Functional characterization of the human PRUNE protein: implications in cancer.

Thesis

PhD thesis in Life sciences

Functional characterization of the human PRUNE protein: implications in cancer.

Anna D'Angelo

Telethon Institute of Genetics and Medicine, TIGEM,

Via Pietro Castellino 111, 80131 Naples, Italy.

Director of studies: Dr. Massimo Zollo

Telethon Institute of Genetics and Medicine, TIGEM,

Via Pietro Castellino 111, 80131 Naples, Italy.

Supervisor of studies: Prof. Ashok Venkitaraman

CRC Department of Oncology - Wellcome Trust Centre for Molecular Mechanisms in Disease - Wellcome Trust/MRC building

Hills Road Cambridge CB2 2QQ

A thesis submitted for the degree in Doctor of Philosophy by research.

August 2004

Submission date: 24 August 2004
Award date: 27 September 2004

To my friend Enzo,

He will always be with me.

He would be very proud of me.

Thanks.

Abstract

The functional characterization of *H-PRUNE* was performed using different approaches, in order to elucidate first the biochemical function of the protein, and then the correlation with other genes and the role in different tumour types.

First, we identified and characterized H-PRUNE phosphodiesterase activity, which is suppressed by dipyridamole. Interestingly, H-PRUNE interacts with NM23-H1, an anti-metastatic protein involved in different processes as proliferation, differentiation and motility, suggesting us to investigate H-PRUNE possible correlation to tumour development and progression with respect to NM23-H1. Our study has consisted in elucidating H-PRUNE function in three different tumour types, as sarcoma, neuroblastoma, and breast cancer.

Both sarcoma and breast cancer analyses revealed that H-PRUNE, localized into the cytoplasm, acts as a negative regulator of NM23-H1. In fact, both aggressive sarcoma subtypes and metastatic breast cancer showed high protein levels of H-PRUNE and low levels of NM23-H1, indicating its involvement in advanced stages of cancer. Moreover, we demonstrated that both the H-PRUNE phosphodiesterase activity and the H-PRUNE and NM23-H1 complex increase cell motility in the MDA-MB-435 breast cancer cell line. The overview of genes and pathways influenced by H-PRUNE overexpression in the MDA-MB-435 breast cancer cellular model has been performed in order to understand the molecular changes in tumour cells.

Interestingly, we found high levels of H-PRUNE, localized into the nuclear compartment, correlated to high levels of both NM23-H1 and NM23-H2 (an isoform of the NM23 family) in advanced stages of neuroblastoma.

We identified a new function of H-PRUNE as a transcriptional regulator of *NM23-H2* and we postulated a transcriptional mechanism of regulation, including activation of *NM23-H1* by NM23-H2 and of *NM23-H2* by H-PRUNE.

This study evidences H-PRUNE function, as a regulator of NM23-H1 anti-metastatic function by two different mechanisms of action, correlated to the different compartmentalization of H-PRUNE protein.

Table of contents

List of figures and tables

Abbreviations

A absorbance

Ab antibody

ATP adenosine triphosphate

bp basepair

cAMP Adenosine 3',5'-cyclic monophosphate

cGMP Guanosine 3',5'-cyclic monophosphate

CMV Cytomegalovirus

Da Dalton

DAB 3,3'-Diaminobenzidine

DAPI 4',6-diamidine-2-phenylindole, hydrocloride

dNTP deoxyribonuceotide triphosphate

DNA deoxyribonucleic acid

DTT dithiothreitol

E.coli Escherichia coli

FBS fetal bovine serum

FCS fetal calf serum

KO knock out

LMS Leiomyosarcoma

LS Liposarcoma

Ma Mammary Carcinoma

MFH Malignant Fibrous Histiocytoma

MS Malignant Schwannoma (Malignant Peripheral Nerve Sheath Tumour)

NB neuroblastoma

PMSF phenylmethylsulfonyl fluoride

SDS sodium dodecyl sulphate

SDS/PAGE sodium dodecyl sulphate polyacrylamide gel electrophoresis

WDLPS Well-differentiated liposarcoma

Introduction

The human prune

The *PRUNE* gene was first identified in *Drosophila melanogaster*. The *Drosophila prune* gene was characterized based on its mutant phenotype that showed a brownish-purple eye colour due to the reduction of drosopterins, in contrast to the bright red eye of the wild-type fly (Timmons and Shearn, 1996). Homozygous *prune* mutants are viable and fertile. In the presence of even a single copy of the gain-of-function mutation in the abnormal wing disc gene (*awd/K-pn*; also named Killer-of-Prune) *prune* mutants are synthetically lethal, developing pseudo-melanotic tumors. The flies die at the third larval instar stage (Biggs et al., 1988; Orevi and Falk, 1975), suggesting a synergism between the *prune* and *awd* genes. Mutations in *awd* result in developmental abnormalities of imaginal disc structures (Rosengard et al., 1989).

The human *PRUNE* gene (*H-PRUNE*) homologue of the Drosophila *prune* gene was identified through dbEST searches and cloned in Dr. Zollo's laboratory (Reymond et al., 1999). The gene is composed of eight exons and is located in the 1q21.3 chromosomal region; a pseudogene has been sequenced and mapped to chromosomal region 13q12.

Reymond et al. (1999) and recent results (Zollo, personal comunication) indicate that *Prune* mRNA pattern of expression is predominant in the development of central nervous system (CNS), and specifically in the regions derived from neural crest cells (dorsal root ganglia, V and VIII cranial nerves), in which neuroblastoma tumour cells originated. *H-PRUNE* is ubiquitously expressed in adult human tissues (Reymond et al., 1999).

The H-PRUNE protein belongs to the DHH superfamily, which includes several phosphoesterases, such as the RecJ nuclease from bacteria and the pyrophosphatases from yeast and bacteria (Aravind and Koonin, 1998b). The DHH superfamily can be divided into two main groups on the basis of a C-terminal motif that is very well conserved within each group, but not across the groups. The first group is represented only in the Archaea and the bacteria, while the second group is also found in eukaryotes (Figure 1). All the members of the superfamily possess the shared N-terminal domain containing the motifs with the absolutely conserved signatures of the form DXD (Motif-1), D (Motif-2), DHH (Motif-3) and D/E (Motif-4). These residues are all on the same face of this domain and together form the catalytic site that chelates at least two divalent cations. The DHH family is so named due to the third motif DHH. The first group of the DHH family includes the RecJ protein, a DNA repair protein, and other nucleases and poorly characterized bacterial proteins; the second group include the exo-polyphosphatases from yeast. The recently availability of the structures of the RecJ protein (Yamagata et al., 2002) and the bacterial pyrophosphatases (PPASEs) (Ahn et al., 2001) reveal that these two major classes of DHH proteins share an N-terminal α/β domain with a five-stranded parallel sheet, but have somewhat different C-terminal domains. The first four motifs are the most conserved portions of the N-terminal domain and define the active site of these enzymes, whereas the group-specific fifth motif maps to the divergent C-terminal domains. In both DHH families, the C-terminal domain contains a core sheet of five strands, four of which form two β-strand hairpins. However, differences in the C-terminal domains between the first and the second families of DHH proteins may contribute prominently to substrate specificities of the two superfamilies.

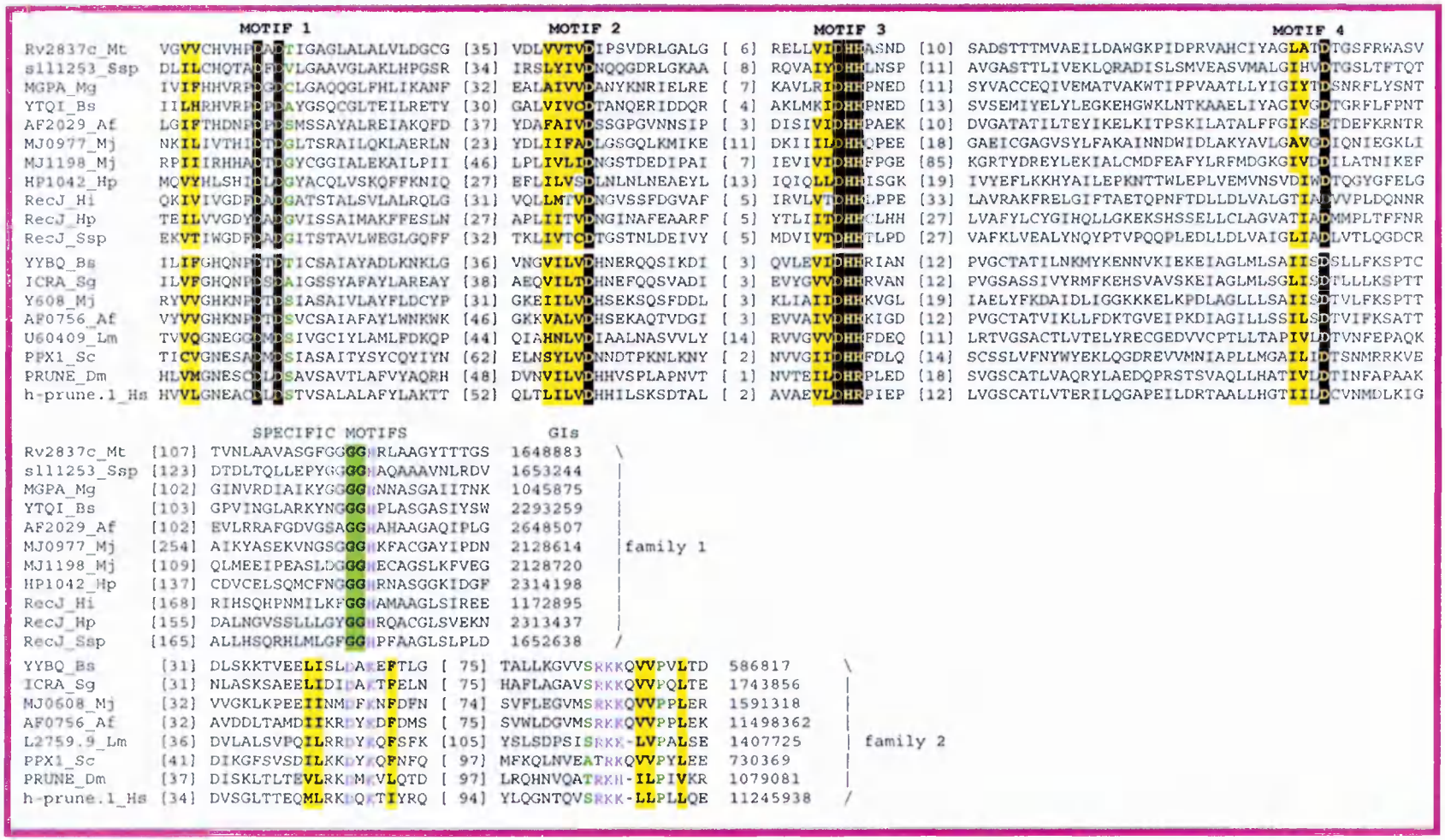

Figure 1. Alignment of DHH family phosphoesterases.

Multiple alignment of the DHH family phosphoesterases, showing separately the four generic motifs (1-4) and the motifs diagnostic of the two distinct subfamilies that map to the second domain. The position of the first aligned residue in each protein sequence and the distances between the motifs are indicated by numbers. The Gene Identification (GI) numbers in the NCBI/GenBank protein sequence database are indicated to the right of each sequence. Species name abbreviations: Af-*Archaeoglobus fulgidus*, Bb-*Borrelia burgdorferi*, Bs-*Bacillus subtilis*, Dm-*Drosophila melanogaster*, Ec–*Escherichia coli*, Hi–*Hameophilus influenzae*, Hp-*Helicobacter pylori*, Lm-*Leishmania major*, Mg-*Mycoplasma genitalium*, Mj-*Methanococcus jannaschii*, Mp-*Mycoplasma pneumoniae*, Mt-*Mycobacterium tuberculosis*, Sc-*Saccharomyces cerevisiae*, Sg-*Streptococcus gordonii*, Ssp-*Synechocystis species*.

A clustering analysis of the DHH proteins shows that PRUNE proteins (human and *Drosophila*) belong to the second group of the DHH family, along with the inorganic pyrophosphatases and exopolyphosphatases (Figure 1). Evolutionary studies on DHH family have shown that phosphoesterases derived from a number of protein folds that encode diverse phosphoesterases and hydrolases. These include: the HD fold, from which the classic signalling cyclic nucleotide phosphodiesterases (PDEs) are recognized (PDE1-11) (Aravind and Koonin, 1998a, Aravind and Koonin, 1998b, Galperin et al., 1999); the metallo-β-lactamase fold (Aravind, 1999; Galperin et al., 1999), from which the PdsA-like PDEs are derived; and the calcineurin-like phosphoesterase fold (Aravind and Koonin, 1998b), from which Icc-like PDEs are derived.

The cyclic nucleotide phosphodiesterases catalyze the hydrolysis of 3':5'-cyclic nucleotides to their corresponding nucleoside 5'-monophosphates. Cyclic nucleotides cAMP and cGMP are well known as second messengers and regulate many functions in various tissues; to date, phosphodiesterases are divided into eleven distinct families on the basis of substrate specificity and sensitivity to endogenous/exogenous regulators and genetically on the basis of sequence homology (Beavo et al., 2002).

Structural analysis of H-PRUNE showed similarities to RecJ (Figure 2) and pyrophosphatase proteins (Ahn et al., 2001; Yamagata et al., 2002), thus suggesting potentially similar activities to those proteins. Additionally, C-terminal to the DHH motif, mammalian PRUNE contains a non-globular extension within which there are some conserved serines that could be phosphorylated to modulate H-PRUNE function.

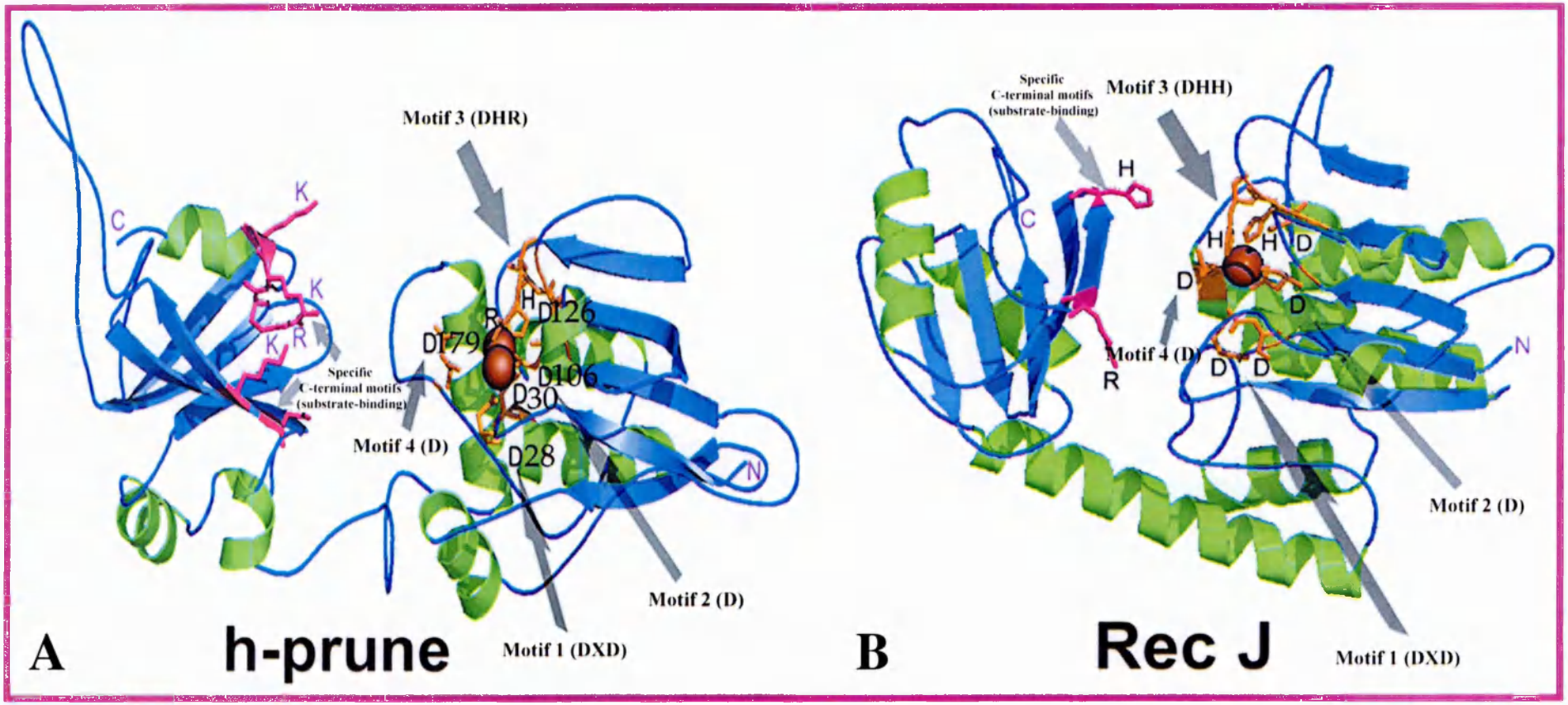

Figure 2. Ribbon structure of the h-prune and RecJ proteins.

A) Ribbon structure of the h-prune protein based on the crystal structure of PPASE and the RecJ protein. Red balls indicate potential cofactor ions (Mg^{2+} and/or Mn^{2+}) and the region of binding to motif 3. Arrows indicate the aspartic acids (D). Aspartic acids of the four DHH motifs are represented, indicating the potential catalytic site of DHH protein family.

B) Ribbon structure of the RecJ protein. Red balls indicate cofactor ions (Mg^{2+} and/or Mn^{2+}) and the region of binding to motif 3. Arrows indicate the aspartic acids (D) characteristic of DHH protein family.

H-PRUNE and *Drosophila* PRUNE proteins belong to DHH family and contain the DHR form, which is conserved in the catalytic sites of some known PDEs, as PDE5 and PDE8, PDE10A and PDE11A. The presence of the DHR form in the PRUNE proteins could result in different structural properties correlated to the different charges of the amminoacids with respect to the other proteins of the DHH family. In fact, the optimum of pH for the phosphodiesterase activity is pH 7.5-8.0, a value at which the arginine is positively charged and the histidine is not charged, since the isoelectric points of the histidine and of the arginine are 7.6 and 10.8, respectively.

Hence, since evolutionary studies on DHH family have shown that phosphoesterases derived from protein folds hallmarks of the classic signalling cyclic nucleotide phosphodiesterases (PDEs) are recognized (PDE1-11) (Aravind and Koonin, 1998a, Aravind and Koonin, 1998b, Galperin et al., 1999) and the Drosophila and human PRUNE proteins contain the DHR form, the two proteins could define a new class of PDEs, characterized by different putative activities as phosphodiesterase, pyrophospatase and/or exonuclease.

Moreover, an interesting example of a family protein characterized by both phosphodiesterase and pyrophospatase activities is the type I phosphodiesterase / nucleotide pyrophosphatase family (NPP1) consisting of phosphodiesterases, including human plasma-cell membrane glycoprotein PC-1 / alkaline phosphodiesterase / nucleotide pyrophosphatase (NPPase). These enzymes catalyse the cleavage of phosphodiester and phosphosulfate bonds in NAD, deoxynucleotides and nucleotide sugars (Cimpean et al., 2004).

Furthermore, a ScanProsite analysis (http://www.expasy.com) revealed the presence of a leucine zipper domain (positions from 157 to 185) in H-PRUNE primary sequence (Figure 3), thus suggesting a possible DNA binding capability or transcriptional activation activity of H-PRUNE associated with a nuclear localization.

Hence, the sequence alignments indicate that the H-PRUNE could potentially have exonuclease, pyrophosphatase, polyphosphatase and/or phosphodiesterase activities. Additionally, the motif scan analysis indicates also a potential DNA binding and/or transcriptional activation activity.

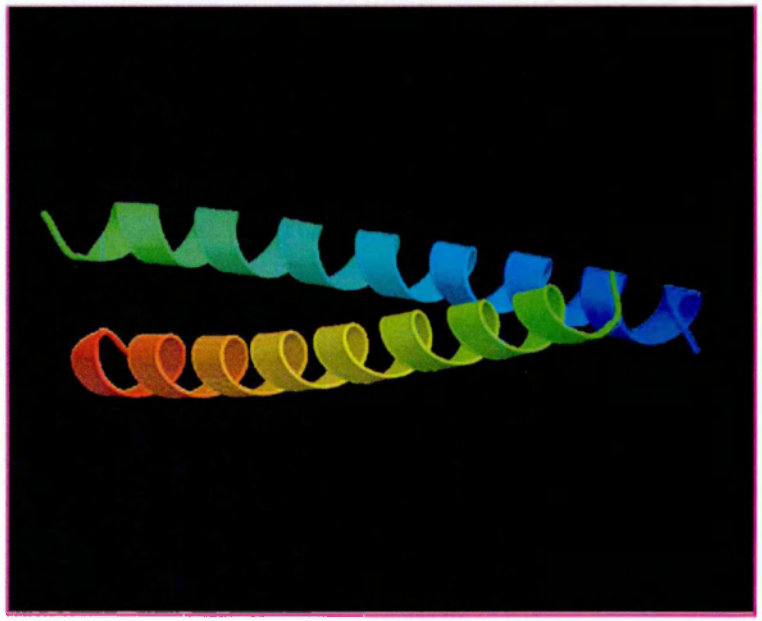

1-MEDYLQGCRAALQESRPLHVVLGNE
ACDLDSTVSALALAFYLAKTTEAEE
VFVPVLNIKRSELPLRGDIVFFLQK
VHIPESILIFRDEIDLHALYQAGQL
TLILVDHHILSKSDTALEEAVAEVL
DHRPIEPKHCPPCHVSVELVGSCAT
LVTERILQGAPEILDRQTAALLHGT
IILDCVNMDLKIGKATPKDSKYVEK
LEALFPDLPKRNDIFDSLQKAKFDV
SGLTTEQMLRKDQKTIYRQGVKVAI
SAIYMDLEAFLQRSNLLADLHAFCQ
AHSYDVLVAMTIFFNTHNEPVRQLA
IFCPHVALQTTICEVLERSHSPPLK
LTPASSTHPNLHAYLQGNTQVSRKK
LLPLLQEALSAYFDSMKIPSGQPET
ADVSREQVDKELDRASNSLISGLSQ
DEEDPPLPPTPMNSLVDECPLDQGL
PKLSAEAVFEKCSQISLSQSTTASL
SKK-453

Figure 3. H-prune as a putative DNA binding protein.
Schematic representation of a leucine zipper domain (left panel) and h-prune primary aminoacidic sequence (right panel). The putative leucine zipper domain is showed in underlined red.

The NM23s: the protein partners of H-PRUNE.

Nm23-H1, the human homologue of *awd Drosphila* gene, is a tumour metastasis suppressor that was originally identified by subtraction cloning in murine melanomas of differing metastatic potential (Steeg et al., 1988). *Nm23-H1* encodes for the nucleoside diphosphate kinase (NDPK-A or NM23-H1), which shares almost 70% similarity at amino acid level to the AWD protein by *Drosophila*. Reymond et al. (1999) demonstrated the physical interaction between H-PRUNE and NM23-H1. Humans encode up to eight orthologs (-H1 to -H8) of *awd*, at least four of which are active nucleoside diphosphate kinases (NDPKs). The NDPKs are 17-20 kDa proteins that are distributed ubiquitously and catalyze the phosphorylation of nucleoside diphosphate to the corresponding nucleoside triphosphate, mainly at the expense of the ATP synthesised through oxidative phosphorylation (Lombardi et al., 2000).

The NM23 family divides into two distinct groups (Table 1): the group I encode proteins that generally have highly homologous counterparts in other vertebrate species and possess the classic enzymatic activity of a NDP kinase. This group includes NDP kinase A-D (*NM23-H1* to *-H4*), which share 58 to 88% identity with each other.

The protein products of the group II genes (*NM23-H5* to *-H8*) are more divergent as the sequences share only 25 to 45% identity with the first group proteins and between each other (Lacombe et al., 2000). NM23-H1 and -H2 can form *in vitro* and *in vivo* homohexamers as well as heterohexamers possessing different ratios of the respective subunits.

Isoform	Size (aa)	Mass (Da)	Locus	Tissutal expression	Subcellular localization	NDPK activity	Comments
nm23-H1	152	17,149	17q21.3	ubiquitous	cytoplasmatic	Yes	overexpressed in tumors; inverse correlation with metastatic potential
nm23-H2	152	17,298	17q21.3	ubiquitous	cytoplasmatic, nuclear	Yes	overexpressed in tumors; transcription factor (PuF) for *CMYC* proto-oncogene
nm23-H3	168	18,903	16q13[a]	ubiquitous	cytoplasmatic	Yes	overexpression suppresses granulocyte differentiation and induces apoptosis of myeloid cells. N-terminus of 17 aa
nm23-H4	187	20,659	16p13.3	ubiquitous	mitochondrial	Yes	associated with mitochondrial membranes; N-terminus of 33 aa
nm23-H5	212	24,236	5p21.3	testis (traces in brain and kidney)	Nd[d]	Not found	expressed in male germinal cells; C-extension of 51 aa
nm23-H6	186	21,142	3p21.3	ubiquitous	mitochondrial, cytoplasmatic	Yes	A role in regulation of cell growth and cell cycle progression?
nm23-H7	376	42,492	1q24	mainly in testis (also in liver, heart, brain, ovary, small intestine, and spleen)	Nd[d]	Nd[d]	Duplicated NDP kinase domain; N-terminus of 85 aa
m23-H8	588	67,270	7	mainly in testis	Nd[d]	Nd[d]	N-terminal thiredoxin domain; triplicated NDP kinase domain

Table 1. The Human Nm23/NDP Kinase family.

[a] another chromosomal localization was reported in 16p13.3 (GenBank acc. no. AL031718)

[d] Nd, not determined

(Lacombe et al., 2000).

The NM23-H1 and NM23-H2 proteins share 88% identity (Figure 4A) and are about 95% and 98% identical to the murine Nm23-M1 and Nm23-M2 proteins, respectively. The *NM23-H1* and *NM23-H2* genes both localize on chromosome 17q21.3 (Backer et al., 1993).

The well characterized biochemical activities of NM23-H1 include nucleoside diphosphate kinase, serine autophosphorylation (MacDonald et al., 1993) and protein histidine kinase (Engel et al., 1995; Hartsough et al., 2002; Wagner et al., 1997; Wagner and Vu, 2000). The nucleoside diphosphate kinase activity functions via a high-energy nm23-phosphohistidine intermediate; in fact, the NM23-H1 and -H2 mutants in H118 lack NDPK activity (MacDonald et al., 1993). For NM23-H1, two proteolytic fragments containing serines 44 and 120, 122 and 125 exhibited serine autophosphorylation (Figure 4A) (MacDonald et al., 1993). Furthermore, NM23-H1 is able to phosphorylate *in vitro* KSR (kinase suppressor of Ras), a scaffold protein for the mitogen activated protein kinase (MAPK cascade), suggesting that the histidine protein kinase activity could be correlated to metastasis-suppressor activity (Hartsough et al., 2002); this observation, coupled to observations that NM23 transfected MDA-MB-435 breast cancer cells had lower levels of phosphorylated MAPK led to the conclusion that NM23 signals through the ERK-MAPK pathway (Steeg, 2003).

NM23-H1 associates with the cytoskeleton through an interaction with β-tubulin (Lombardi et al., 1995) and the centrosomal kinase Aurora-A/STK15 (Du et al., 2002). Physical interaction with NM23-H1 has also been demonstrated for the Epstein-Barr virus nuclear protein EBNA-3C (Subramanian et al., 2001), for small and heterotrimeric G-proteins (Kikkawa et al., 1990; Kimura et al., 2003; Randazzo et al., 1991), and their exchange factors (Otsuki et al., 2001).

A new role of NM23-H1, alternatively named GzmA-activated Dnase, is of note in the nucleus, by creating single-stranded DNA nicks, in a caspase-independent apoptosis pathway (Fan et al., 2003). The NM23-H1 role, correlated to apoptotic pathways, may offer an alternative mechanism for metastasis suppression. Recently, Ma et al. (2004) have demonstrated that NM23-H1 has a 3'-5' exonuclease activity.

While NM23-H1 is a predominantly cytoplasmatic protein, NM23-H2 is found mainly in the nucleus (Kraeft et al., 1996) and has been implicated in transcription regulation of *CMYC* "via" its specific binding to a single strand DNA, a nuclease-hypersensitive polypurine/polypyrimidine element (NHE-PuF) (Berberich and Postel, 1995; Postel et al., 1993; Postel, 1996; Postel et al., 1996). NM23-H2 binding to the *CMYC* NHE sequence can result in double-stranded DNA breaks and in the formation of a covalent protein-DNA complex (Grand et al., 2004; Postel et al., 1999), suggesting that NM23-H2 is involved in DNA structural transactions necessary for the activity of *CMYC* regulation of expression.

Several mutations of NM23 that affect folding, oligomerization, DNA binding and NDPK activity have been described in NM23-H1 and NM23-H2 (Ouatas et al., 2003) (Figure 4B). In particular, the NM23H1-P96S mutation, a *Drosophila* developmental mutation homolog (*awd/K-pn*), is able to interact with H-PRUNE and exhibits autophosphorylation and NDPK normal function, while it is deficient for protein histidine kinase activity (Reymond et al., 1999; Freije et al., 1997a). The NM23-H1P96S shows failure in folding properties associated to oligomeric NM23-H1 protein complexes and it is not able to reduce motility with respect to the NM23-H1 wild-type protein (Lascu et al., 1992; Freije et al., 1997a).

A second mutation, NM23H1-S120G, associated with advanced stages of neuroblastoma (Chang et al., 1994) retains NDPK activity and exhibits deficient downstream serine autophosphorylation and histidine protein kinase activity (Freije et al., 1997a). The NM23H1-S120G mutant is able to increase cell motility in a breast cancer cellular model (MacDonald et al., 1996), and it is impaired in its interaction with H-PRUNE (Reymond et al., 1999). The NM23H2-S122P mutation, found in melanoma cell lines of high metastatic potential, shows reduced NDPK activity of the protein and promotes cell motility (Hamby et al., 1995; Schaertl et al., 1999).

Thus, NM23s represent a protein family implicated in different physiological processes, as motility, proliferation and differentiation.

A

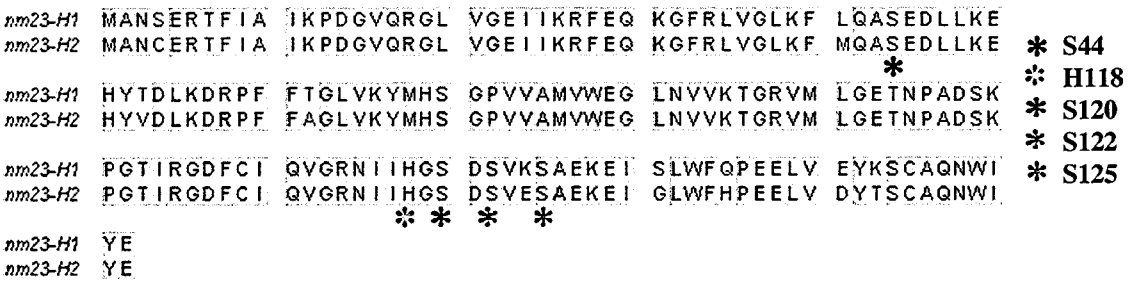

B

Isoform	NDPK activity	Auto phosphorylation	Histidine protein kinase	DNA cleavage	MDA-MB-435 Motility
nm23-H1	+++	+++	+++	+++	–
nm23-H1 P96S	+++	+++	+	ND	+++
nm23-H1 S120G	+++	++	++	+++	+++
nm23-H1 H118F	–	–	–	+++	ND
nm23-H2	+++	ND	ND	+++	ND
nm23-H2 S122P	++	ND	ND	ND	+++

Note - ND: not determined

Figure 4. The nm23s partners of h-prune.

A) Clustal alignment of nm23-H1 and nm23-H2 isoforms. The asterisks indicate the serines involved in autophorylation and the histidine of the catalytic site.
B) Effect os site direct mutagenesis on nm23-H1 and nm23-H2 biochemical characteristics and biological function in motility (Outas et., 2003).

H-PRUNE and NM23: correlations with cancer.

Tumorigenesis in human is a multistep process; the steps reflect genetic alterations that drive the progressive transformation of normal human cells into highly malignant derivatives. Many types of cancers are diagnosed in the human population with an age-dependent incidence implicating four to seven rate-limiting, stochastic events. Pathological analyses of a number of organ sites reveal lesions that appear to represent the intermediate steps in a process through which cells evolve progressively from normal status via a series of pre-malignant states into invasive cancers. The genomes of tumour cells are invariably altered at multiple sites, having suffered disruptions through lesions as subtle as point mutations and as obvious as changes in chromosomal complement (Hanahan et al., 2000). Amplification represents one of the major molecular pathways through which the oncogenic potential of proto-oncogenes is activated during tumorigenesis (Schwab, 1998; Savalyeva and Schwab, 2001).

Various authors suggested that the vast catalog of cancer cell genotypes is a manifestation of six essential alterations in cell-physiology that collectively dictate malignant growth: self-sufficiency in growth signals, insensitivity to growth-inhibitory (anti-growth) signals, evasion of programmed cell death (apoptosis), limitless replicative potential, sustained angiogenesis, and tissue invasion and metastasis.

To date, the main cause of treatment failure and death for cancer patients is metastasis. Metastatic processes require a complex set of ordered cellular functions, many of which can be initiated by multiple, redundant stimuli (Steeg, 2003).

Examples are acquisition of invasive ability, changes in adhesion, initiation of motility and extra-cellular matrix proteolysis (Figure 5).

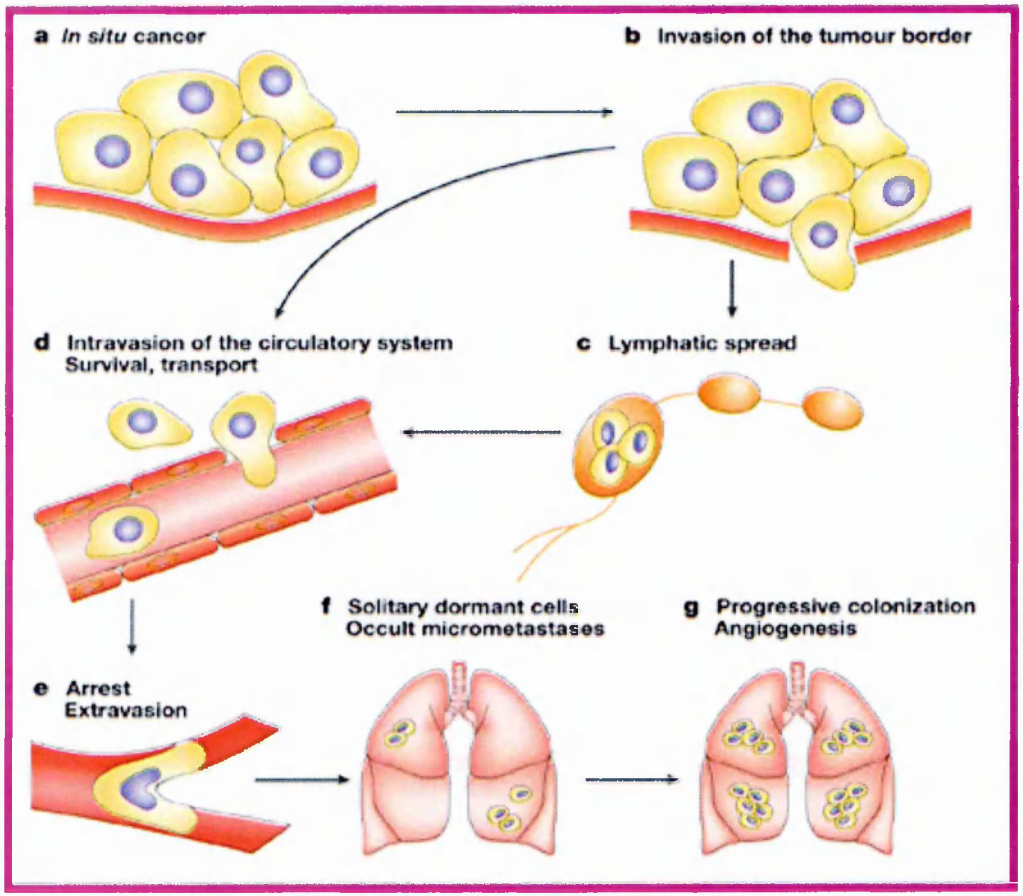

Figure 5. Metastasis is a complex, multistep process.

A schematic of the metastatic process, beginning with a) an *in situ* cancer surrounded by an intact basement membrane. b) Invasion requires reversible changes in cell-cell and cell-extracellular-matrix adherence, destruction of proteins in the matrix and stroma, and motility. Metastasizing cells can c) enter via the lymphatics, or d) directly enter the circulation. e) Survival and arrest of tumour cells, and extravasation of the circulatory system follows. f) Metastatic colonization of the distant site progresses through single cells, which might remain dormant for years, to occult micrometastases and g) progressively growing, angiogenic metastases (Sleeman, 2000).

In breast cancer, metastatic spread is responsible for virtually all cancer deaths. To become invasive, tumour cells need to change their adhesive properties, to lose contact with other cells in the primary tumour and make new contacts with the extracellular matrix of host cells they encounter as they invade. They also need to be able to penetrate into the surrounding host tissue and here the modulation of protease activity in the vicinity of the tumour cells plays a critical role. To migrate away from the primary tumour, tumour cells also need to gain motility functions. These same properties are also thought to be important when circulating tumour cells exit the circulatory system and start metastatic colonization in secondary organs (Sleeman, 2000).

Tumorigenicity and metastasis are distinct, but interrelated phenotypes. Tumorigenicity is necessary, but not sufficient, for metastasis. Tumour progression results from genetic instability coupled with selection of subpopulations of cells. Eventually some cells accumulate sufficient capacity to dissociate and spread. Depending on whether the mutations occur early or late in tumour progression determines proportions of metastatic cells within tumours of a given size. In part, metastasis is also determined, to a great extent, by tumour-host interactions (Liotta et al., 2001).

By screening cDNA libraries of matched metastatic/non-metastatic K1735 murine melanoma cell lines by differential hybridization, "non-metastatic clone 23" gene, was identified as the first metastasis suppressor gene (Steeg et al., 1988).

To date, eight metastasis suppressor genes (*NM23-H1, KAI1, KiSS1, BrMS1, MKK4, RHOGDI2, CRSP3* and *VDUP1*) have been isolated and characterized.

Within this group, NM23-H1 plays a major role for its ability to reduce cellular motility if overexpressed in aggressive breast cancer cells, influencing anchorage-independent colonization and induction to differentiation (Freije et al., 1997a; Freije et al., 1997b; Hartsough et al., 2001). The *NM23-H1* gene has proved to have a clear role as metastasis suppressor gene in breast cancer (Hartsough and Steeg, 1998; Howlett et al., 1994; Kantor et al., 1993; Leone et al., 1993a; Lombardi et al., 2000). Moreover, overexpression of NM23-H1 in rat PC12 cells promotes neuronal differentiation upon nerve growth factor (NGF) induction (Gervasi et al., 1996).

Numerous tumours and highly proliferative cells overexpress nm23-H1 both at mRNA and protein levels, and in most cases this overexpression is linked to early stages of cancer, with a loss of expression in more advanced and aggressive stages. In breast, colon, gastric and ovarian carcinomas and in melanomas, high expression of human NM23-H1 is associated with a decreased metastatic potential (Florenes et al., 1992; Hennessy et al., 1991; Schneider et al., 2000; Muller et al., 1998; Srivatsa et al., 1996). The relation between the expression of NM23 and the control of metastatic potential is somehow controversial. In fact, in other cancers such as non-Hodgkin lymphomas and neuroblastomas, high NM23-H1 expression is associated with an adverse outcome (Hartsough and Steeg, 2000; Niitsu et al., 2001).

Furthermore, in neuroblastoma a mutated *nm23-H1* mRNA, the *nm*23H1-S120G, was often found associated with advanced stages of disease and poor patient survival (Chang et al., 1994).

In sarcomas, NM23-H1 expression was found to increase with the metastatic potential for some tumours, but some aggressive cases also showed loss of expression (Royds et al., 1997).

Clinical studies assessing NM23 as a marker for metastasis were recently reviewed (Salerno et al., 2003). Briefly, decreased expression (as would be expected for a metastasis suppressor) correlated in many, but not in all cancers. Thus, NM23 has shown promise for some cancer types, but is not yet considered an independent prognostic factor.

The synergism between the *awd* (the orthologue of *NM23-H1*) and *prune* genes observed in *Drosophila*, the amplification of the 1q21 chromosomal region within which *H-PRUNE* maps (Muleris et al., 1994; Nilsson et al., 2004), the interaction between H-PRUNE and NM23-H1, which is impaired with the NM23H1-S120G mutation suggest us a possible involvement of H-PRUNE in tumorigenesis and/or metastatic processes. Since the opposite correlation of *nm23-H1* to cancer (high levels of *nm23-H1* correlate with low metastatic potential in breast cancer but low levels of *nm23-H1* correlate with low metastatic potential in neuroblastoma), we decided to investigate H-PRUNE function in association to NM23-H1 in three different types of tumours:

sarcomas, which do not show a unique correlation between *nm23-H1* levels and aggressiveness of the tumour and present the amplification of the chromosomal region 1q21;

neuroblastoma, where advanced stages of the tumour present high levels of *nm23-H1* and are frequently associated to a gain of function mutation, the *nm*23H1-S120G;

breast cancer, in which low levels of *nm23-H1* are associated with poor prognosis and amplification of the chromosomal region 1q21 is reported.

H-PRUNE, NM23-H1 and sarcoma

Sarcomas, tumours of mesenchymal origin (Enzinger and Weiss, 1995) are rare tumours occurring at different sites of the body and varying greatly in their degree of aggressiveness. Approximately 60% of sarcomas are high grade and approximately half of these will metastasize, predominately to the lung. Bone and soft tissue tumours (BSTT) belong to a heterogeneous group of tumours that involve a large number of histological subtypes and affect persons of all ages (Fletcher et al., 2002). The pattern of chromosome changes, including numerical and structural aberrations, is diverse. Some tumour types exhibit highly specific translocations, occurring in 90-95% of a particular tumour type, such as t(12;16)(q13;p11) in myxoid liposarcoma and t(X;18)(p11;q11) in synovial sarcoma. These translocations result into the formation of fused genes encoding chimeric proteins. Other tumours exhibit characteristic, but not tumour-specific, aberrations such as supernumerary ring chromosomes and giant marker chromosomes in atypical lipomatous tumours (ALT), low-grade malignant fibrous histiocytomas (MFH) and parosteal osteosarcomas. Finally, some BSTTs, such as highly malignant osteosarcomas, low-grade malignant fibrous histiocytomas (MFH) and leiomyosarcomas display an extensive cytogenetic heterogeneity with numerous structural and numerical aberrations.

Sarcomas have been widely studied at the molecular level, and this has provided insight into mechanisms of importance for tumour development in general. Notably, amplification and overexpression of *MDM2* and *CDK4*, representing alternative pathways for inactivation of the tumour suppressors *p53* and *pRb*, were first described in this group of tumours (Khatib et al., 1993; Oliner et al., 1992). Chromosome bands 12q13-15 are frequently altered in different types of sarcomas (Schwab, 1998). The gene *GLI*, which encodes a nuclear zinc finger phosphoprotein, presumably a transcription factor, maps to 12q13-15 chromosomal region. In malignant fibrous histiocytoma amplified sequences derived from chromosome 12q13-14 and encoding a gene designated *SAS* (*sarcoma amplified sequence*) were reported (Smith et al., 1992). Comparative genomic hybridisation (Kallioniemi et al., 1992) revealed novel amplified regions that seem to be important for the development of sarcomas, in particular 1q21-q22 (Forus et al., 1995a,b; Szymanska et al., 1996). Recently, Nilsson et al. (2004) demonstrated the presence of an amplicon originating from 1q21-23, containing the candidate oncogenes *COAS1*, *COAS2* and *COAS3* (Chromosome One Amplified Sequence) in lipomatous tumours.

In sarcomas, the *nm23-H1* expression increase in line with metastatic potential in many cases analysed but has no value as a prognostic factor for these mesenchymal tumours. Metastatic sarcomas with low expression of *nm23-H1* have also been reported (Royds et al., 1997). Because of the different correlation of *nm23-H1* to sarcomas progression and of the amplification of the 1q21 region, the study of H-PRUNE in association with NM23 will be interesting to elucidate H-PRUNE function related to NM23-H1.

H-PRUNE, NM23s and neuroblastoma

Neuroblastoma (NB) is a malignant tumour consisting of undifferentiated neuroectodermal cells derived from the neural crest. Neuroblastoma is one of the most common malignant disease in children with 7-5 cases in every 100.000 infants (Bown, 2001; Schwab et al., 2003). In addition, an interesting phenomenon is observed of spontaneous neuroblastoma regression, with a significant frequency, most often observed in infants younger than 1 year (Guin et al., 1969). Finally, at low frequency, estimated 1% - 2% of all neuroblastoma world wide reported tumours, has been also observed as a familial complex hereditary NB disease (Tonini et al., 2003). NB tumours are heterogeneous in their biological, genetic, and morphological characteristics and demonstrate diverse clinical phenotype. To date three clinical patterns of NB have been identified: i) spontaneously regressing widespread disease; ii) non-metastatic local-regional disease, and iii) metastatic disease (stage 4, 4S).

The study of the molecular genetics of NB in the last two decades has elucidated several non-random genetic events: allelic losses on chromosomes 1p, 2q, 3p, 7q, 11q, 14q and 19q, implicating putative tumour-suppressor gene (Ejeskar et al., 1998; Fong et al., 1992; Guo et al., 1999; Maris and Matthay, 1999; Maris et al., 2002; Marshall et al., 1997), allelic gains on chromosomes 1q, 5q, 7q, 17q, 18q and probably affecting growth control genes (Bown et al., 1999; Janoueix-Lerosey et al., 2000; Meltzer et al., 1996; Mora et al., 2002; Takita et al., 2000); amplification of the oncogene *MYCN* (Schwab, 1991; Seeger et al., 1985) and, changes in the normal diploid chromosomal content (Kaneko et al., 2000). *MYCN* amplification, found to be relatively specific for tumours of neural origin is an important prognostic marker and it is well known to correlate with advanced stage disease and in general with an

increased risk of fatal outcome. *MYCN* maps to 2p23-24 chromosomal region and it is retained in single copy at its normal position during amplification in human neuroblastoma cells (Corvi et al., 1994). Because *MYCN* amplification occurs only in approximately half the cases of advanced neuroblastoma, it has been suggested that *MYCN* independent pathways exist in neuroblastoma progression (Brodeur et al., 1997; Schwab et al., 1997).

High expression of the neurotrophin receptor TRKA is a favourable indicator – perhaps mediating either apoptosis or differentiation in NB tumours. TRKA expression levels are inversely correlated to *MYCN* amplification, indicating that this gene is not prognostic factor independent of *MYCN* amplification (Brodeur et al., 1984; Nakagawara et al., 1993; Tanaka et al., 1998). Conversely, high expression of TRKB with its ligand might provide an autocrine survival pathway in unfavourable tumours, particularly those with *MYCN* amplification (Brodeur, 2003).

Recently, Takita et al. (2004) performed DNA microarray analysis on early- and advanced-stage neuroblastoma in order to identify candidate genes involved in neuroblastoma progression. In the early stage group *BIRC3 (Baculoviral IAP repeat-containing 3, API2)* and *CDKN2D (Cyclin-dependent kinase inhibitor 2D)* genes were found significantly increased in their expression levels while *SMARCD3 (SWI/SNF related, subfamily d, member 3)* expression resulted reduced, indicating that these genes are possible candidates for being novel prognostic markers for neuroblastoma.

Another prognostic example is measured on 1p NB deletion, which correlates with unresectable and metastatic disease, whereas localised and clinically favourable tumours showed an intact chromosome 1.

Among genetic alterations in neuroblastoma, amplifications on 1p at bands 1p34.2 and 1p36.3 were also found (Fix et al., 2004). Between the most occurring neuroblastoma chromosome abnormalities, chromosome 17 is often found as gain and the hot region of constant gain has been defined between 17q23.1 and 17qter. About 41% of tumours show 17q22 gain. Alternatively, gain of whole chromosome 17 is more likely to be seen in tumours showing favourable clinical outcome, while unbalanced partial 17q gain is significantly associated with a clinical risk in neuroblastoma. In chromosome 17q21 region there are several genes implicated in apoptosis, cell cycle control and neuroblastoma cell differentiation. This region includes *NM23* genes (*-H1* and *-H2*) located at 17q21-22 (Backer et al., 1993). A striking correlation between *MYCN* amplification and mRNA and protein expression of both *NM23-H1* and *NM23-H2* genes was reported for neuroblastoma (Godfried et al., 2002). The gain of function mutation (nm23H1-S120G) has been identified in a high proportion of advanced neuroblastomas (Chang et al., 1994), as an indicator of poor prognosis and unfavourable outcome.

Because of the mRNA pattern of *prune* expression predominant in the mouse central nervous system, and of the interaction of H-PRUNE, impaired into the gain of function mutation, nm23H1-S120G, frequently encountered in NB (Chang et al., 1994; Hailat et al., 1991; Lascu et al., 1997) we decided to investigate the role of H-PRUNE in neuroblastoma tumour.

H-PRUNE, NM23-H1 and breast cancer.

Breast cancer is the most common malignancy and the second most common cause of cancer-related death in Western European and North American women. Mutations in *BRCA1* and *BRCA2* genes, as well as *p53*, *Her2/neu* and some regulatory proteins of the cell cycle, such as cyclinD1 and p27 Kip1 are used as molecular markers to predict breast cancer prognosis. In particular, mutations in *BRCA1* and *BRCA2* are found in hereditary breast cancer; the BRCA1 and BRCA2 proteins are implicated in DNA repair and recombination, checkpoint control of cell cycle, and transcription. However, only about 10% of breast cancer cases cluster in families. The majority of cases ("sporadic") exhibit no clear-cut familial clustering and probably result from the collective effect of multiple, poorly penetrant variations in a much larger group of genes, modified by environmental factors (Venkitaraman, 2002).

Several genes, such as *ERBB2* (at 17q12), *MYC* (8q24), and *CCND1* (11q13) are amplified in 10-25% of tumours, and their amplification is associated with advanced stages of the disease (Ross et al., 1999; Cuny et al., 2000). The 17q23 amplification is associated with poor prognosis of breast cancer patients (Bärlund et al., 2000); several genes as *RPS6KB1*, a mediator involved in G1- to S-phase progression of the cell cycle (Chou and Blenis, 1995) and *APPBP2*, a cytoplasmatic protein that is involved in cellular trafficking of amyloid precursor protein (Zheng et al., 1998) have been proposed as targets for the 17q23 amplification.

About chromosomal abnormalities the gain of the whole long arm (1q) is most frequent in breast cancers; local amplification affecting 1q21-q22 has been observed (Tirkkonen et al., 1998).

A significant association between reduced NM23-H1 expression, at the mRNA and protein levels, and aggressive breast cancer behaviour was observed. The NM23-H1 is able to induce "low motility cellular processes" if overexpressed in aggressive breast cancer cells (Freije et al., 1997a; Freije et al., 1997b). Transfection studies, in which human nm23-H1 cDNA was expressed in the metastatic human MDA-MB-435 breast carcinoma cell line, indicate that NM23-H1 suppresses *in vivo* metastatic potential by the means of 50-90% (Leone et al., 1993a).

The anti-motility effect of NM23-H1 demonstrated in breast cancer and the amplification of the chromosomal region 1q21 in which *H-PRUNE* maps, suggest us that breast cancer could be an interesting model for studying H-PRUNE function correlated to NM23-H1.

Aim of the project

The aim of this project is to investigate the functional role of *H-PRUNE*, focusing the attention on the biochemical characterization of the protein and its possible correlation to tumour development and progression with respect to NM23-H1. The starting point of the work was the interaction between H-PRUNE and NM23-H1, an anti-metastatic protein involved in different processes as proliferation, differentiation and motility.

Confirmed sequencing analysis has associated both *Drosophila* and human PRUNE proteins to a new family of proteins named DHH phosphoesterases, including RecJ (exonuclease) and exopolyphosphatases (Aravind and Koonin, 1998b). Among the different putative H-PRUNE activities, we decided to investigate first the phosphodiesterase (PDE) activity, which could be inversely correlated to the cAMP levels in the cell. In order to identify H-PRUNE catalytic activity, we plan to purify eukaryotic H-PRUNE to get a functionally active protein, using the Baculovirus expression system. After the identification of the enzymatic activity, the characterization of H-PRUNE could be performed defining the kinetic properties and the sensitivity to PDE inhibitors.

Since interaction between H-PRUNE and wild-type NM23-H1 and some mutants has already been demonstrated (Reymond et al., 1999), it would be interesting to demonstrate the interaction of H-PRUNE with NM23-H2, which shows high homology to NM23-H1.

By using a variety of known mutations in NM23-H2 already characterized, *in vivo* co-immunoprecipitations will be performed in order to define the role of H-PRUNE in the binding capability, which can elucidate the role of H-PRUNE with respect to NM23s proteins.

In order to clarify the role of H-PRUNE and NM23-H1 in oncogenesis, we want to verify the expression level of both genes in sarcoma, neuroblastoma and breast cancer using specimens from early and advanced stages of tumours, to study also the correlation with the tumour progression.

Furthermore, *NM23-H1* shows a clear role of in breast cancer (Leone et al., 1993a). To study the role of H-PRUNE correlated to NM23-H1 in motility, we will produce stable clones transfecting h-prune and NM23-H1, alone or in combination, in human MDA-MB-435 breast carcinoma cell line and we will perform motility assays.

Reymond et al. (1999) showed a *Prune* mRNA pattern of expression specifically in central nervous system (CNS) during mouse development. It would be interesting to create a conditional FLIP/FRT prune KO mouse. We plan to prepare the construct to generate "null" prune mice by directing the complete disruption of the *Prune* gene using the FLIP recombinase system and, on the basis of the peculiar expression pattern of prune in mouse embryo, to verify a conditional FLIP/FRT KO mice in brain tissues.

Thus, this thesis represents an approach, both biochemical and functional, to elucidate H-PRUNE role in tumour development and progression.

Experimental procedures

Cell culture

COS-7, HeLa, MDA-MB-435 breast cancer cell line and IMR-32 and SH-SY5Y neuroblastoma cell lines were cultured in Dulbecco's modified Eagles' medium supplemented with 10% fetal bovine serum, 100 units/ml penicillin, and 100 μg/ml streptomycin at 37°C with 5% CO_2. Human neuroblastoma SK-N-BE and SK-N-SH cell lines were cultured in RPMI medium supplemented with 10% fetal bovine serum, 100 units/ml penicillin, 100 μg/ml of streptomycin, 1% non-essential aminoacids and 2% HEPES buffer at 37°C with 5% CO_2.

Antibodies purification

The A59 polyclonal antibody was produced against a synthetic peptide designed on the basis of the primary aminoacidic sequence, containing the DHR motif (conserved in some PDEs as PDE5, PDE10A, PDE11A). The peptide sequence is: NH_2-ALEEAVAEVLDHRPIEPK-COOH (PRIMM).

The purification of rabbit IgG was performed on ProteinA Sepharose column (Amersham-Pharmacia) using 20 mM Na-phosphate pH 7.4 buffer. Column elution was performed with 100 mM glycine, pH 2.5. Buffer 1 M Tris-HCl, pH 9.0 was immediately added to each fraction (1/10 of the fraction volume) in order to avoid antibody denaturation. The fractions were further dialysed against 20 mM Na-phosphate pH 7.4. The antibody concentration was determined considering A_{280}: 1,33 O.D. corresponding to an IgG concentration of 1mg/ml.

Transient transfection and lysate preparation

Transient COS-7 cell co-transfection of prune-FLAG-pcDNA (previously prepared in Dr. Zollo's laboratory) was performed by LipofectAMINE (Life Technologies, Inc.) according to the manufacturer's instructions. COS-7 cells were seeded in 100-mm dishes at 75% confluence. Forty-eight hours after transfection, the cells were washed twice with ice-cold phosphate-buffered saline and scraped in ice-cold homogenization buffer (20 mM Tris-HCl, pH 7.4, 2 mM magnesium acetate, 0.3 mM calcium chloride, 1 mM dithiothreitol, 2 μg/ml leupeptin, 2 μg/ml aprotinin, 2 μg/ml pepstatin A, 0.2 mM PMSF). The cell suspension was disrupted with a sonicator for 10 s (twice, with a 30 s interval) and the homogenates were centrifuged at 10,000×g for 20 min. The resulting whole extracts were assayed for total protein concentration.

Quantification of protein

Protein concentrations were determined using Bradford's method (Bradford, 1976). Protein samples were mixed with Bradford reagent (Bio-Rad) and the absorbance at 595 nm was measured on a spectrophotometer. Protein absorbances were converted to mg/ml concentrations using a standard curve constructed by measuring the absorbance of a range of bovine serum albumin (BSA) concentrations.

SDS/PAGE and Western blot analysis

Protein samples were resuspended in disruption buffer (1×: 20 mM Tris-HCl pH 6.8, 2% SDS, 5% β-mercaptoethanol, 2.5% glycerol and 2.5% bromophenol blue) and denatured at 100°C for 5 min. Fifteen μg of protein were analyzed by SDS-

PAGE on a 10% (w/v) polyacrylamide gel, using a Bio-Rad mini gel equipment in accordance with the manufacturers instructions. New England Biolabs protein molecular weight markers were used (175-6.5 kDA range) to establish the apparent molecular weight of proteins resolved on SDS-polyacrilamide gels. All gels were run at 150V for an appropriate length of time, using SDS running buffer (25 mM Tris, 192 mM glycine, 0.1% SDS). Proteins were electroblotted onto a PVDF membrane (Immobilon-P, Millipore) using a wet blotter (Bio-Rad) at 100V for 1h in blotting buffer (25 mM Tris, 192 mM glycine, 20% methanol). The membranes were blocked against non-specific binding of antibodies with blocking buffer (PBS containing 5% skimmed milk powder and 0.1% Tween 20). H-PRUNE protein overexpressed was immuno-detected with polyclonal anti-A59 used at 1:500 dilution and anti-FLAG M2 (Sigma) used at 1:3000 dilution, incubated for 2 hrs at room temperature. After primary antibody incubation, membranes were washed (3×, 5 min) in a large excess of blocking buffer and then incubated with horseradish peroxidase-labeled anti-rabbit IgG and anti-mouse IgG for anti-A59 and anti-FLAG respectively, for 1h at room temperature. Membranes were again washed (3×, 5 min) in a large excess of blocking buffer and the visualization was performed by enhanced chemiluminescence system (Amersham-Pharmacia), according to the manufacturer's protocol.

In vitro site directed mutagenesis for h-prune mutants

In order to produce the h-prune mutant cDNAs, site-directed mutagenesis of the h-prune construct (prune-FLAGpcDNA, available in Dr. Zollo's laboratory) was performed using the QuikChange III Kit (Stratagene) according to the manufacturer instruction. The following oligonucleotides were used to generate h-prune mutants:

h-pruneΔ (DHRP126-129AAAA): 5' – GTA GCA GAG GTG CTA **GCC** **G CT** **GCA** **GCC** ATC GAG CCG AAA CAC – 3'.

D28A: 5' – GAA GCC TGT **GCT** TTG GAC TCC – 3'.

D106A: 5' – ACC CTC ATC CTT GTC **GCT** CAT CAT ATC TTA TCC – 3'.

D179A: 5' – GAA CCA TCA TCC TGG **CA**T GTG TCA ACA TGG – 3'.

Mutated nucleotides are noted in boldface type and the altered codon is underlined. All mutations were confirmed by DNA sequencing.

Constructs for expression studies

The cDNAs coding for nm23-H1, nm23H1-S120G, nm23H1-P96S, h-prune, and h-prune mutants: h-pruneΔ, D28A, D106A, D179A, D28A-D106A, D28A-D106A-D126A, D28A-Δ, 4DΔ (D28A-D106A-Δ-D179A) (for the mutants preparation see "*In vitro site directed mutagenesis for h-prune mutants*" paragraph) were subcloned into the *EcoRI/XhoI* digested pFastBac-Hta vector (Invitrogen). The full-length h-prune, nm23-H1, nm23H1-S120G and nm23H1-P96S cDNAs were *EcoRI/XhoI* digested and isolated from the pcDNA vectors, available in Dr. Zollo's laboratory.

Restriction enzyme digestion of DNA

DNA was digested in a final volume of 20 µl at 37°C for 1 h. All the restriction enzymes were New England Biolabs, and digestions were performed in appropriate buffers, supplied by the manufacturer with the enzyme. All digestions were analysed by agarose gel electrophoresis.

Agarose gel electrophoresis

Agarose gels (1% w/v in TAE; 40 mM Tris-Acetate pH 7.5, 2 mM EDTA) were prepared and supplemented with ethidium bromide (1μg /ml). The percentage of the agarose in gels was determined depending on the size of the DNA fragments to be solved. Gels were generally run at 120V in 1× TAE buffer, and DNA was visualized on a UV transilluminator.

Isolation of DNA from agarose gel

Following agarose gel electrophoresis, DNA gel slices were excised under UV light. DNA was extracted from these gel slices using QiaexII Gel Extraction Kit (QIAGEN) following the protocol supplied by the manufacturer. Purified DNA was eluted from the resin using 20 μl dH_20.

DNA sequence analysis

For DNA sequence analysis, plasmids or PCR were processed by the DNA sequencing core at TIGEM.

Quantification of plasmidic DNA

DNA concentration was determined for 1:100 dilutions of stocks according to the following formula: absorbance of one A_{260} unit indicates a DNA concentration of approximately 50 μg/ml.

Ligation reaction

The ligation reactions were generally set up as follows:

X ng vector DNA : Y ng insert DNA = 1: 2

1 µl 10× ligation

0,5 µl T4 DNA Ligase (400U/µl) (New England Biolabs)

dH_20 to 10µl

Ligation was carried out 16°C over night; the whole reaction was used for transformation of chemical competent DH5α *E.coli* cells. The resulting clones were analysed by restriction digestion and sequencing.

Transformation of E.coli with plasmidic DNA

E.coli DH5α cells were prepared for transformation as follows: cells were grown to mid-log phase (A_{600}=0.6) in Luria Broth (LB: 1% bactotryptone, 1% NaCl and 0.5% Bacto-yeast extract) at 37°C with shaking. Cells were collected by centrifugation at 2000×g at 4°C, resuspended into 30 ml (for each 100 ml of culture) of RF1 and kept on ice for 90 min. This suspension was then centrifuged at 2000×g for 15 min. The resulting pellet was resuspended in 4 ml (for each 100 ml of culture) of ice cold RF2 and kept on ice for 30 min. At this point cells were aliquoted and stored at -80°C. For each transformation, DNA was added to 50 µl of competent cells and incubated on ice for 20 min; then, cells were subjected to heat shock at 42°C for 2 min and successively incubated on ice for 10 min. Cells were recovered in 1ml of LB and incubated for 40 min at 37°C, before plating on LB-agar containing appropriate antibiotics and incubation at 37°C overnight.

Solutions:

RF1 (V=250ml)	**RF2 (V=250ml):**
1.86g KCl	0.52g MOPS
2.47g $MnCl_2$ $4H_20$	0.187g KCl
0.74g CH_3COOK	2.75g $CaCl_2$ 2 H_20
0.367g $CaCl_2$ 2 H_20	37.5ml glycerol
37.5ml glycerol	pH 7.0 (with HCl)
pH 5.8 (with CH_3COOH)	

Isolation of plasmid DNA from E.coli

Large-scale (midi-preps) and mini-preps plasmidic DNA preparations were carried out using the QIAGEN MIDI and MINI prep kits, respectively. Both procedures are based on the alkaline lyses method (Sambrook et al., 1989), but use a support column to purify isolated plasmid DNA. Purified DNA was always checked by enzymatic digestion with appropriate enzymes.

Protein expression and purification in Baculovirus

Protein expression of H-PRUNE, H-PRUNE mutants (H-PRUNEΔ, D28A, D106A, D179A, D28A-D106A, D28A-D106A-D126A, D28A-Δ, 4DΔ), NM23-H1, NM23H1-S120G and NM23H1-P96S, was performed using Baculovirus Expression System (Invitrogen). Virus infection and purification conditions were set up in the

Dr. Zollo's laboratory and described in (Garzia et al., 2003). Histidine-tagged H-PRUNE and H-PRUNEΔ were further purified on a MonoQ HR 5/5 column (Amersham-Pharmacia) using 10 mM Tris-HCl pH 8.0 buffer. Column elution was performed with a linear gradient from 0 to 0.8 M NaCl, over 20 min and at a flow rate of 1 ml/min. The fractions were further dialysed against 10 mM Tris-HCl pH 8.0 buffer, and tested for activity. The purity of isolated proteins was measured by electrophoresis SDS page analysis.

Identification of the H-PRUNE phosphodiesterase activity

Phosphodiesterase (PDE) activity was measured by a cAMP/cGMP scintillation proximity assay (Amersham-Pharmacia). Samples were diluted as required and incubated at 30°C in 100 µl assay buffer (50 mM Tris-HCl pH 7.4, 8.3 mM $MgCl_2$, 1.7 mM EGTA) containing the desired concentrations of cAMP or cGMP as substrate (3:1 ratio unlabeled to ^{3}H-labeled). All reactions, including buffer-only blanks, were conducted in triplicate and allowed to proceed for an incubation time giving <25% substrate turnover (empirically determined). Reactions were terminated by adding 50 µl Yttrium silicate SPA beads (Amersham-Pharmacia). Enzyme activities were calculated for the amount of radiolabeled product detected according to the manufacturer protocol. We performed the assay on H-PRUNE, H-PRUNEΔ mutant and H-PRUNE pre-incubated with the A59 polyclonal antibody. As positive control we used the PDE2 (Sigma). In particular, for H-PRUNE and H-PRUNE mutants PDE activity, 200 ng of purified enzymes were incubated for 10 min at 30 °C.

Lineweaver-Burk plots with K_m and V_{max} values were determined by measuring hydrolysis with a range of substrate concentrations (0.05-10.0 µM) and a

fixed amount of diluted enzyme over a time course of 5-40 min. Initial rates were calculated at each substrate concentration and plotted against substrate concentration, from which the kinetic parameters were determined.

Characterization of the H-PRUNE phosphodiesterase activity

To study the influence of different buffers on H-PRUNE PDE activity we modified PDE assays, using 50 mM Tris-HCl pH 7.4 or 50 mM HEPES buffer pH 7.5 with increasing concentrations (0, 1, 2, 4, 8, 16 and 32 mM) of $MgCl_2$. To study the ion influence we performed the PDE assays in 50 mM HEPES buffer pH 7.5 (in order to avoid oxido-reduction reactions) at increasing concentrations (1, 2, 4, 8, 16, 32 and 64 mM) of $MgCl_2$ or $MnCl_2$ salt. As a negative control, we used H-PRUNEΔ in the same conditions used for H-PRUNE. H-PRUNE activity in the absence of ions was tested after extensive dialysis of the protein against 50 mM Tris-HCl pH 7.4, 1.7 mM EGTA or 50 HEPES buffer pH 7.5, 1.7 mM EGTA.

The influence of NM23 (NDPK) activity on H-PRUNE PDE activity was investigated performing the assays with a pre-incubation of purified H-PRUNE with NM23s (yield of purification 70%, -H1, -H1-S120G or -H1-P96S). We tested the possible influence of NM23-H1 on H-PRUNEΔ pre-incubating the mutant purified protein with NM23-H1 and performing the PDE assay.

For the inhibitor studies, eight different potential inhibitors were tested: cilostamide, dipyridamole, 3-isobutyl-1-methylxanthine (IBMX), milrinone, rolipram, vinpocetine, sulindac and zaprinast (Sigma). A low concentration of cAMP (0.01 μM) was employed in order to approximate the IC_{50} to the K_i. All inhibitor studies were carried out in triplicates and were repeated three times.

Immunohistochemical analysis in sarcomas

All immunohistochemical analyses were done on paraffin sections from individual samples or the tissue array. Thirty cases comprising leiomyosarcomas, liposarcomas, malignant fibrous histiocytomas, malignant Schwannomas (malignant peripheral nerve Sheath tumour), and well-differentiated liposarcomas were analyzed. Also, six mammary carcinomas were analysed by immunohistochemical analysis.

The ABC procedure was used for immunohistochemistry (VECTASTAIN from Vector, Vector Laboratories, Inc). Colorimetric reaction was performed by using DAB (Vector, Vector Laboratories, Inc). Microwave pre-treatment was used for NM23-H1 detection for 15' at 90°C in 10 mM NaCitrate pH 6. The monoclonal antibody anti-NDP kinase nm23-H1, clone NM301 (Santa Cruz, USA) was used at 1:25 dilution; the prune A59 polyclonal antibody was used at 1:300 dilution. The primary antibody was omitted for negative controls. Positive controls included sections from tissues known to be positive. The controls gave satisfactory results.

Evaluation of results

Tumours were considered positive if at least 10% of the tumour cells were stained. Signal intensity was grouped as follows: negative (0, expression in <10% of the cells), weakly positive (1, expression in 10-30% of the cells), moderately positive (2, expression in 30-50% of the cells) and strong (3, expression in >50% of the cells).

Transient transfection in NIH3T3 cells

1×10^6 NIH3T3 cells were transfected by Lipofectamine reagent (Gibco-BRL) with 10 μg of pcDNA vector containing h-prune cDNA-FLAG gene under a CMV promoter. Forty-eight hours after transfection, cells were plated for proliferation assay.

pBABE vector modification

pBABE puro-PC3 vector was modified to include a FLAG epitope at the carboxy-terminal region of the protein and an SP6 promoter and primer site at the 3' terminus in the poly-linker sequence at the *EcoRI* site (modification performed in Dr. Zollo's laboratory). The vector was used to subclone, into the *EcoRI/XhoI* sites, the entire h-prune full-length cDNA, digested from the HA-prune-pcDNA.

The pBABE-pruneFLAG construct was further modified in order to include a His-tag at the NH_2-terminal region. The His-tag was amplified from the pFastBac-Hta vector (Invitrogen) by using the Polymerase Chain Reaction (PCR). The following oligonucleotides were used to amplify the His-tag with *BamHI* and *EcoRI* ends:

His Forward: 5'–CCG GGA TCC ACC ATG TCG TAC TAC–3'

His Reverse: 5'–CGC GAA TTC GGC GCC CTG AAA ATA CAG–3'

We used *Pfu* Polymerase as follows:

40 ng DNA template

5 μl Pfu buffer

20 pmol forward primer

20 pmol reverse primer

1 µl Pfu polymerase (3U/µl)

0.2 mM of each dNTP

dH_20 to 50µl

The PCR reaction was performed with the following cycling parameters:

1 cycle: 1 min at 95°C

20 cycles: 30 sec at 95°C

30 sec at the annealing temperature

30 sec at 72°C (1min per each Kb of DNA to amplify)

1 cycle: 10 min at 72°C.

The resulting purified PCR product was analysed by agarose gel electrophoresis, and extracted from the gel using Qiaquick columns (QIAGEN), according to the manufacturer's protocol. The purified DNA was then digested with *BamHI* and *EcoRI* restriction enzymes and the fragment was subcloned in frame into the *BamHI/EcoRI* digested pBABE-pruneFLAG eukaryotic vector, in order to obtain the pBABE-HispruneFLAG vector (pBABE-h-prune).

H-prune retrovirus production

The pBABE-h-prune vector was used in transient transfection of BOSC 23 ecotropic retroviruses cells as described (Pear et al., 1993). High titer retrovirus supernatant was collected and used to infect NIH3T3 cells lines. After 4 days on puromycin (2 mg/ml) selection, the cells were tested by a cellular proliferation assay.

Cellular proliferation assay

To test cellular proliferation we used the viability assay `MTS protocol (Cell-Titer 96TM AQueous proliferation assay-Promega), which is based on the cellular conversion of a tetrazolium salt into a formazan product. The assay measures dehydrogenase enzyme activity found in metabolic active cells. Cells, both transfecetd and infected, were plated in a 96 well plate and measured by MTS protocol (48, 72 and 96 h later). The cell concentrations were ranging from 2.5, 5 and 10×10^3 cells per well. A colorimetric reaction was performed after incubation of the cells for 2 h at 37°C measuring the absorbance (O.D.) at 490 nm using a Packard 96-well reader spectrophotometer.

Immunofluorescence analysis on neuroblastoma cell lines

Neuroblastoma SH-SY5Y, IMR-32, SK-N-BE and SK-N-SH cell lines were attached to slides (Lab-Tek II Chamber Slide, Nalge Nunc International). Twenty-four h after coating, the cells were washed twice with ice-cold phosphate-buffered saline (PBS) and treated by immunofluorescence analyses following standard techniques. Fixed cells were incubated for 3 h at room temperature with primary antibody diluted (1:100) in PBS/porcine serum. Slides were then washed three times in PBS and incubated in PBS/porcine serum containing directly conjugated secondary antibodies (1/100). Secondary antibodies were FITC-conjugated goat anti-mouse IgG and Texas red-conjugated pig anti-rabbit IgG. After labelling, slides were washed three times in PBS and mounted in 10% glycerol. For immunostaining, the following antibodies were used: rabbit polyclonal anti-h-prune (A59), monoclonal

antibody anti-NDP kinase nm23-H1, clone NM301 (Santa Cruz, USA) and monoclonal anti-human nm23-H2, clone H2-206 (Seikagaku Corporation). We performed immunofluorescence analysis on transiently trasfected COS-7 cells using anti-FLAG M2 (Sigma) or anti-HA clone12CA5 (Roche) antibodies. Nuclei were counterstained with 4',6-diamidino-2-phenyl-indole (DAPI).

In vitro site directed mutagenesis for nm23-H2 mutants

To produce the human nm23-H2, -H2-H118F, -H2-N69H, -H2-S122P mutants, site directed mutagenesis of nm23-H2 construct (HA-nm23-H2pcDNA available in Dr. Zollo's laboratory) was performed using QuikChange III Kit (Stratagene) according to the manufacturer's directions. The following oligonucleotides were used to generate the asparagine to histidine mutant (N69H): 5'–GGG CTG GTG AAG TAC ATG **CAC** TCA GGG CCG GTT GTG–3'. To create the histidine to phenylalanine (H118F) mutant we used the oligonucleotide 5'–CAG GTT GGC AGG AAC ATC ATT **TTT** GGC AGT GAT TCA GTA AAA AG–3' and for the serine to proline (S122P) mutant we used the oligonucleotide: 5'–GGC AGT GAT **CCA** GTA AAA AGT GC–3'. Mutated nucleotides are noted in boldface type, and the altered codon is underlined. All mutations were confirmed by DNA sequencing.

Co-immunoprecipitation and immunoblotting

The co-immunoprecipitation assays were performed on both SH-SY5Y neuroblastoma cells and transiently transfected COS-7 cells. Transient COS-7 cells were co-transfected with prune-FLAG-pcDNA and HA-nm23-pcDNAs by

LipofectAMINE (Life Technologies, Inc.) according to the manufacturer's instructions. The resulting whole extracts of both SH-SY5Y and transiently transfected COS-7 cells (see *"Transient transfection and lysate preparation"* paragraph for lysate preparation) were assayed for total protein concentration. Each lysate of SH-SY5Y neuroblastoma cells was divided into two aliquots and incubated with rabbit polyclonal anti-h-prune (A59) and monoclonal anti-human nm23-H2, clone H2-206 (Seikagaku Corporation) overnight at 4°C. Each lysate of transiently transfected COS-7 cells was divided into two aliquots and incubated with anti-FLAG M2 (Sigma) or with anti-HA clone12CA5 (Roche) overnight at 4°C. Twenty μg of Protein-A beads (Amersham-Pharmacia) were added, and the mixtures were incubated for 1 h at 4 °C. The immunoprecipitates were washed three times in extraction buffer and the pellets were resuspended in electrophoresis sample buffer. Samples were boiled for 5 min and proteins were analyzed by SDS-PAGE on a 10% (w/v) or 12.5% (w/v) polyacrylamide gel. Proteins were electroblotted onto a PVDF membrane (Immobilon-P, Millipore). For the SH-SY5Y neuroblastoma cells, H-PRUNE and NM23-H2 proteins were immuno-detected with rabbit polyclonal anti-h-prune (A59) and monoclonal anti-human nm23-H2, clone H2-206 (Seikagaku Corporation), respectively. For the transiently transfected COS-7 cells, NM23 and H-PRUNE proteins were immuno-detected with monoclonal anti-HA and anti-FLAG antibodies, respectively. After incubation with horseradish peroxidase-labeled anti-mouse IgG, visualization was performed by enhanced chemiluminescence (Amersham-Pharmacia).

Stable clone analysis in neuroblastoma SH-SY5Y cell line

The neuroblastoma SH-SY5Y cell line was transfected with the pBABE-h-prune expression vector. The transfections were performed using LipofectAMINE (Invitrogen), according to the manufacturer instructions. Transfectants were selected in Dulbecco's modified Eagles' medium (DMEM) containing 10% fetal bovine serum, 100 Units/ml penicillin, 100 μg/ml streptomycin and 2 μg/ml puromycin (Sigma). For the bulk transfected lines, plates containing forty puromycin-resistant colonies were trypsinized, and cell lines were established. Two pBABE-h-prune-SH-SY5Y puromycin-resistant clones (SH-5YSY-prune #2 and #3) were isolated and characterized both by western blot analyses.

For western blot analysis, 15 μg of protein lysate in sample buffer were analyzed by SDS-PAGE on 10% (w/v) or 12.5% (w/v) polyacrylamide gels and were electroblotted onto a PVDF membrane (Immobilon-P, Millipore). The lysates were immuno-detected with the A59 polyclonal antibody for H-PRUNE, with the nm23-H1 antibody (clone NM301; Santa Cruz, USA) for NM23-H1 and with the monoclonal anti-human nm23-H2, clone H2-206 (Seikagaku Corporation), as described in "*SDS/PAGE and Western blot analysis*" paragraph. For normalization the lysates were immuno-detected with the polyclonal anti-histone H3 for histone H3 used at 1:1000 dilution (Upstate Biotechnology).

Immunofluorescence analysis on neuroblastoma stable clones

An immunofluorescence analysis was performed on the SH-5YSY-prune #2 and #3 stable clones following the protocol reported in "*Immunofluorescence analysis on neuroblastoma cell lines*" paragraph. For immunostaining, the following

antibodies diluted (1:100) were used: rabbit polyclonal anti-prune (A59), monoclonal anti-NDP kinase nm23-H1 antibody, clone NM301 (Santa Cruz, USA), monoclonal anti-human nm23-H2, clone H2-206 (Seikagaku Corporation) and the monoclonal Penta-His antibody against the His-tag (QIAGEN).

Expression analysis in neuroblastoma cohorts

An immunohistochemical analysis of H-PRUNE, NM23-H1 and NM23-H2 in 47 cases of neuroblastoma (4 from San Raffaele Scientific Institute, 14 from Bari, 2 from Children Hospital Vittore Buzzi and the remaining from Associazione Italiana lotta al Neuroblastoma databank) was performed using the following antibodies: the rabbit polyclonal anti-prune (A59) used at 1:100 dilution, the monoclonal antibody anti-NDP kinase nm23-H1, clone NM301 (Santa Cruz, USA) at 1:25 dilution and the monoclonal anti-human nm23-H2, clone H2-206 (Seikagaku Corporation) at 1:150 dilution. The ABC procedure was performed as described as in "*Immunohistochemical analysis in sarcomas*" paragraph.

Chromatin immunoprecipitation of h-prune, nm23-H2, and nm23-H1 promoter sequences

The chromatin immunoprecipitation assay (ChIP) was performed on SH-SY5Y neuroblastoma cell lines. Cells, plated 7-9x10^5 in 100mm Petri dish, were cultured in 8ml DMEM supplemented with 10% FBS. The experiment was divided in different steps as described below.

CROSS-LINKING: Cells were fixed by adding 800µl (1/10vol) of cross-linking solution (11% formaldehyde, 0.1 M NaCl, 1 mM Na-EDTA pH 8, 0.5 mM Na-

EGTA pH 8, 50 mM Hepes pH 8), and by leaving cells in the incubator for an additional 20 min. Cross-linking reaction was stopped by addition of 10ml of quenching solution (0.125 M Glycine in Phosphate-Buffered Saline (PBS)) and 2-3 minutes incubation at room temperature. Plates were put on ice and washed once with ice-cold 0.5 mM PMSF in PBS. All of the passages reported below were performed on ice. One ml buffer A (0.25% Triton X-100, 10 mM Na-EDTA pH 8, 0.5 mM Na-EGTA pH 8, 10 mM Tris-HCl pH 8, 0.5 mM PMSF, 10 μg/ml aprotinin, 10 μg/ml leupeptin, 5 mg/ml pepstatin, 0.1 mM sodium orthovanadate, 1 mM tetra-sodium pyrophosphate, 1 mM NaF) was added, cells were scraped and collected in final 10 ml buffer A/dish in a 15 ml tube. After 10 min incubation at 4°C on a rotating wheel, cells were centrifuged for 5 min at 1000×g, and the pellet was resuspended in 10ml of buffer B (0.2 M NaCl, 10 mM Na-EDTA pH 8, 0.5 mM Na-EGTA pH 8, 10 mM Tris-HCl pH 8, 0.5 mM PMSF, 10 μg/ml aprotinin, 10 μg/ml leupeptin, 5 mg/ml pepstatin, 0.1 mM sodium orthovanadate, 1 mM tetra-sodium pyrophosphate, 1 mM NaF). Incubation and centrifugation steps were then repeated, and the pellet was resuspended in 440 μl of sonication buffer (0.2 M NaCl, 10 mM Na-EDTA pH 8, 0.5 mM Na-EGTA pH 8, 10 mM Tris-Cl pH 8, 0.5 mM PMSF, 10 μg/ml aprotinin, 10 μg/ml leupeptin, 5 mg/ml pepstatin, 1 mM sodium orthovanadate, 10 mM tetra-Sodium pyrophosphate, 10 mM NaF). Samples were sonicated for 3x30 sec, yielding genomic DNA fragments with a bulk size of 500-2000 base pairs, and the sonication buffer was adjusted to a RIPA buffer (IP buffer) by adding to the sonication buffer 1% Triton X-100, 0.1% SDS, and 0.1% Sodium Deoxycholate (DOC) final concentration. Samples were incubated for 10 min on a rotating wheel at 4°C and then centrifuged for 10 min at 10000×g. Fifty μl/sample

were kept to recover total DNA input, and the lysates were subjected to immunoprecipitation.

PRE-CLEARING: Twenty µg of Protein A-sepharose (Amersham-Pharmacia) in PBS was incubated in IP buffer without anti-proteases and anti-phosphatases, with 1 mg/ml BSA and 0.25 mg/ml sheared Salmon sperm final concentration, at 4°C over night on a wheel. Eighty µl of blocked protein A beads were then added to the lysates and incubated for 30 min-1hr at 4°C on a wheel and centrifuged for 2 min at 5000×g at 4°C.

IMMUNOPRECIPITATION: Supernatants were transferred to new tubes and incubated over night, either with 2 µg of antibody (anti-human MYCN clone 2 - Santa Cruz - for h-prune promoter; anti-h-prune A59 for *NM23-H2* promoter; anti-human nm23-H2 clone H2-206 - Seikagaku Corporation - for *NM23-H1* promoter) or without antibody, at 4°C on a wheel. Immune complexes were recovered by adding 80 µl of blocked protein A-beads and incubated 1h at 4°C on a wheel. Beads were washed for 5 times in RIPA buffer, once with LiCl buffer (0.25 M LiCl, 0.5% NP-40, 0.5% DOC, 10 mM Tris-HCl pH 8, 1 mM Na-EDTA pH 8, 0.1 mM PMSF, 10 µg/ml aprotinin, 10 µg/ml leupeptin, 5 µg/ml pepstatin, 0.1 mM sodium orthovanadate, 1 mM tetra-sodium pyrophosphate, 1 mM NaF) and twice with TE buffer. DNA-protein complexes were eluted by adding 250 µl of elution buffer (1% SDS, 0.1% $NaHCO_3$) and incubated for 15 min on a wheel at RT. After 1 min centrifugation at 5000×g at RT, supernatant was transferred to a new tube and elution was repeated.

REVERSAL of CROSS-LINKING: In order to revert cross-linking, NaCl 0.2 M final concentration was added to ChIP samples and DNA input, and incubated over night at 65°C. Proteins were then digested by incubating for 1h at 45°C after adding 20

μM Tris-HCl pH 6.5 and 0.8 mg/ml proteinase K final concentration, and extracted once with phenol chloroform and once with chloroform. DNA was precipitated in 2.5 volumes ethanol 100%, 1/10 volume 3M Na-Acetate pH 4.8, and 20 μg glycogen, washed with ethanol 70%, centrifuged for 2 min at 10000×g and resuspended in TE buffer (10 mM Tris-HCl pH 8 and 1 mM Na-EDTA pH 8) 50μl for input DNA samples and 100μl for ChIP DNA.

PCR: For total chromatin immunoprecipitated both with anti-Nmyc (Santa Cruz, USA) and the monoclonal antibody anti-NDP kinase nm23-H1, clone NM301 (Santa Cruz, USA) as negative control, PCR reactions were performed using the following oligonucleotides:

E1- Forward: 5'- ACC TTA AAG GGG GTG C – 3'

E1- Reverse: 5' – CTC CAG TGC CCC CAG TAC T – 3'

E2- Forward: 5'– GTT GTG GCC ACT TCC GGA CT – 3'

E2- Reverse: 5' – TTT CTT CGT CCT GAT GAG AAC – 3'

For total chromatin immunoprecipitated both with anti-human prune A59 and the monoclonal antibody anti-NDP kinase nm23-H1, clone NM301 (Santa Cruz, USA) as negative control, PCR reactions were performed using the following oligonucleotides:

H2-A Forward: 5'- TCAGAGTCCTGAGGGGAAGCAAG – 3'

H2-A Reverse: 5' – GGAAAGTCTAGACCCTGTCATAGAGA – 3'

H2-B Forward: 5'– CACTGCAAGTAGGAAGTGTCTAC – 3'

H2-B Reverse: 5' – GCCTCCCCACCTACATTTCC – 3'

H2-C Forward: 5' – AAAACTCGACCGCACTTTAGTGC –3'

H2-C Reverse: 5' – CTTTGCTCAGCACCTCAAACG –3'

H2-D Forward: 5' – TCATCAAGGCAGGGCAGAGG – 3'

H2-D Reverse: 5' – CCGGCATTAACCTTGACTTGG – 3'

H2-E Forward: 5' – GGATAAGGACCGTGGGTGCAC – 3'

H2-E Reverse: 5' – CCTATGAGTTCAACTACGCACGT - 3'

H2-F Forward: 5'- ACTGAGAGGTGAGGAGTGGG – 3'

H2-F Reverse: 5' – GCGGCCGGAGAACAGTGT – 3'

H2-G Forward: 5' – GTCTCGATCTCTGCCTGGC – 3'

H2-G Reverse: 5' – GAGAGCAGAGAGCTGGTGCG – 3'

H2-H Forward: 5' – TGTGGTGGTCGCACCAGCTC – 3'

H2-H Reverse: 5' – GGGACCTGCGGGAAATC – 3'

H2-I Forward: 5' – GATTTCCCGCAGGTCCC – 3'

H2-I Reverse: 5' – CCCTCTGCGGAGCCCGAA – 3'

For total chromatin immunoprecipitated both with the anti-human nm23-H2, clone H2-206 (Seikagaku Corporations) and the anti-human prune A59 as negative control, PCR reactions were performed using the following oligonucleotides:

H1-A Forward: 5'- TTTCCAGCGTGCTGGGATTAC – 3'

H1-A Reverse: 5' – CAAAATGAATCATAGATTTAAATG – 3'

H1-B Forward: 5' – CCCCATAAGTGATTTATTG – 3'

H1-B Reverse: 5' – AACATTCCCACTGCTCTAAGG – 3'

H1-C Forward: 5' – TATTAGCATCTCACAACATAAG – 3'

H1-C Reverse: 5' – GCAAATTAATATGTAATAGATCGC – 3'

H1-D Forward: 5' – CCTTTTCTTCACAGCACTTAC – 3'

H1-D Reverse: 5' – GACTTTTCGCTCCCGCTTTGT – 3'

H1-E Forward: 5' – CTTGACAGGCTAGAAAAGG – 3'

H1-E Reverse: 5' – GGCGCTAGCTTTTTCAGACC – 3'

H1-F Forward: 5' – AAGAAAGCAAGCAGCTAACC – 3'

H1-F Reverse: 5' – GCACGCACGGAACGCTTC – 3'

For all the PCR reactions, we used *AmpliTaq* Polymerase (Perkin Elmer) as follows:

2 µl DNA immunoprecipitate or 2 µl of a 1:100 dilution of the total sample

5 µl Taq buffer

20 pmol forward primer

20 pmol reverse primer

1 µl *Taq* polymerase (2.5U/µl)

2.5 mM $MgCl_2$

0.2 mM of each dNTP

dH_20 to 50µl

The PCR reactions were performed with the following cycling parameters:

1 cycle	10 min at 95°C
20 cycles	30 sec at 95°C
	30 sec at the annealing temperature
	30 sec at 72°C (1min per each Kb of DNA to amplify)
1 cycle	10 min at 72°C

The resulting purified PCR products were analysed on agarose gels.

pBABE constructs for expression studies

H-pruneΔ and h-prune4DΔ cDNAs were subcloned into the *EcoRI/XhoI* digested pBABE-His-FLAG vector, in order to obtain pBABE-pruneΔ and pBABE-h-prune4DΔ constructs.

The human PDE5A cDNA was PCR amplified from PDE5A-pSVL construct (a gift from Dr. Keni Omori), adding *EcoRI* and *XhoI* restriction ends, in order to clone it into the same His-tagged vector. The following oligonucleotides were used:

PDE5 Forward: 5'–ATA GAA TTC ATG GAG CGG GCC GGC CCC AGC–3'

PDE5 Reverse: 5'–ATA CTC GAG GTT CCG CTT GGC CTG GCC GCT–3'

For the PCR reaction, we used *Pfu* Polymerase as follows:

40 ng DNA template

5 µl Pfu buffer

20 pmol forward primer

20 pmol reverse primer

1 µl Pfu polymerase (3U/µl)

0.2 mM of each dNTP

dH_20 to 50µl

The PCR reaction was performed with the following cycling parameters:

1 cycle	1 min at 95°C
30 cycles	30 sec at 95°C
	30 sec at the annealing temperature
	2 min 30 sec at 72°C (1min per each Kb of DNA to amplify)
1 cycle	10 min at 72°C

The resulting purified PCR product was cloned into the pBABE-His-FLAG vector in order to obtain the pBABE-His-PDE5-FLAG construct (pBABE-PDE5A).

Stable clones analysis in MDA-MB-435 breast cancer cell line

The MDA-C100, MDA-H1-177, MDA-nm23H1-S120G and MDA-nm23H1-P96S clones (produced by Dr. P.S. Steeg) were transfected with the pBABE-h-prune expression vector. The MDA-C100 clone was transfected with the pBABE-h-pruneΔ, pBABE-h-prune4DΔ, and pBABE-PDE5A expression vector. The transfections were performed using LipofectAMINE (Invitrogen), according to the manufacturer instructions. Transfectants were selected in Dulbecco's modified Eagles' medium (DMEM) containing 10% fetal bovine serum, 100 Units/ml penicillin, 100 μg/ml streptomycin and 2 μg/ml puromycin (Sigma). For the bulk transfected lines, plates containing one hundred puromycin-resistant colonies were trypsinized, and cell lines were established. Several pBABE-h-prune, pBABE-h-pruneΔ, pBABE-h-prune4DΔ and pBABE-PDE5A puromycin-resistant clones were isolated for every MDA clone transfected and characterized by western blot analyses. For western blot analysis, 15 μg of protein lysate in sample buffer were analyzed by SDS-PAGE on 10% (w/v) or 12.5% (w/v) polyacrylamide gels and were electroblotted onto a PVDF membrane (Immobilon-P, Millipore). The lysates were immuno-detected with the specific h-prune A59 polyclonal antibody for H-PRUNE, with the nm23-H1 antibody (clone NM301, Santa Cruz, USA) for NM23-H1 and with the Penta-His antibody against a His-tag (QIAGEN) for PDE5A. After incubation with horseradish peroxidase-labeled anti-IgG, visualization was performed by enhanced chemiluminescence (Amersham-Pharmacia). Eleven cell lines, MDA-prune (clone #3 and #4), MDA-H1-177-prune (clone #7 and #8), MDA-nm23H1-S120G-prune (clone #2 and #3), MDA-nm23H1-P96S-prune (clone #4 and

#5) and MDA-pruneΔ (clone #11), MDA-prune4DΔ (clone #19), MDA-PDE5A (clone #14), were selected and proteins were normalized on Western blots.

In vitro cell motility assay

Stable MDA clones overexpressing h-prune, h-pruneΔ, h-prune4DΔ and human PDE5A were analyzed by motility assay, using the trans-well technology (6-well - Corning-Costar). In the lower wells, we incubated 2.5 ml of "motility" medium (DMEM containing 0.1% BSA, 100 Units/ml penicillin, 100 μg/ml streptomycin, 5 mM HEPES buffer) and the diluted chemo-attractant; in the upper wells, we incubated 1×10^5 cells in 1.5 ml of motility medium. The trans-wells were incubated for 3 h at 37 °C with 5% CO_2. After the attraction procedure, the cells were fixed and stained with Hematoxylin solution Gill n°1 following manufacturer protocol (Corning-Costar); the cells were finally counted under the microscope. The control MDA-C100 breast cancer cell line was used in the cell motility assay, as described (Leone et al., 1993a, Leone et al., 1993b), with the cell line overexpressing NM23-H1 (MDA-H1-177), which shows an inhibition of metastasis processes *in vivo*. Cellular motility was determined using the trans-well technology (6-well - Corning-Costar) using 0.25%, 0.5% FCS, and 2.5, 5.0 ng/ml fibronectin (Sigma) final concentrations as chemo-attractants. The *in vitro* h-prune inhibition motility assay was performed as follow. The MDA-prune (clone #3 and #4) and MDA-pruneΔ (clone #10 and #11) were incubated with dipyridamole (8 μM, a 10-fold higher concentration with respect to its IC_{50}) for 24 h to obtain the complete enzyme inactivation, and then the motility assay was repeated as described above.

cAMP content in MDA stable clones

cAMP levels were determined by an immunoassay (R&D systems). For the quantitative determination of cAMP in MDA-C100 and MDA-prune #3 and #4 stable clones, 0.1 M HCl was added to a pellet of 1×10^5 cells to prepare the lysates. Each experiment was repeated three times in duplicate.

Statistical analyses

All the assays including PDE activity and cellular motility were validated using the unpaired T-test method using the tool available at http://www.graphpad.com/quickcalcs/index.cfm.

Immunohistochemical analysis on breast cancer samples

Multiple Tissue Array (MTA) breast were immunodetected with the specific A59 h-prune polyclonal antibody at 1:300 dilution and the nm23-H1 antibody clone K73 at 1:25 dilution (specific for the -H1 and H2 isoforms; Apotech Corporation, CH). The ABC procedure was performed as described as in "*Immunohistochemical analysis in sarcomas*" paragraph. Intensity of immunohistochemical staining was used to classify the tumor samples as positive if present in at least 20% of cells analyzed under the microscope (strong +++, moderate ++, diffusely weak staining + or negative 0 (absent or focally weak staining) for H-PRUNE and NM23-H1 proteins expression.

Tumour case collection and TNM selection

Tumour cases have been collected by AUSL1 of Sassari (Italy), including patients with a minimum of five years follow-up. The TNM system classification applied to this study and since described by Sobin et al. 1997 was used for describing the anatomical extent of disease and is based on the assessment of three components: T corresponds to the extent of the primary tumour (from T0 to T4), N corresponds to absence or presence and extent of regional lymph node metastasis (from N0 to N4), and M stands for the absence or presence of distant metastasis (M0 or M1). Our collection of fifty-nine tumour breast cases has been categorized as TxNxM1 positive.

Bioinformatic analysis of differentially expressed genes in breast cancer stable clones

A gene expression profiling was performed in Dr. Zollo's laboratory (D'Angelo et al., 2004). We selected the genes differentially expressed (P value ≤ 0.05) in MDA-H1-177-prune #8 clone with respect to MDA-H1-177 clone. To study the possible pathways altered upon H-PRUNE overexpression, we performed a literature search using PubMed annotation (http://www.ncbi.nlm.nih.gov/entrez/).

Construct for conditional Knock Out mouse model

In order to prepare the construct for conditional KO mouse model, we planned to isolate two *Prune* genomic regions (named Intron Arm and Right Arm), which are required to recombine with the entire *Prune* genomic region in order to insert a cassette into the region containing exon2-intron2. The removal of exon2 will

disrupt the *Prune* open reading frame, creating a truncated protein. The Intron Arm (5000bp) contains a fragment of intron 1. The Right Arm is a genomic region of 4350bp, containing exon3-intron3-exon4-intron4-exon5-intron5. The two arms will be cloned into the KO conditional vector, the pUC19FRT5, which is a pUC19 vector modified by Dr. Cobellis (at TIGEM). The pUC19FRT5 contains a cassette with the *hygromicine* gene to confer resistance and the *GreenFluorescent Protein (GFP)* as a reporter gene. At the ends of the cassette, two Frt sites (Frt5 at 5' and Frt1 at the 3' end) are present and necessary for recombination.

At the stage of the preparation of this PhD thesis work, we subloned the two arms into the pBLUESCRIPT SK(+). Hence, the RPCI-21 PAC library (YAC Screening Center, DIBIT, Milan) was screened in Dr. Zollo's laboratory and the PAC containing the *Prune* genomic region was then used as template in Polymerase Chain Reactions (PCRs), in order to amplify and isolate the two arms.

The following oligonucleotides were used to amplify the Intron Arm:

Armintron1F: 5'–CAT CTT GGA CAA TCT TTG GAG TCT–3'

Armintron1R: 5'–GGG AGA ACT GAT AAA CCA TCT CTG–3'

We used *Taq* Polymerase as follows:

400 ng DNA template

5 µl Taq buffer

50 pmol forward primer

50 pmol reverse primer

1.25 µl *Taq* polymerase (2.5U/µl)

3.0 mM $MgCl_2$

0.2 mM of each dNTP

dH_20 to 50µl

The PCR reaction was performed with the following cycling parameters:

1 cycle	10 min at 95°C
30 cycles	1 min at 95°C
	1 min at the annealing temperature (61°C)
	6 min at 72°C (1 min per each Kb of DNA to amplify)
1 cycle	10 min at 72°C

The resulting purified PCR product was analysed by agarose gel electrophoresis, and extracted from the gel using Qiaquick columns (QIAGEN), according to the manufacturer's protocol. The purified DNA was then phosphorylated with the T4 Polynucleotide Kinase (New England Biolabs) as follows:

10 µl Intron Arm

1 µl T4 Polynucleotide Kinase (2.5U/µl)

1mM ATP (final concentration)

5 µl T4 Polynucleotide Kinase buffer

dH_20 to 50µl

The reaction was incubated for 30 min at 37°C. Then, the DNA was extracted with phenol chloroform and precipitated in 2.5 volumes ethanol 100% with 1/10 volume 3M Na-Acetate pH 4.8. The DNA was resuspended in 10µl dH_20. The Intron Arm was therefore cloned into *SMA1* digested pBLUESCRIPT SK(+), which was previously incubated with the Alkaline Phosphatese, Calf intestinal enzyme (New England Biolabs) in order to remove the phosphate at the 5' end. Thus, we obtained the IntronArm pBLUESCRIPT SK(+) vector, which was confirmed by DNA sequencing.

The following oligonucleotides were used to amplify the Right Arm, adding *NotI* restriction ends:

RightarmF:

5'–ATG CGG CCG CAG TGG GTG TGT AAG TAT GTA GGA TGA–3'

RightarmR:

5'–ATG CGG CCG CTC TTG CAT TTT CCT AAG CCT TAT TAT–3'

For the PCR reaction, we used *Pfu* Polymerase as follows:

400 ng DNA template

5 µl Pfu buffer

50 pmol forward primer

50 pmol reverse primer

2 µl Pfu polymerase (3U/µl)

0.2 mM of each dNTP

dH_20 to 50µl

The PCR reaction was performed with the following cycling parameters:

1 cycle	1 min at 95°C
30 cycles	1 min at 95°C
	30 sec at the annealing temperature (60°C)
	10 min at 72°C (2 min per each Kb of DNA to amplify)
1 cycle	5 min at 72°C

The resulting purified PCR product was analysed by agarose gel electrophoresis, and extracted from the gel using Qiaquick columns (QIAGEN), according to the manufacturer's protocol. The purified DNA was then digested with *NotI* and sublconed into the *NotI* digested pBLUESCRIPT SK(+) in order to generate RightArmpBLUESCRIPT SK(+) vector, which was confirmed by DNA sequencing.

The scheme of the final pUC19FRT5 vector containing the two arms required for homologous recombination is represented below. Frt1 and Frt5 are the sites for the FLIP recombination; the red boxes indicate the *Prune* exons and the SA-Ires HyGFP/A+ indicate the cassette, which will be exchanged with genomic DNA in order to remove the exon 2.

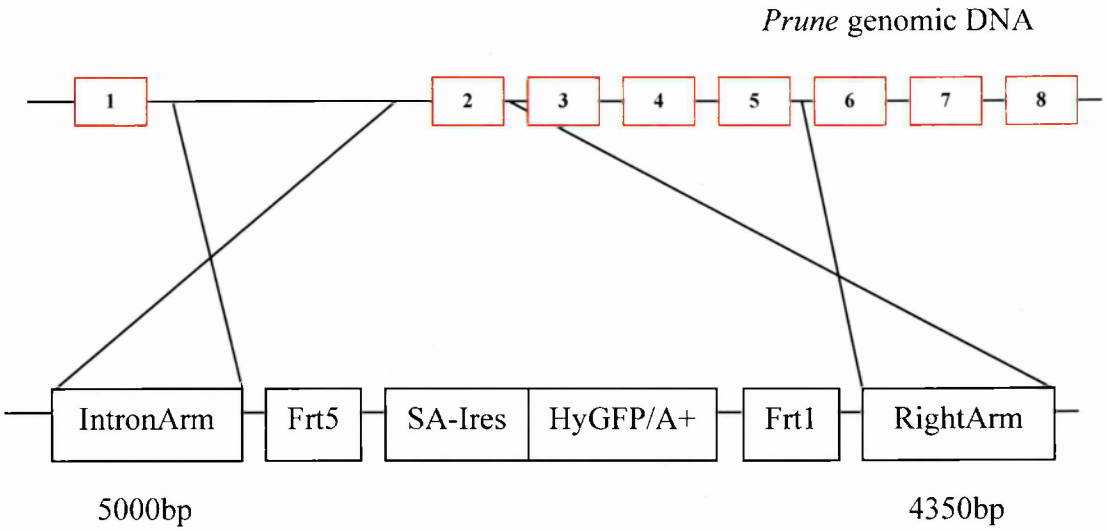

pUC19FRT5 vector

H-PRUNE biochemical characterization

Expression and purification of H-PRUNE protein

To test the specificity of h-prune A-59 polyclonal antibody, we performed transient transfection using a prune-FLAGpcDNA in COS-7 cells. The lysates, both transfected and untransfected (control), were analysed by western blot analysis using both anti-FLAG and A59 antibodies. The A59 polyclonal antibody reveals with high specificity the 60 kDa H-PRUNE protein (Figure 6A). To perform biochemical studies, we cloned and expressed H-PRUNE and H-PRUNEΔ, a mutation created in the motif 3 region (DHRP126-129AAAA) using the Baculovirus expression system (Figure 7A and B). His-tagged H-PRUNE and H-PRUNEΔ, were purified by affinity chromatography (Figure 9).

Identification of the H-PRUNE phosphodiesterase activity

To determine the ability of H-PRUNE to disrupt the phosphoester bonds in cyclic nucleotides (cAMP and cGMP) and to determine the specific substrate, we used the PDE scintillation proximity assay. H-PRUNE possesses significant PDE activity that is higher for cAMP than for cGMP as substrate, while H-PRUNEΔ shows a 40% reduction of this activity. In fact, the H-PRUNEΔ has a 60% of cAMP PDE activity with respect to the H-PRUNE (2.1 $pmol \times min^{-1} \times \mu g^{-1}$ versus 3.5 $pmol \times min^{-1} \times \mu g^{-1}$) indicating a reduction of 40% compared to the wild type protein. As positive control we used PDE2. In addition, we performed the assay on both H-PRUNE pre-incubated with the A59 specific polyclonal antibody and H-PRUNEΔ (Figure 6B). These results indicate that H-PRUNE protein shows PDE activity.

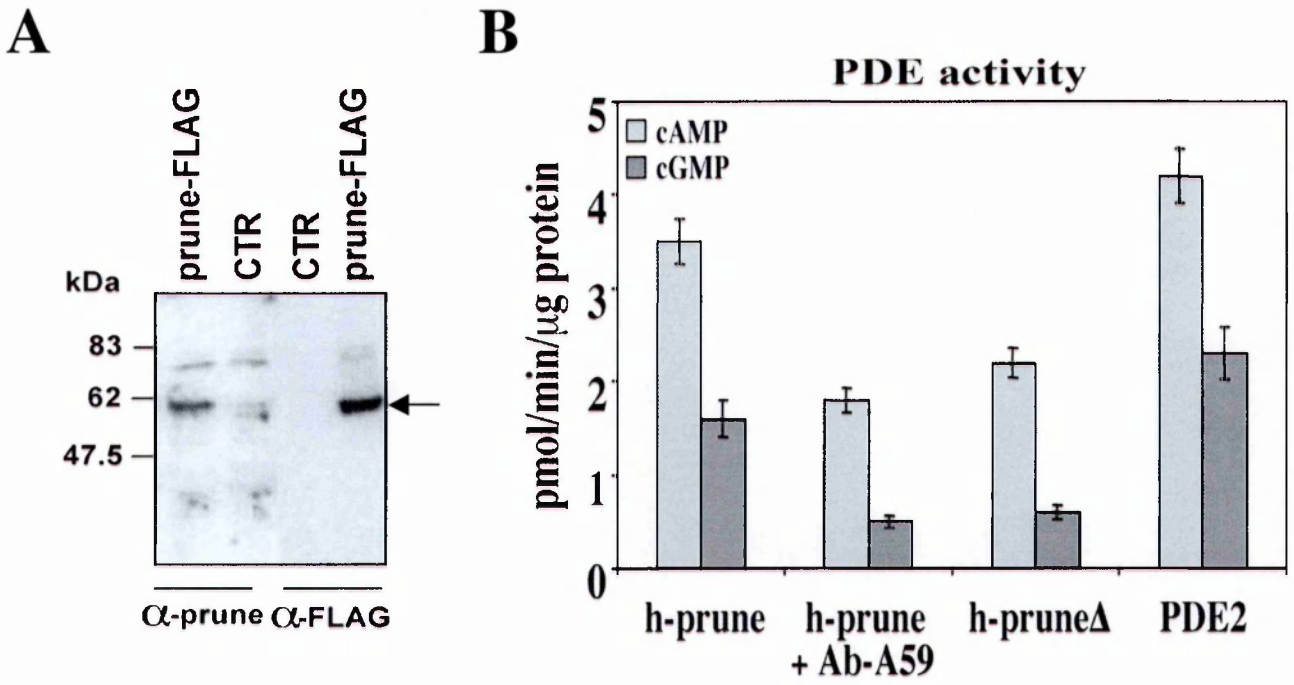

Figure 6. Western blot analysis of h-prune and identification of PDE activity.

A) Western blot analysis of crude protein extracts derived from transient transfected COS-7 cells with pcDNA vector containing h-prune cDNA-FLAG. Lanes 1 and 2 were revealed with the polyclonal anti-prune A59. Lanes 3 and 4 were revealed with the monoclonal anti-FLAG. An arrow shows the specific immuno-reactivity against 60kDa prune protein.

B) H-prune PDE activity for cAMP and cGMP as substrates. H-prune, h-prune pre-incubated with A59 specific antibody, and h-pruneΔ, a mutant protein in the motif III characteristic of DHH protein family were tested ($p<0.03$). Positive Control: purified PDE2 protein.

Characterization of the H-PRUNE phosphodiesterase activity

Mutational analysis

Homology modelling of H-PRUNE structure was performed by Dr. L. Aravind (in collaboration with Dr. Zollo) on the basis of the crystal structure of PPASE and RecJ proteins. The structural model (Figure 2), together with the sequence alignment of the DHH superfamily (Figure 1) allowed us to identify the aminoacids to mutagenesize in order to define the catalytic site. Thus, a mutation analysis at single and multiple sites affecting H-PRUNE PDE activity was conducted. We expressed the mutants using the Baculovirus expression system (Figure 7B, C and D; Figure 8) and purified them by affinity chromatography to homogeneity (with a 80% yield of purification, Figure 9 and Table 2). We tested the proteins for cAMP-PDE activity; all the aspartic acids of the DHH characteristic motifs were mutated alone and in combination (Figure 10A). We observed an 80% decrease in the H-PRUNE4DΔ (D28A, D106A, Δ, D179A) mutant (Figure 10B). In summary, D28, D126, H127, R128, P129 and D179 aminoacids were found essential for H-PRUNE PDE activity, thus indicating that most likely they are part of the catalytic site. Instead, D106A mutation in motif 2 did not influence H-PRUNE PDE activity.

H-PRUNE: K_m and V_{max}

To further characterize H-PRUNE activity, we purified to homogeneity the His-tagged H-PRUNE protein by another step of purification using an ion-exchange chromatography (Mono-Q column) with a high yield of purification (90%) (Table 2).

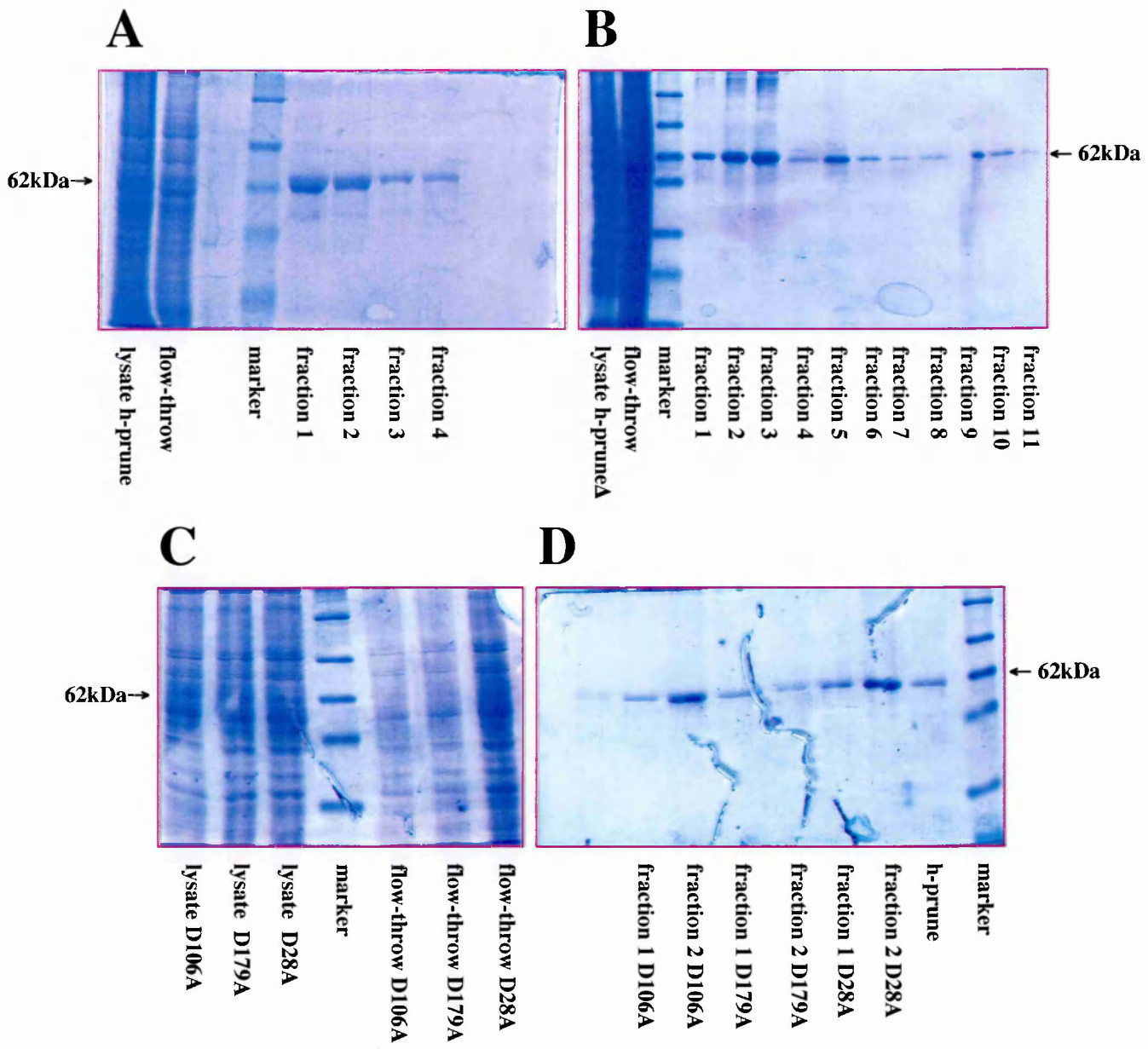

Figure 7. Purification by affinity chromatography (Ni-NTA resin) of h-prune and h-prune mutants. Coomassie staining of the purified h-prune and h-prune mutants. In panel A the lysate, flow-throw and the eluted fractions of the h-prune were loaded. In panel B the lysate, flow-throw and the eluted fractions of the h-pruneΔ mutant were loaded. In panel C the lysates and flow-throws of the D106A, D179A and D28A mutants were loaded. In panel D the eluted fractions (fractions 1 and 2) for the D106A, D179A and D28A mutants and the purified h-prune as positive control were loaded.

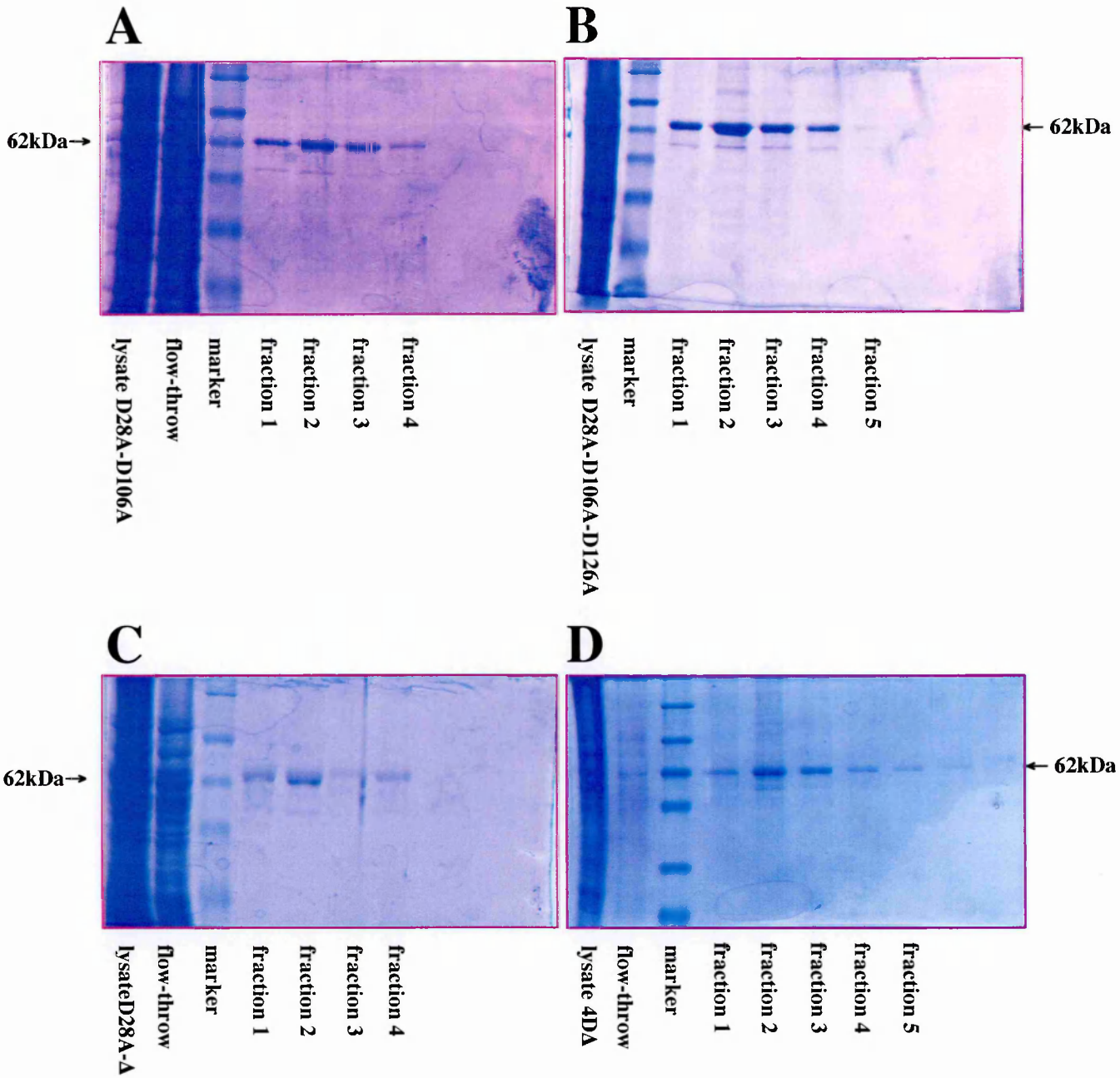

Figure 8. Purification by affinity chromatography (Ni-NTA resin) of h-prune mutants. Coomassie staining of the purified h-prune mutants. In panel A, C and D the lysate, flow-throw and the eluted fractions of the D28A-D106A, D28A-Δ and 4DΔ mutant were loaded respectively. In panel B the lysates and and eluted fractions of the D28A-D106A-D179A mutant were loaded.

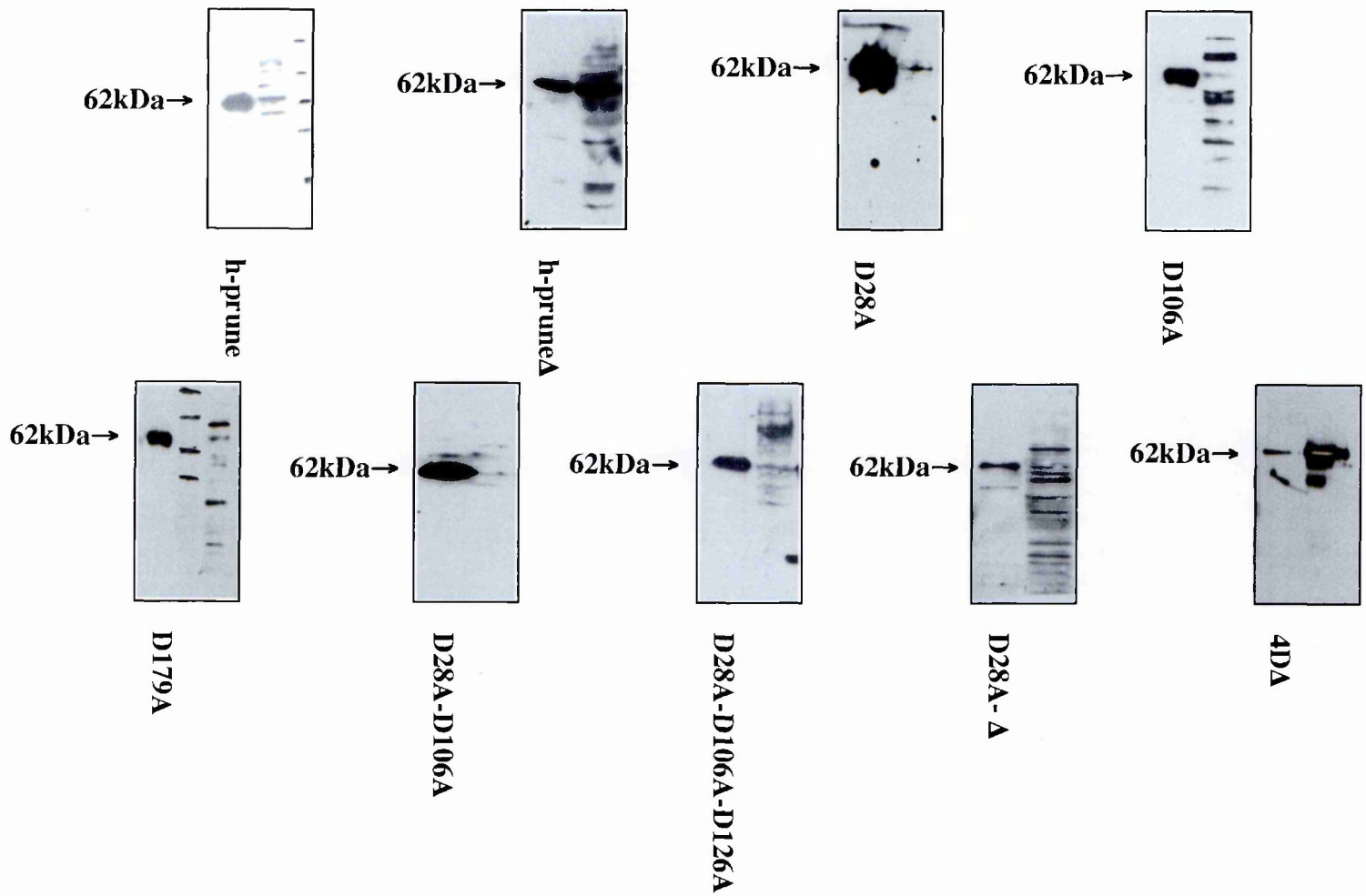

Figure 9. Western blot analyses for h-prune and h-prune mutants.

On the left lane of each panel is indicated the purified protein; on the right lane the lysate of Lepidottera cells overexpressing the corresponding protein. The proteins were revealed with the monoclonal anti-His (used at 1:100 dilution).

	$\frac{\text{specific activity of the fraction}}{\text{specific activity of the lysate}}$	Yield of purification
h-prune purified by affinity chromatography	$\frac{3.5\ \text{pmol}\times\text{min}^{-1}\times\mu\text{g}^{-1}}{4.4\ \text{pmol}\times\text{min}^{-1}\times\mu\text{g}^{-1}}$	80%
h-prune purified by ion-exchange chromatography	$\frac{3.2\ \text{pmol}\times\text{min}^{-1}\times\mu\text{g}^{-1}}{3.5\ \text{pmol}\times\text{min}^{-1}\times\mu\text{g}^{-1}}$	90%

Table 2. Table of purification for h-prune protein.
For h-prune two steps of purification were performed and the ratio between the specific activity of the purified fraction and the specific activity of the lysate loaded onto the column was calculated.

A

Mutated aminoacids

Δ { D126, H127, R128, P129 } — Motif 3

D28 — Motif 1

D106 — Motif 2

D179 — Motif 4

B

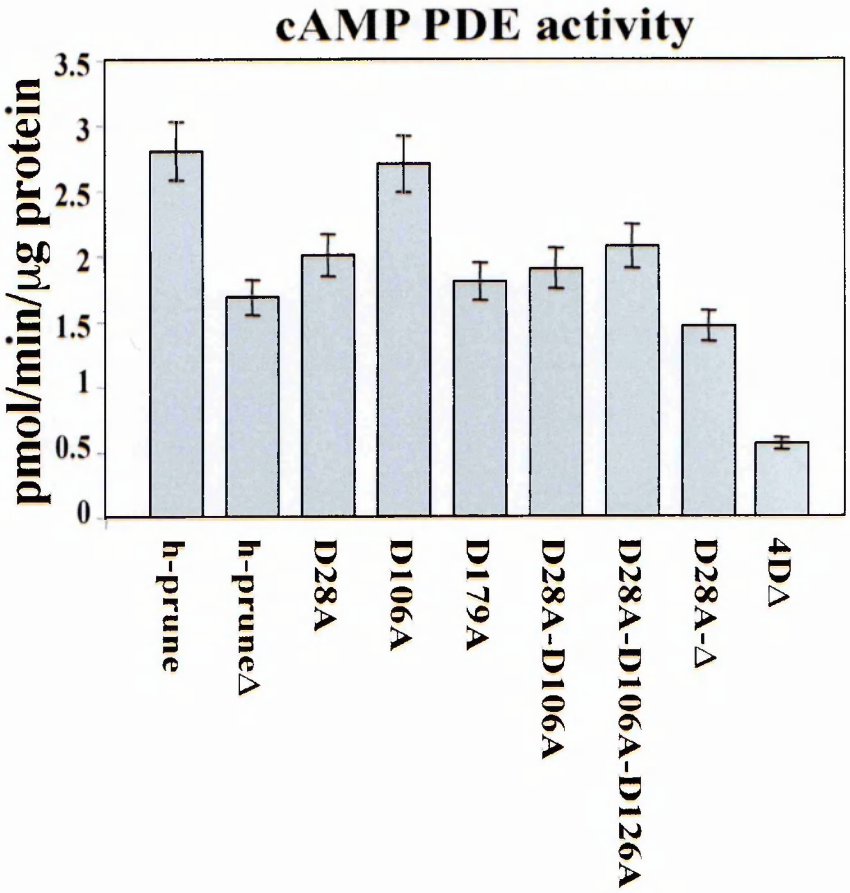

Figure 10. Mutational analyses in the potential catalytic site of h-prune protein.

A) List of the mutated aminoacids and their corresponding motif characteristic of the DHH family.

B) Single and multiple mutations in all the aminoacids of the DHH characteristic motifs and their cAMP-PDE activities are reported in the histogram (h-prune/mutant $p<0.03$).

The K_m and V_{max} values were determined by measuring nucleotides hydrolysis with a fixed amount of H-PRUNE purified enzyme in a range of substrate concentrations (0.05-10.0 μM) and taking those data points in the linear part of the reaction. Both cAMP and cGMP are substrates for H-PRUNE, with K_m values of 0.9±0.03 μM and 2.3±0.11 μM, respectively. The maximal rates of turnover of substrate (V_{max}) were found to be 12.8±0.5 $pmol \times min^{-1} \times \mu g^{-1}$ and 16.1±0.8 $pmol \times min^{-1} \times \mu g^{-1}$ purified enzyme for cAMP and cGMP, respectively (Figure 11A and B). The affinity of H-PRUNE is 2.5-fold higher for cAMP as compared with cGMP and the maximal rate of turnover substrate is approximately equal for both these cyclic nucleotides. Unlike other PDEs with dual-substrate specificity, H-PRUNE exhibits very similar K_m and V_{max} suggesting that the protein could define a new class of PDEs, which could exhibit also other more specific putative activities (i.e. pyrophospatase and/or exonulcease).

Thus, we present evidence of a cyclic nucleotide phosphodiesterase activity for a protein of the DHH superfamily.

Buffer influence and ion dependence of H-PRUNE PDE activity

To study the buffer influence on H-PRUNE PDE activity, we tested Tris-HCl and HEPES buffers in the presence of the same salt and we observed a higher PDE activity in the presence of Tris-HCl buffer (Figure 12A). Considering the ion dependence of DHH proteins, we investigated the Mg^{2+} and Mn^{2+} ion dependency of H-PRUNE in the PDE cAMP assay. Although the higher activity found of H-PRUNE in Tris-HCl buffer, we performed PDE assays in the presence of HEPES buffer to avoid oxido-reduction reactions of the Mn^{2+} and Mg^{2+} divalent ions in Tris buffer.

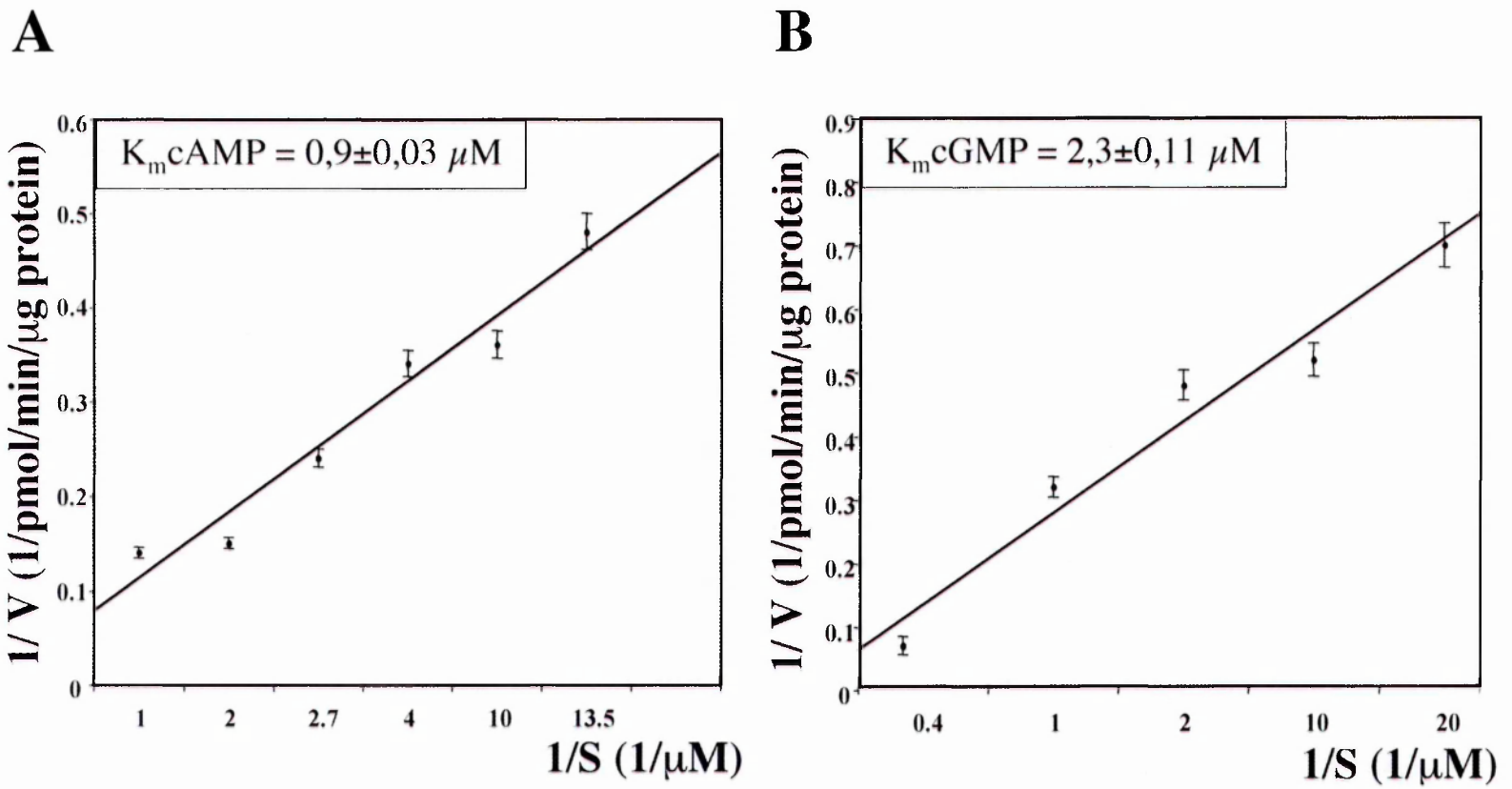

Figure 11. Lineweaver-Burk plots to determine K_m and V_{max} for both cAMP (panel A) and cGMP (panel B) as substrate, respectively.

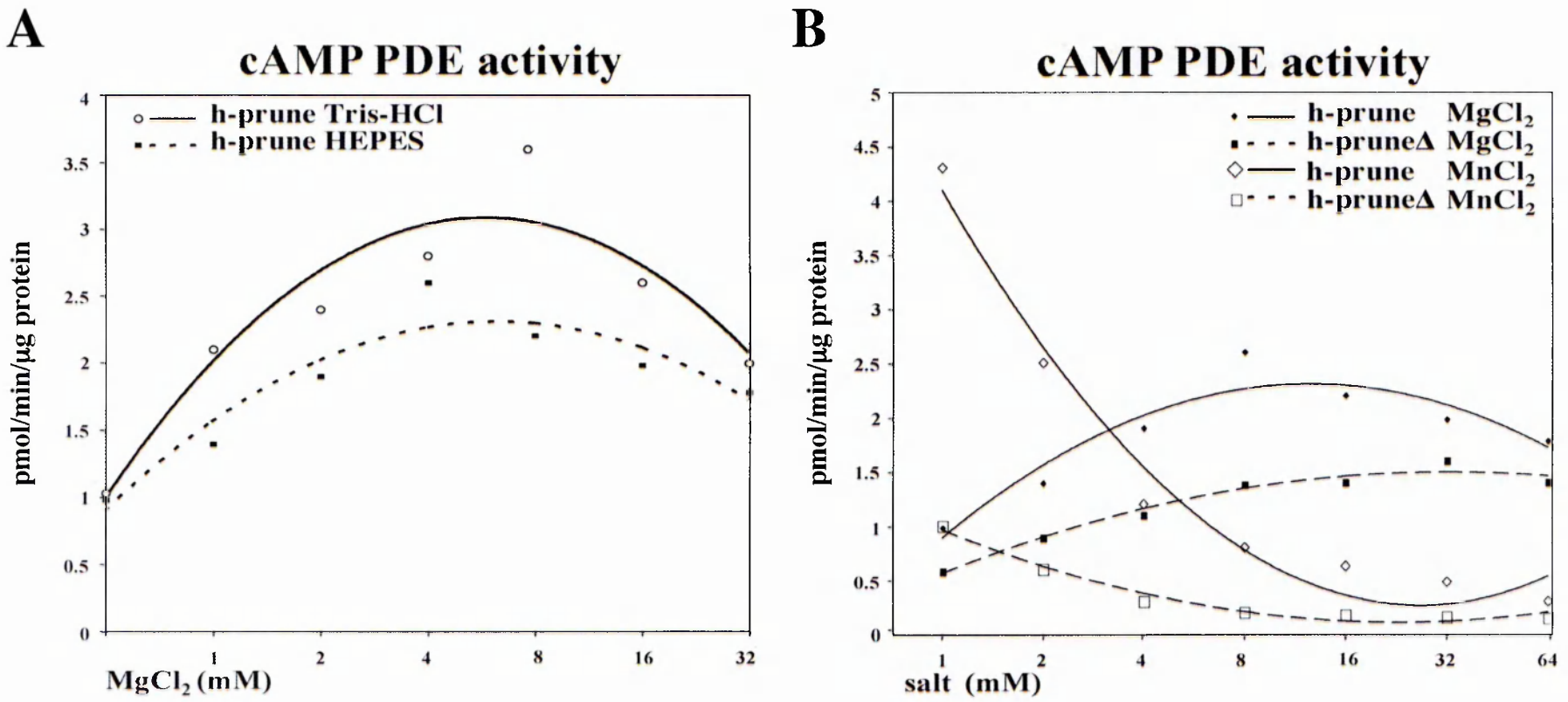

Figure 12. Characterization of h-prune PDE activity.

A) cAMP-PDE activity measured in the presence of two different buffers at increasing concentrations of Mg^{2+}.

B) cAMP-PDE activity measured in the presence of increasing concentrations of Mg^{2+} (black points) or Mn^{2+} (white points). Activity plots of both h-prune (solid lines) and h-pruneΔ (scattered lines) are shown. In all the assays presented the activities values are arithmetical means±SD for five independent assays each conducted in triplicate.

We used increasing concentrations of two different divalent ions. Although some PDE activity was measured in the no-ion buffer, Mg^{2+} stimulated H-PRUNE PDE activity; in contrast, in the presence of $MnCl_2$ this activity is inhibited (Figure 12B). The *in vitro* characterization of H-PRUNE activity indicates that the protein does prefer Mn^{2+} as cofactor at 1 mM of concentration but it is inhibited by the ion at higher concentrations. Since the Mn^{2+} ion is present only in traces in the cell, the *in vitro* analysis could not be correlated to the *in vivo* H-PRUNE PDE activity. Thus, we demonstrated that H-PRUNE PDE activity is influenced by two different ions *in vitro*.

In addition, the Mg^{2+} ions, as well as the wild-type protein do not activate the H-PRUNEΔ mutant thus, indicating that the motif 3, modified in H-PRUNEΔ mutant, is necessary for phosphodiesterase activity. In conclusion, we show here that H-PRUNE cAMP-PDE activity is influenced by both the Mg^{2+} and Mn^{2+} ions.

Influence of NM23-H1 on H-PRUNE PDE activity

Considering that H-PRUNE and NM23-H1 physically interact (Reymond et al., 1999), we investigated whether NM23s may influence the PDE activity of H-PRUNE and the biochemical significance of the NM23-H-PRUNE interaction. This was achieved by pre-incubating NM23-H1 with H-PRUNE purified protein and measuring the cAMP-PDE activity *in vitro*. H-PRUNE PDE activity showed up to a 2-fold increase over the control in the presence of NM23-H1 (Figure 13A).

In addition, to verify that this increased activity is due to a physical interaction, we tested different NM23 mutants.

A

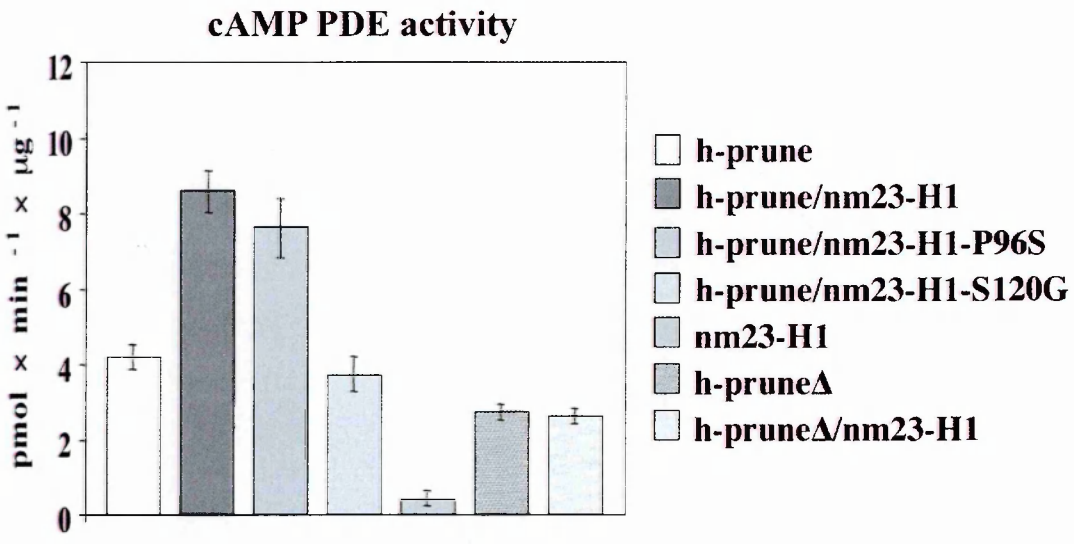

B

Inhibitor	Selective for PDE type	$IC_{50}\mu M$	h-prune $IC_{50}\mu M$
Cilostamide	PDE3	0.05	>100
Dipyridamole	PDE5/6/9/10/11	0.9/0.38/4.5/1.1/0.37	0.78±0.05
IBMX	nonselective	2-59	40.2±0.8
Milrinone	PDE3	1.3	>100
Rolipram	PDE4	2.0	>100
Vinpocetine	PDE1C	8.1	22.3±1.1
Zaprinast	PDE1/5/6	6.9/0.76/0.15	>100
Sulindac	cGMP PDEs	n.a.	>100

Figure 13. Influence of nm23-H1 on h-prune activity and PDE inhibitor studies.

A) H-prune and h-pruneΔ cAMP-PDE activity in the presence of nm23 proteins ($p<0.03$). Negative control: nm23-H1 and h-pruneΔ purified proteins. Positive control: h-prune purified protein. The activities values are arithmetical means±SD for five independent assays each conducted in triplicate.

B) Eight inhibitors were tested for h-prune PDE activity. In second and third columns are listed for each inhibitor the specific or selective PDEs and their respective IC_{50} values. On the latest column h-prune IC_{50} is reported for the most sensitive compounds: dipyridamole, IBMX, and vinpocetine. The activities values presented are arithmetical means±SD for three independent assays each conducted in triplicate.

The non-interacting mutant NM23H1-S120G was not able to increase H-PRUNE PDE activity; in contrast, the interacting mutant NM23H1-P96S increased H-PRUNE PDE activity almost as the wild-type NM23-H1, although to a lesser extent (Figure 13A). This is possible because of the lower binding affinity to H-PRUNE, previously reported (Reymond et al., 1999).

The NM23-H1 wild-type, the NM23H1-S120G and the NM23H1-P96S mutants were expressed in Lepidottera cells by Baculovirus infection and purified by affinity chromatography in Dr. Zollo's laboratory. As a further control experiment, we tested H-PRUNEΔ PDE activity in the presence of NM23-H1 protein. These two proteins do not interact by coimmuno-precipitation assays (data not shown). Indeed, there is no increase in H-PRUNEΔ PDE activity measured (Figure 13A). Altogether these results demonstrate a correlation between the direct physical interaction of H-PRUNE and NM23-H1 and the increase of H-PRUNE PDE activity.

PDE inhibitor studies of H-PRUNE

To identify the physiological role(s) of H-PRUNE cAMP PDE activity in the cell we tested a panel of selective PDE inhibitors (Figure 13B) and verified if any were affecting H-PRUNE protein activity. The ability of H-PRUNE to hydrolyze cAMP was inhibited selectively by dipyridamole (already known to act against PDE5, PDE6, PDE9, PDE10 and PDE11). The IC_{50} measured for dipyridamole inhibition of H-PRUNE PDE activity was 0.78±0.05 μM and this value is lower (higher specificity) if compared to the other dipyridamole selective PDEs (PDE5, PDE9, PDE10). Only PDE6 and PDE11 have a lower IC_{50} compared to H-PRUNE IC_{50} value (Figure 13B).

The effect of dipyridamole was determined only at a fixed concentration of substrate (0.01μM cAMP). Therefore, we cannot exclude that the kinetic properties of H-PRUNE PDE activity could be influenced by dipyridamole.

H-PRUNE was also moderately sensitive to IBMX (IC_{50}: 40.2±0.8 μM), a non-selective specific PDE inhibitor, and to vinpocetine (IC_{50}: 22.3±1.1 μM), a PDE1C specific inhibitor.

Several other inhibitors used in this study did not affect H-PRUNE hydrolysis of cAMP, even when applied at 100-fold higher concentrations than those defined as their IC_{50} values against the other PDEs. The results of the inhibitor studies are summarized in Figure 13B.

H-PRUNE and sarcoma tumours

Immunohistochemical analysis of H-PRUNE and NM23-H1 in sarcomas

In order to clarify the role of H-PRUNE in sarcoma tumours, we performed immunohistochemical analysis. Expression of H-PRUNE and NM23-H1 proteins was examined on paraffin embedded tissues from 14 of the samples analysed by FISH (Forus et al., 2001), and in 16 additional LS and MFH cases. In sarcomas, samples with increased copy numbers of *H-PRUNE* in more than 40% of the nuclei generally showed moderate to high expression of the protein (Figure 14), with some exceptions: in MS8x, LMS2x and LMS15, no protein could be detected, and in LS3x, only very low levels. The absence of protein signal was probably due to improper fixation of the tissues.

Generally, most of the LS and MFH cases examined showed moderate to high levels of H-PRUNE, and more variable expression levels of NM23-H1

(examples are shown in Figure 14A and B). Within the study of H-PRUNE expression, also five breast cancer samples with amplification of *H-PRUNE* were analysed. The mammary carcinoma cases had low or moderate expression of the protein, although mRNA levels were generally high. Expression of NM23-H1 protein was moderate to high in most of the breast carcinoma samples, except for Ma215, where no expression could be detected (examples are shown in Figure 14A and B). The amplification of *H-PRUNE* reported for sarcoma and breast carcinoma tumours is frequently associated to H-PRUNE overexpression (Forus et al., 2001); in our hypothesis, H-PRUNE is involved in a mechanism of negative regulation on NM23-H1 activity. In fact, high levels of H-PRUNE correlate with low levels of NM23-H1, suggesting that H-PRUNE could subtract free NM23-H1 forms, inhibiting the anti-metastatic function.

Cellular proliferation assay

To further understand the role of H-PRUNE overexpression we tested its cell proliferation activity in transient transfection experiments. We observed a 1.2-fold increase in proliferation (measured after 48, 72 and 96 h) in transient transfection experiments (48 h post transfection) (Figure 15A and B). In retro-viruses infected NIH3T3 cells H-PRUNE increased cellular proliferation 2-fold compared to the control (Figure 16A). Western blot analysis of both transfected and infected clones was performed as a control of H-PRUNE overexpression (Figure 15C and 16B).

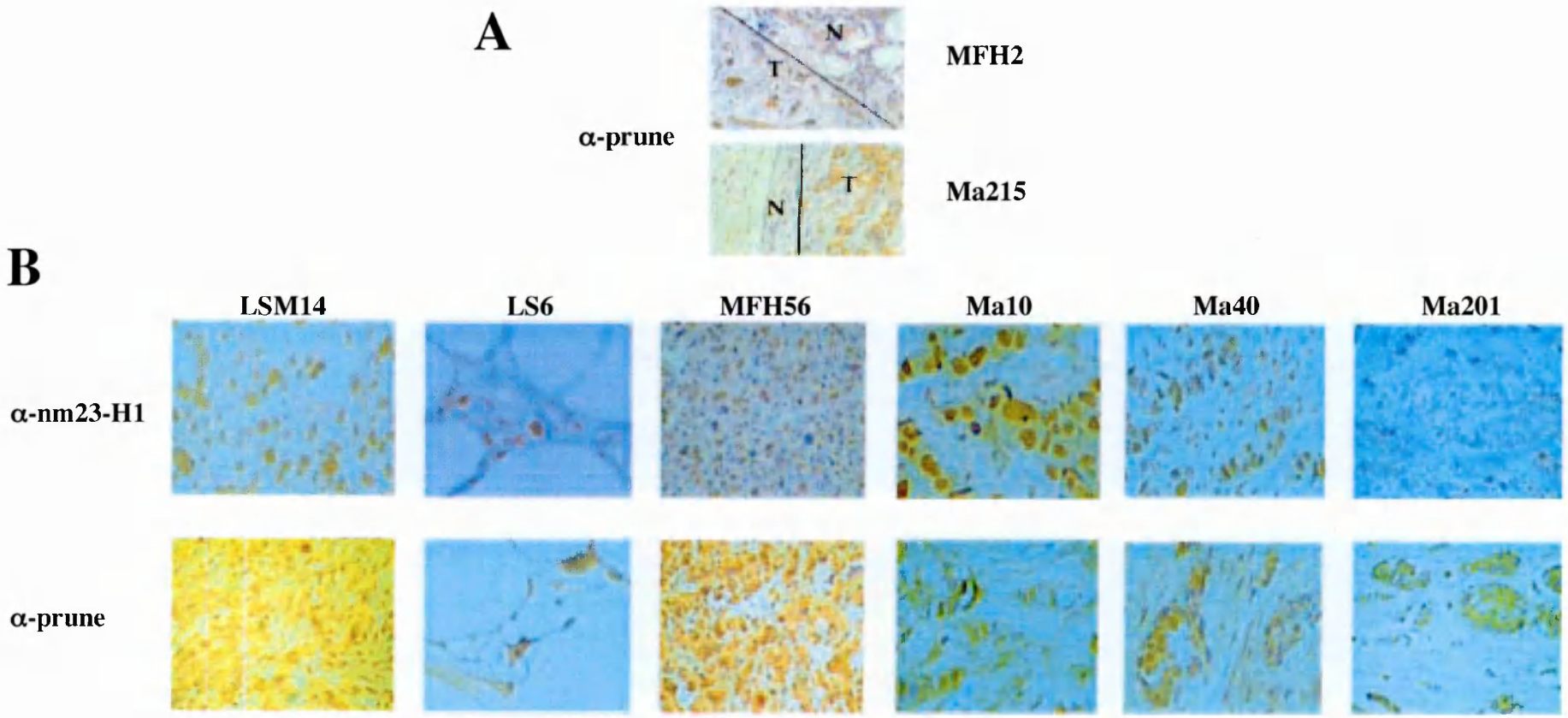

Figure 14. Immunohistochemical analysis in sarcoma tumors.

A) Representative IHC analyses using antibodies recognising prune protein (α-prune) of MFH2 (upper panel) and Ma215 (lower panel) cases. T=tumour tissue; N=normal tissue. Upper panel: On the left side some MFH2 cells (T) with strong nuclear and cytoplasmic immunoreactivity, on the right side (N) adipocytes, inflammatory cells and vascular endothelial cells with little or no immunoreactivity. Lower panel: On the right side, Ma215 cells (T) with strong nuclear and cytoplasmatic immunoreactivity, on the left side (N) terminal ductal lobular unit, with little or no immunoreactivity. 400× magnification.

B) Representative IHC analyses panel using antibodies recognising nm23-H1 and prune proteins.

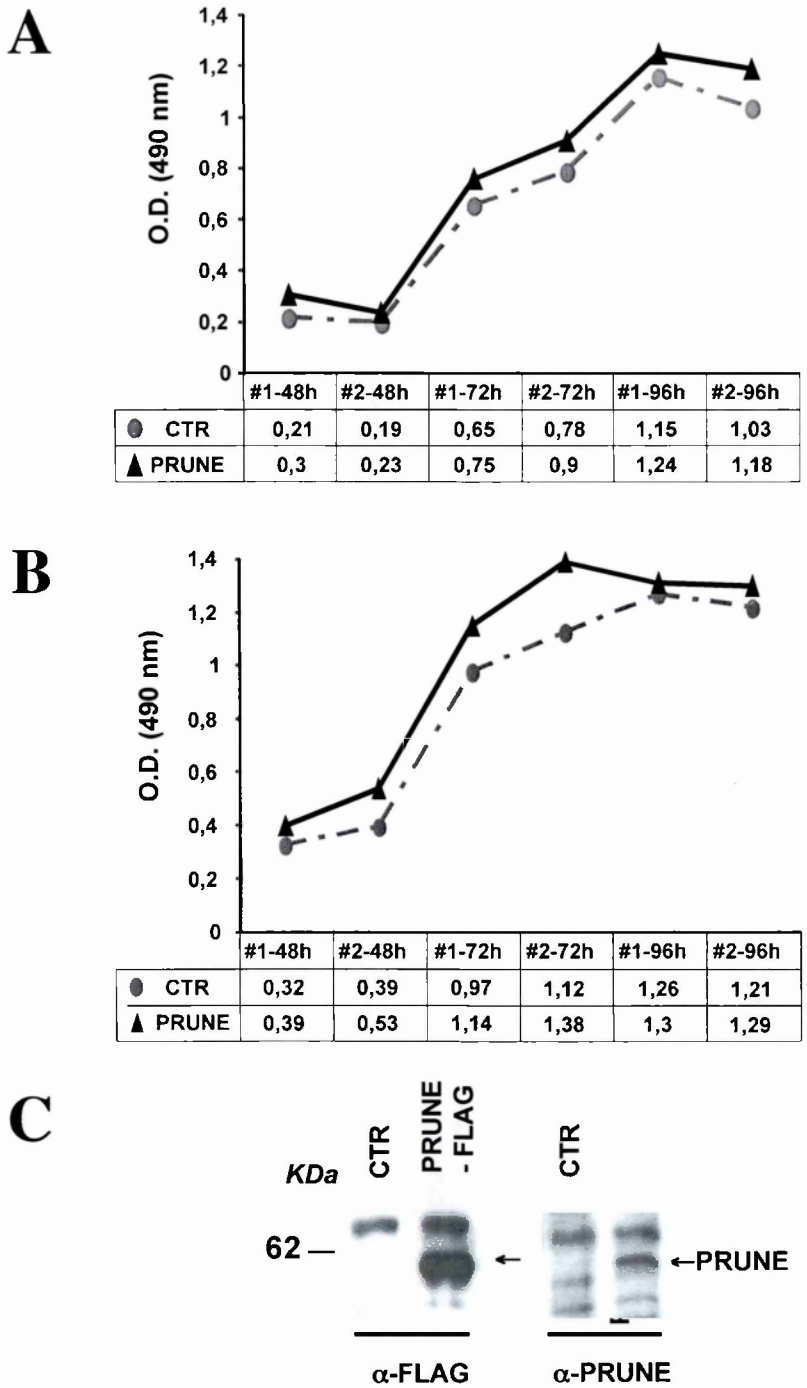

Figure 15. MTS cellular proliferation assay and prune protein content in NIH3T3 transfected cells. A) 5.000 cells/well were analysed. Time points have been scored for 12 independent wells corresponding to two independent replica clones (#1, #2). B) 10.000 cells/well were analyzed. Time points have been scored for 12 independent wells corresponding to two independent replica clones (#1, #2). C) Western blot analysis of transfected clones by using α-prune (A59) and α-FLAG Abs respectively.

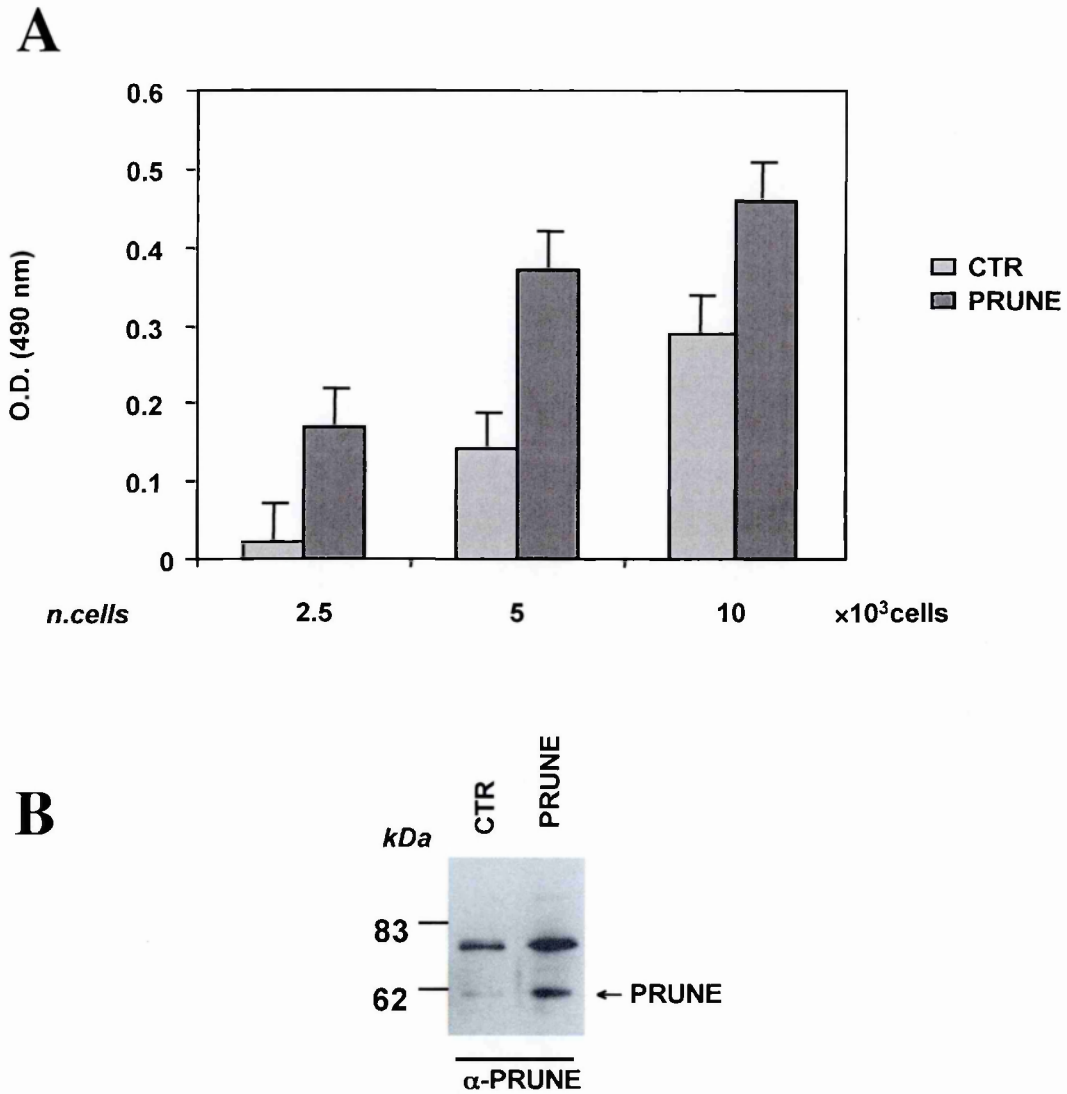

Figure 16. MTS cellular proliferation assay and prune protein content in infected NIH3T3 cells.

A) NIH3T3 cells infected with both h-prune cDNA retrovirus and empty virus. Each column correspond to the average absorbance value (O.D.) obtained in 12 independent wells with the corresponding standard deviation. B) Western blot analysis of infected clones by using α-prune (A59).

H-PRUNE and neuroblastoma tumors

H-PRUNE protein cellular localization in Neuroblastoma cell lines

As a first step towards the identification of the function of H-PRUNE in Neuroblastoma development we investigated its cellular localization in four neuroblastoma cell lines by immunofluorescence analysis. We previously reported that H-PRUNE has mostly a cytoplasmatic localization in breast cancer cells (Reymond et al., 1999). We performed immunofluorescence analysis on IMR-32, SH-SY5Y, SK-N-BE, SK-N-SH neuroblastoma cell lines, using polyclonal antibodies anti-h-prune, monoclonal antibodies anti-nm23-H1 and anti-nm23-H2 to visualize the endogenous proteins localization. The three proteins, H-PRUNE, NM23-H1 and NM23-H2 are distributed both into the cytoplasm and into the nucleus but the nuclear localization in all neuroblastoma cell lines tested is predominant (Figure 17A).

The same localization is observed when both H-PRUNE and NM23-H2 proteins were transfected in COS-7 cells and the transfected proteins were revealed using antibodies against tags (-FLAG and -HA) (Figure 18A). These data indicate the presence of H-PRUNE, NM23-H1 and NM23-H2 in the nuclear compartment of NB cell lines.

NM23-H2 and H-PRUNE protein-protein interactions

Reymond et al. (1999) have previously shown the ability of NM23-H1 to interact with H-PRUNE by yeast interaction mating experiments and co-immunoprecipitation assay.

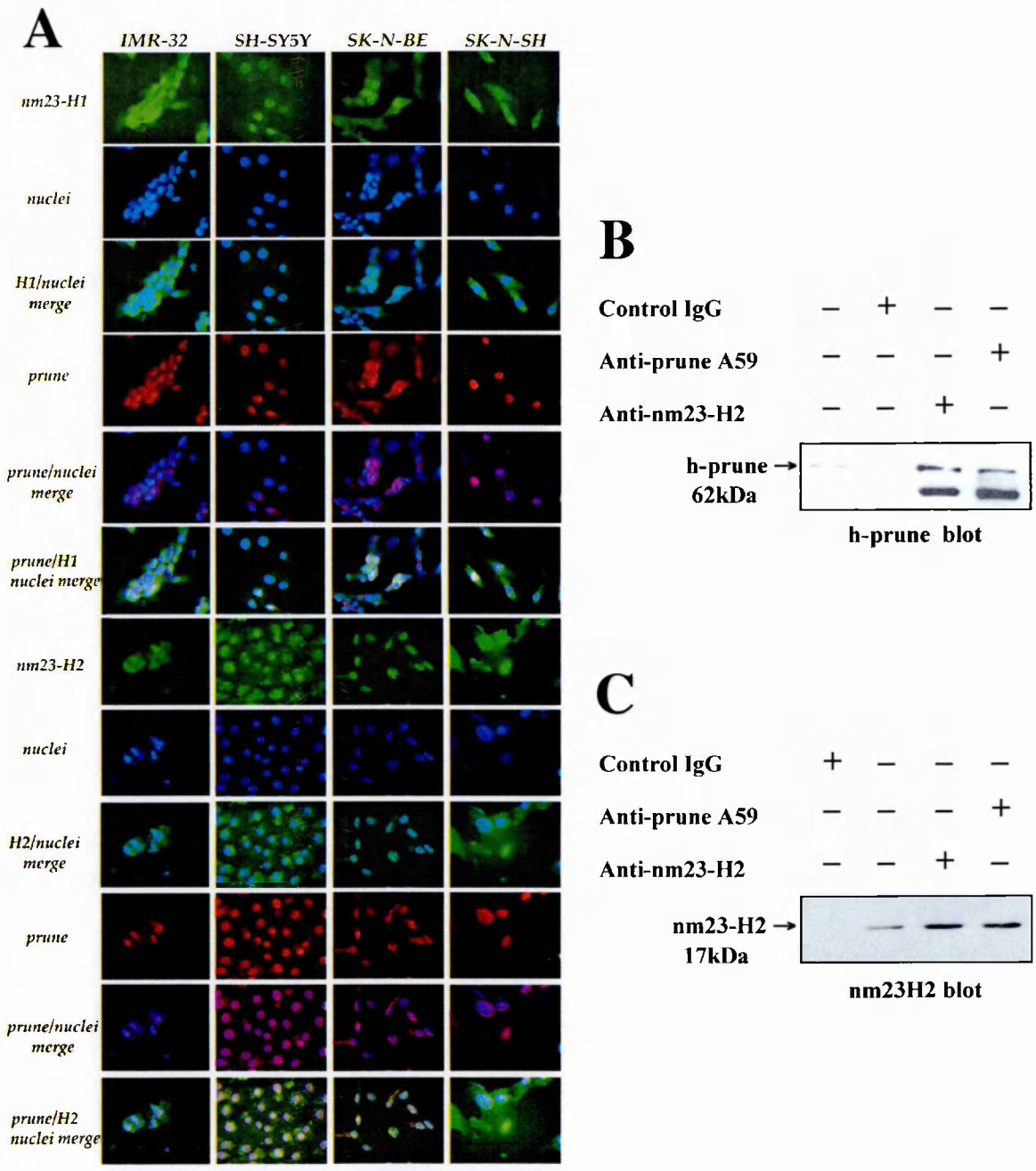

Figure 17. Immunofluorescence analysis and h-prune nm23-H2 co-immunoprecipitation.

A) Immunofluorescence analysis on four neuroblastoma cell lines using a polyclonal prune Ab (A59), a specific Ab for nm23-H1 and a specific Ab for the nm23-H2 protein. H-prune is predominantly nuclear and it co-localizes in the nucleus with both nm23-H1 and nm23-H2. B-C) Co-immunoprecipitations of h-prune and nm23-H2 endogenous proteins performed in SH-SY5Y cells with anti-prune A59 and anti-nm23-H2 antibodies. Interaction between the two proteins is observed.

Because of the 98% similarity at the aminoacidic level between NM23-H1 and NM23-H2 and the peculiar nuclear localization of both H-PRUNE and NM23-H2 proteins, we verified if H-PRUNE is able to bind to NM23-H2. We performed co-immunoprecipitation experiments on endogenous H-PRUNE and NM23-H2 proteins in SH-SY5Y neuroblastoma cells (Figure 17B and C). In addition, we performed co-immunoprecipitation experiments using wild-type H-PRUNE and wild-type or mutated forms of NM23-H2, over-expressing transiently them in COS-7 cells (Figure 18B and Figure 19).

To investigate how H-PRUNE might bind to NM23-H2 (NDPK-B), we constructed three NM23-H2 mutants: N69H, which disrupts the DNA binding domain (Postel et al., 1996); H118F, complete loss of NDPK activity (Hamby et al., 2000) and S122P, similar to the mutation described in melanomas where the suppressor of metastasis function of the protein is negatively affected (Schaertl et al., 1999). Moreover, the mutated residues are conserved between different members of the NDPK family (Lombardi et al. 2000). By co-immunoprecipitations experiments H-PRUNE binds to the wild-type NM23-H2 (Figure 18B) and NM23-H2-N69H (Figure 19A); conversely it does not bind to NM23-H2-H118F (Figure 19B and D) nor NM23-H2-S122P (Figure 19C and E), known to influence, respectively, the catalytic NDPK activity and the autophosphorylation NDPK function, under the same conditions.

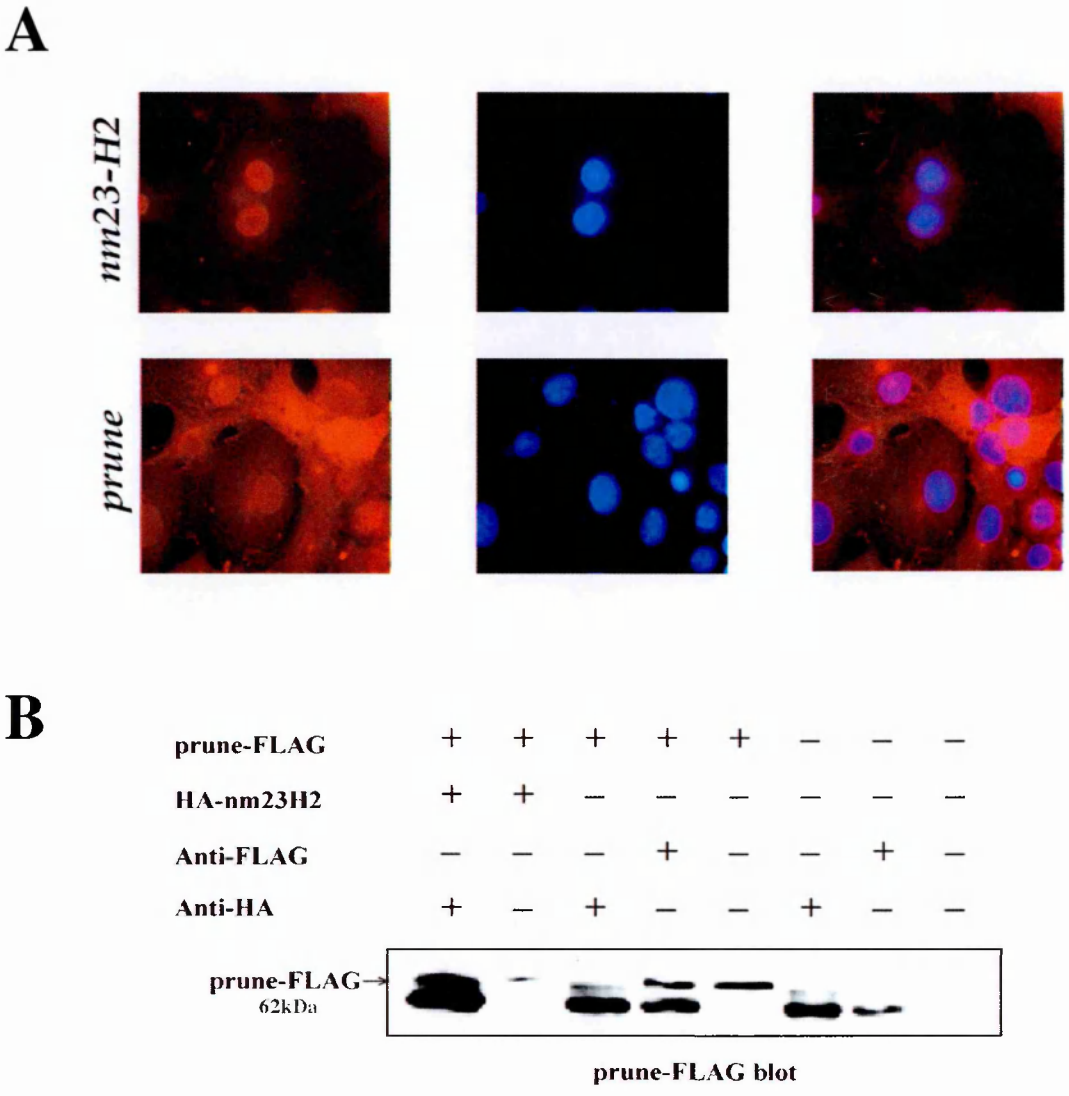

Figure 18. Co-localization and co-immunoprecipitation experiments in COS-7 cells.

A) Immunofluorescence analysis on transiently transfected COS-7 performed with anti- HA and anti- FLAG antibodies used respectively for nm23-H2 and h-prune proteins.

B) Co-immunoprecipitations of h-prune and nm23-H2 performed with anti-FLAG and anti-HA antibodies. Interaction between the two proteins is observed.

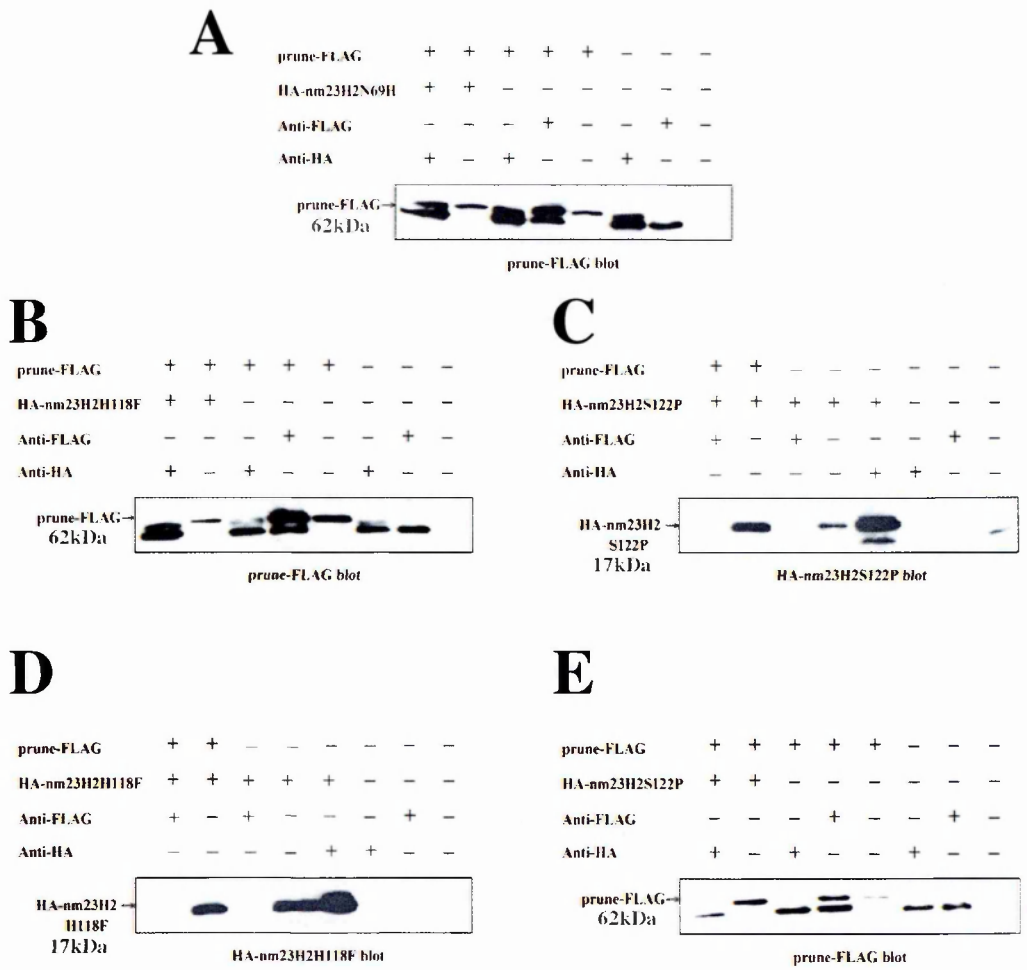

Figure 19. Co-immunoprecipitations assays.

A) Co-immunoprecipitations of h-prune and nm23-H2-N69F performed with anti-FLAG and anti-HA antibodies. Interaction between the two proteins is observed.

B-D) Co-immunoprecipitations of h-prune and nm23-H2-H118F performed with anti-FLAG and anti-HA antibodies. No interaction between the two proteins is observed.

C-E) Co-immunoprecipitations of h-prune and nm23-H2-S122P performed with anti-FLAG and anti-HA antibodies. No interaction between the two proteins is observed.

H-PRUNE, NM23-H1 and NM23-H2 expression in SH-SY5Y stable clone

To study H-PRUNE role in a neuroblastoma cell line, we overexpressed stably h-prune in SH-SY5Y, a well-characterized cell line with no amplification of *MYCN*. We performed expression analysis at protein level of the SH-SY5Y wild-type and SH-SY5Y-h-prune clones #2 and #3. To investigate the protein level of H-PRUNE, NM23-H1 and NM23-H2, we performed a western blot analysis. The lysates were immuno-detected with the polyclonal antibody for H-PRUNE (A59), with the nm23-H1 antibody for NM23-H1 (clone NM301), with the monoclonal anti-nm23-H2 (clone H2-206) and the polyclonal anti-histone H3 for normalization.

The overexpression of H-PRUNE in SH-SY5Y cells induces the expression of NM23-H1 and NM23-H2 at protein levels (Figure 20A), indicating a direct or indirect influence of H-PRUNE on the two NM23 isoforms

Immunofluorescence analysis on neuroblastoma stable clones

An immunofluorescence analysis was performed on the SH-SY5Y-prune #2 and #3 stable clones using the rabbit polyclonal anti-prune (A59), the monoclonal anti-NDP kinase nm23-H1 antibody (clone NM301), the monoclonal anti-human nm23-H2 (clone H2-206) and the monoclonal Penta-His antibody against the His-tag to detect the overexpressed protein. The overexpressed H-PRUNE has the same predominant nuclear localization of the endogenous protein. No mis-localization of both nm23-H1 and nm23-H2 was observed in consequence of H-PRUNE overexpression (Figure 20B).

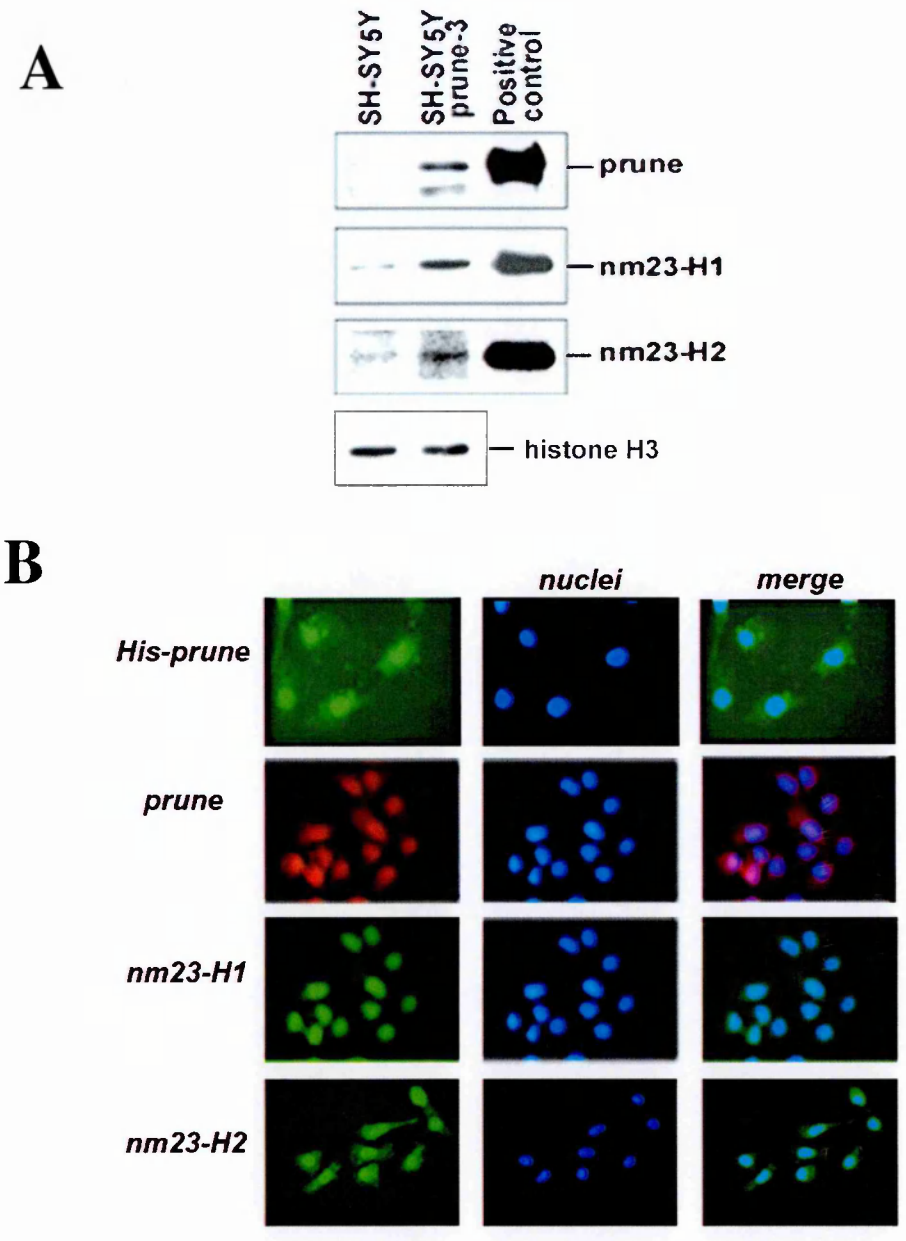

Figure 20. Analysis of SH-SY5Y cells overexpressing h-prune .

A) Western blot analyses on endogenous proteins from wild type and SH-SY5Y-prune cells. Proteins were detected by anti-h-prune, anti-nm23-H1, anti-nm23-H2 and anti-histone H3 Abs.

B) Immunofluorescence analysis on SH-SY5Y-prune-3 clone. Anti h-prune and anti-Histidine Abs were used to detect endogenous and overexpressed proteins. Anti-nm23-H1 and anti-nm23-H2 Abs were used to detect endogenous proteins after overexpression of h-prune. Co-localization of h-prune, nm23-H1 and nm23-H2 in the nucleus is still observed upon h-prune over-expression.

Immunohistochemical analyses of H-PRUNE, nm23-H1 and nm23-H2 in NB cohorts

An inverse correlation of *nm23-H1* and *nm23-H2* expression levels to tumour progression has been observed in neuroblastoma; in fact, both NM23-H1 and NM23-H2 are expressed at high levels in NB cohorts and in NB cell lines (Godfried et al., 2002). We decided to study the *in vivo* H-PRUNE expression correlated to the two nm23s isoform expression levels. We performed immunohistochemical analysis on 47 NB cohorts (classified from stage 1 to stage 4), using Abs directed against the human NM23-H1, NM23-H2 and H-PRUNE proteins.

High expression levels of H-PRUNE, NM23-H1 and NM23-H2 at protein levels, were found in the NB stage 4 cases analyzed (examples are shown in Figure 21).

These data confirmed our *in vitro* analysis on SH-SY5Y-h-prune overexpressing clones correlated to NM23-H1 and NM23-H2 increase of expression, thus suggesting a correlation between NM23-H1, NM23-H2 and H-PRUNE expression in neuroblastoma, both *in vivo* and *in vitro* analyses.

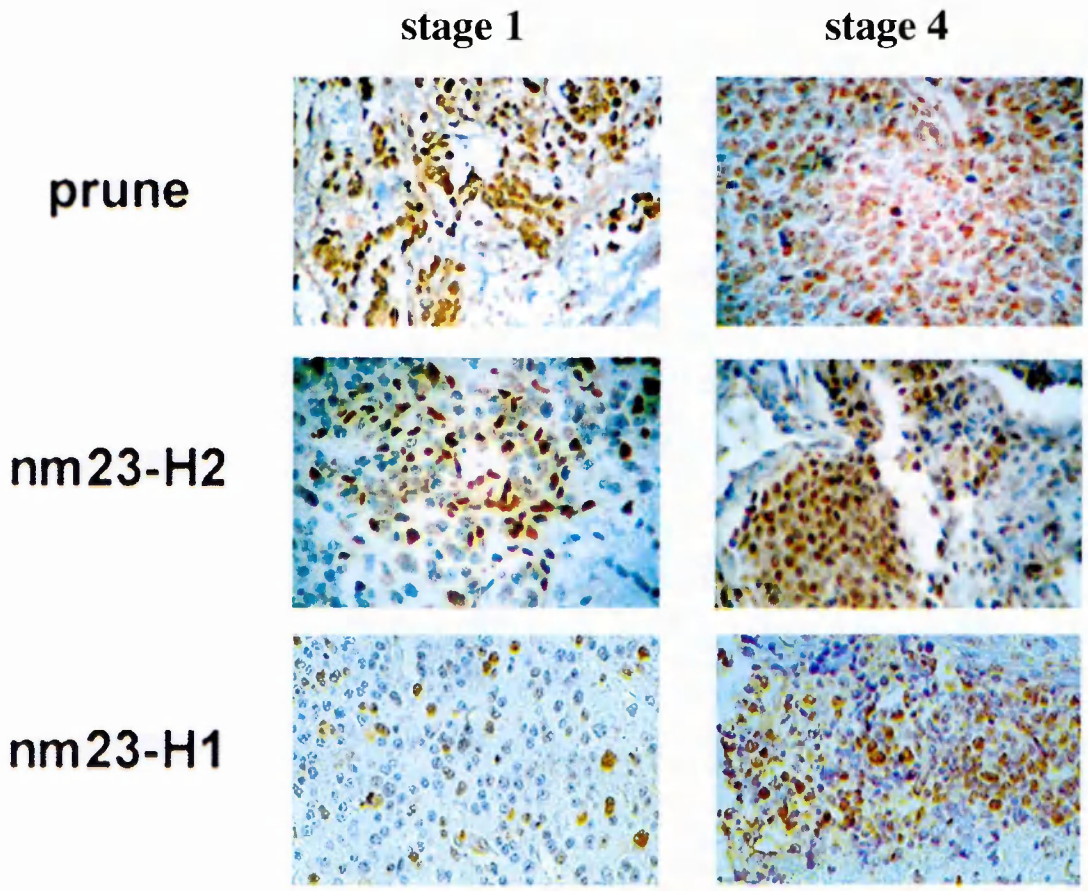

Figure 21. Immunohistochemistry with nm23-H1, nm23-H2 and h-prune specific antibodies on tumour cohorts of neuroblastoma affected patients (stage 1 compared to stage 4). High levels of all the three proteins are observed in the advanced stages of NB.

Chromatin immunoprecipitation analyses on h-prune, nm23-H2 and nm23-H1 promoter sequences

Since over-expression of H-PRUNE is correlated to an increase in NM23-H1 and NM23-H2 protein levels, the primary sequence of H-PRUNE reveals the presence of a leucine zipper domain and H-PRUNE has a predominant nuclear localization in NB cell lines, we hypothesized that H-PRUNE could be able to influence directly *NM23-H1* and *NM23-H2* expression. Luciferase reporter assays performed in Dr. Zollo's laboratory indicate that H-PRUNE is able to drive *NM23-H2* expression but is not able to increase *nm23-H1* transcription. These results shed light on the new role of H-PRUNE protein in the nucleus compartment as a transcriptional activator of NM23-H2 protein.

Since H-PRUNE is not able to transactivate *NM23-H1* expression and *NM23-H2* has been described as a transcription factor able to increase *CMYC* expression, luciferase reporter assays (performed in Dr. Zollo's laboratory) indicate that NM23-H2 is able to increase *NM23-H1* expression.

To explain H-PRUNE increase of expression in stage 4 of NB, we analyzed *h-prune* promoter region, containing two putative E-boxes. We hypothesized that H-PRUNE overexpression *in vivo* could be directly influenced by *MYCN,* a gene frequently amplified in NB tumours and encoding for a transcription factor binding the E-boxes.Luciferase reporter assays performed in Dr. Zollo's laboratory indicate that MYCN increases slightly *h-prune* expression, suggesting that MYCN could be responsible of H-PRUNE increased levels in NB cohorts. All the transactivation assays were performed in Dr. Zollo's laboratory by Dr. A. Andre' and Dr. N. Marino (unpublished results).

To investigate the binding regions of the transcription factors analyzed (MYCN, H-PRUNE and NM23-H2) on their respective promoters (*H-PRUNE, NM23-H2* and *NM23-H1*), we performed the chromatin immunoprecipitation (ChIP) assay using SH-SY5Y neuroblastoma cell lines. To study the capability of MYCN to bind *h-prune* promoter in the regions containing the E-boxes we immunoprecipitated total chromatin with anti-human MYCN clone 2 (Santa Cruz, USA) and anti-nm23-H1, clone NM301 (Santa Cruz, USA) as negative control. Then, we performed PCR reactions using two pairs of oligonucleotides for promoter region containing the two E-boxes. The analysis revealed that MYCN is able to bind weakly the region containg the E-box 2 (Figure 22A).

In order to investigate the H-PRUNE capability to bind the *NM23-H2* promoter, we immunoprecipitated total chromatin with anti-human prune A59 and anti-nm23-H1, clone NM301 (Santa Cruz, USA) as negative control. We performed PCR reactions using nine pairs of oligonucleotides spanning the entire *NM23-H2* minimal promoter region. The analysis revealed that H-PRUNE is able to bind a region of 331bp on *NM23-H2* promoter, containing a GC box (Figure 22B).

To investigate the binding region of NM23-H2 on *NM23-H1* promoter, we immunoprecipitated total chromatin with anti-nm23-H2, clone H2-206 (Seikagaku Corporations) and anti-human prune A59 as negative control. We performed PCR reactions, using seven pairs of oligonucleotides spanning the entire *NM23-H1* minimal promoter region. The ChIP analysis revealed that nm23-H2 is able to bind a region of 217bp on *nm23-H1* promoter, containing TATA boxes and an Oct-2 binding site (Figure 22C).

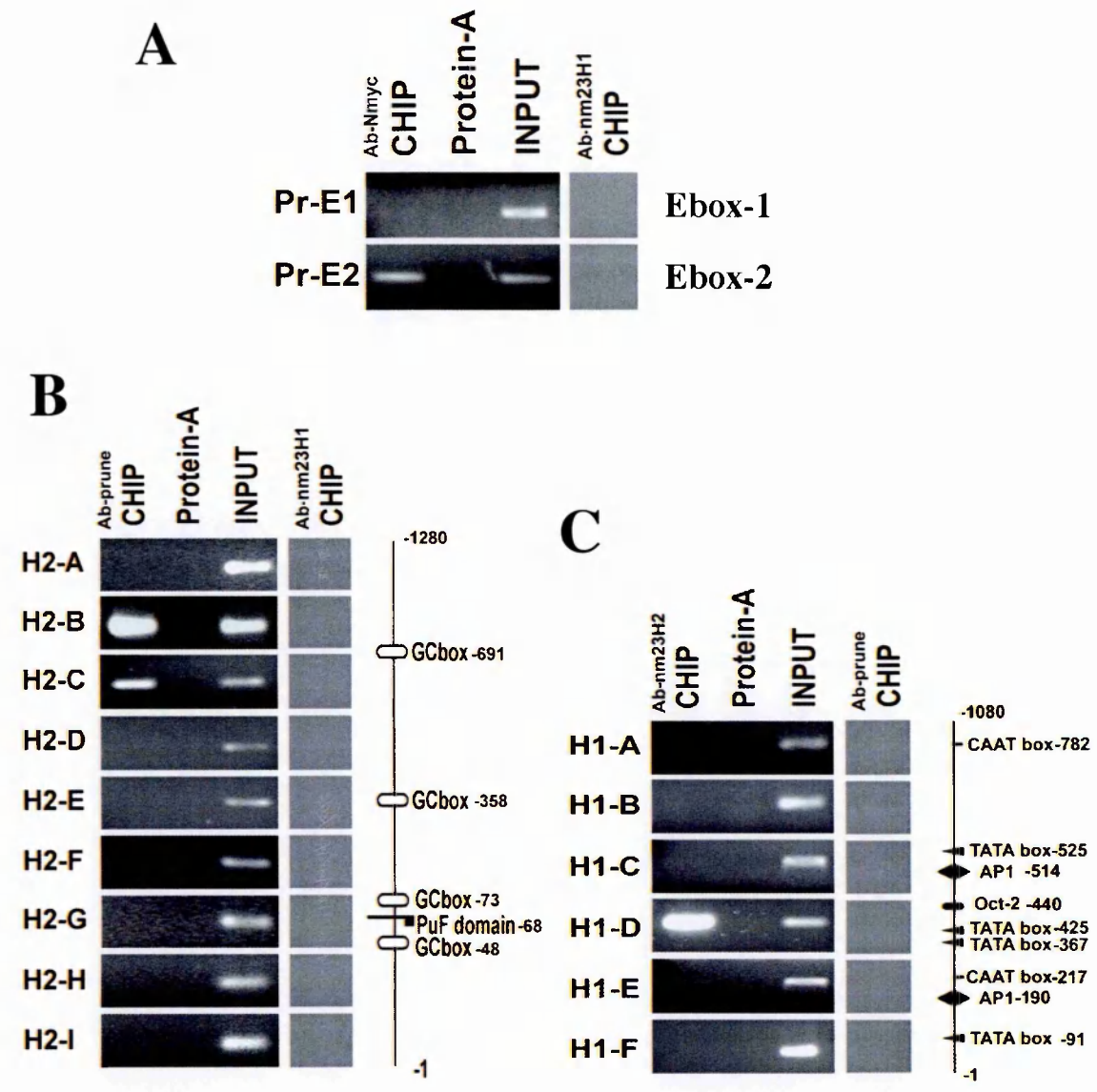

Figure 22. Chromatin immunoprecipitation experiment using SH-SY5Y cells.

A) PCR reactions were performed on total chromatin immunoprecipitated with anti-Nmyc (left lane), only with Protein-A Sepharose resin (center lane) or not immunoprecipitated chromatin. PCR reactions were performed also on total chromatin immunoprecipitated with the unrelated antibody, anti-nm23-H1 (right lane). B) PCR reactions were performed on total chromatin immunoprecipitated with anti-h-prune (left lane), only with Protein-A Sepharose resin (center lane) or not immunoprecipitated chromatin. PCR reactions were performed also on total chromatin immunoprecipitated with the unrelated antibody, anti-nm23-H1 (right lane). C) PCR reactions were performed on total chromatin immunoprecipitated with anti-nm23-H2 (left lane), only with Protein-A Sepharose resin (center lane) or not immunoprecipitated chromatin. PCR reactions were performed also on total chromatin immunoprecipitated with the unrelated antibody, anti-h-prune (right lane).

H-PRUNE and breast cancer

Stable breast MDA h-prune clones

To study the H-PRUNE function in regulating NM23-H1 anti-motility and suppressor metastasis activities well characterized in breast cancer, we have taken advantage of the breast cancer cellular models MDA-C100 and H1-177 (Mao et al., 2001; Tseng et al., 2001).

We produced several stable clones overexpressing the h-prune cDNA (clone #3 and #4), the h-pruneΔ cDNA (clone #10 and #11), the h-prune4DΔ cDNA (clone #19 and #20) and the PDE5A cDNA (clone #14 and #16) in MDA-C100 cells. We stabilized the h-prune cDNA in MDA-H1-177 overexpressing nm23-H1 (clone #7 and #8), in MDA overexpressing nm23H1-P96S (clone #4 and #5) and in MDA overexpressing nm23H1-S120G (clone #2 and #3). Several of these clones were characterized by western blot analyses to determine the expression level of H-PRUNE (Figure 23A), nm23 and PDE5A (Figure 23B) proteins, using anti-h-prune (A59), anti-nm23-H1 (clone NM301) and anti-Penta-His antibodies respectively.

Stable breast MDA h-prune clones and correlation to cellular motility

The stable clones produced were assayed for cellular motility using the Trans-well cell culture chambers (Freije et al., 1997a). Six independent clones (MDA-C100; MDA-prune clone #3 and #4; MDA-H1-177-prune clone #7 and #8; MDA-H1-177) were assayed. Overall, the MDA-prune clones have a 2-folds increase in motility when compared to the control cell line MDA-C100 (Figure 24).

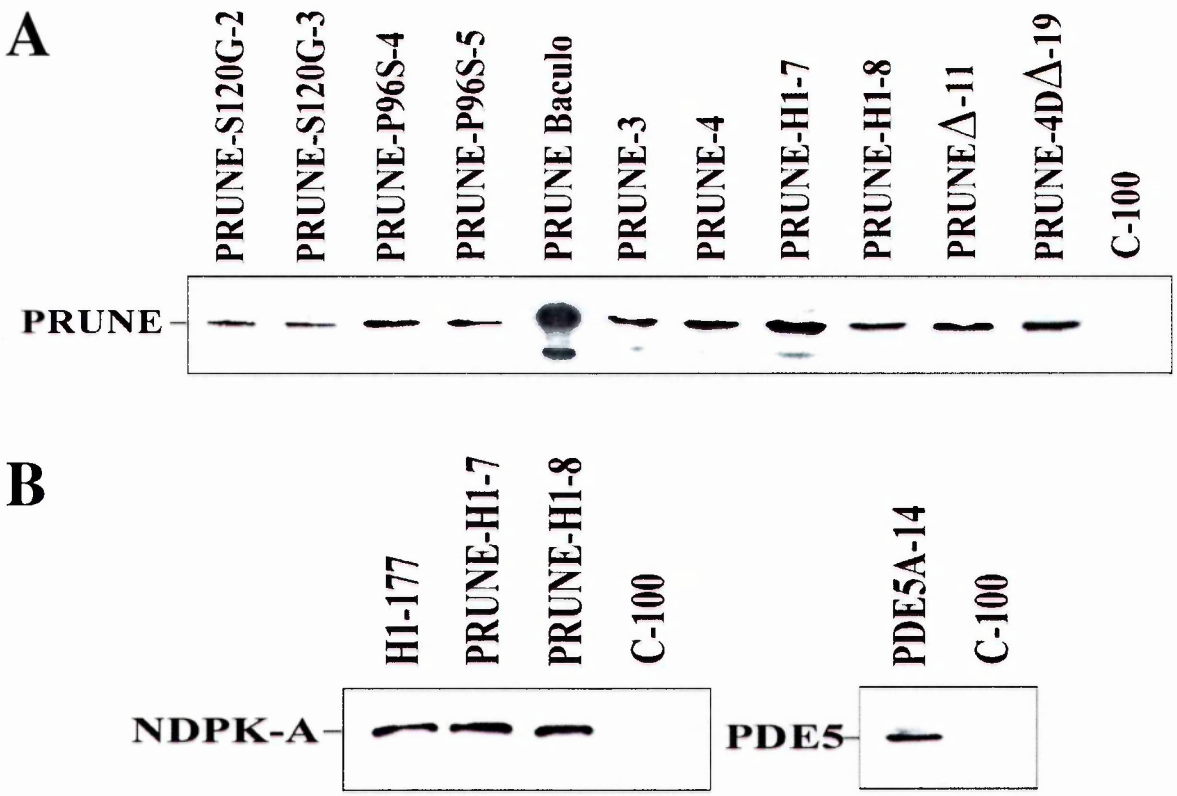

Figure 23. Western blot analyses of MDA-MB-435 stable clones.

A) Western analysis using Ab specific for h-prune indicate the amount of proteins expressed in each individual cell clone. Purified baculovirus h-prune protein was used as a positive control.

B) Western analyses using Abs specific for nm23-H1 and His-tag (for PDE5A) indicate the amount of proteins expressed in each individual cell clone.

Twenty μg total protein cell lysate were loaded in each lane.

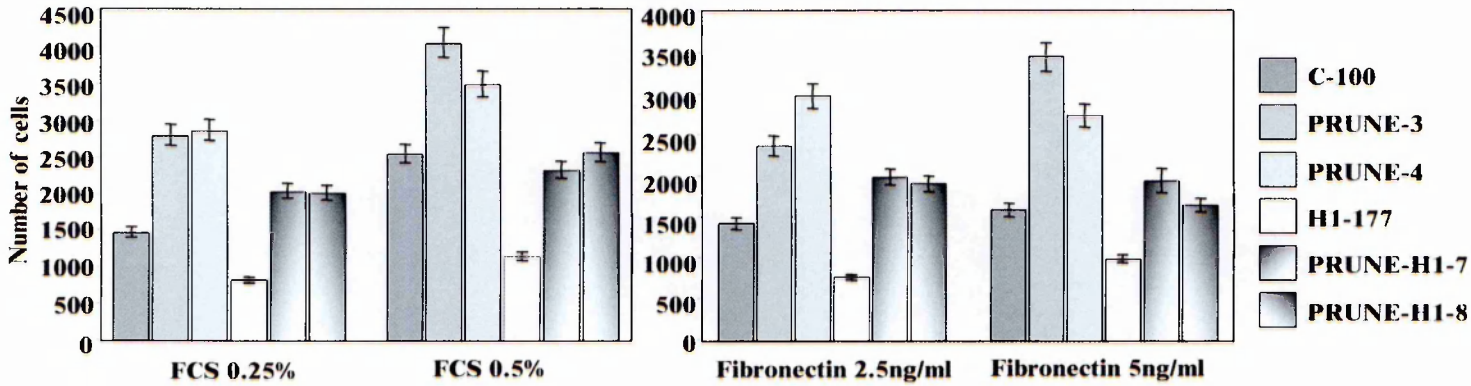

Figure 24. ***In vitro*** **motility assay.**

Cellular motility of MDA C-100 (control cell line), MDA H1-177, MDA-prune and MDA-H1-177-prune cell lines, overexpressing respectively h-prune (clone #3 and #4) alone or h-prune and nm23-H1 (clone #7 and #8) was measured after attraction by two different chemoattractors (Fetal calf serum FCS - left panel; Fibronectin - right panel), as the number of cells subjected to motility and counted, as visualized and counted under the microscope ($p<0.05$).

The values observed for the MDA-H1-177-prune clones are increased of 2.2 folds as compared to the cell line MDA-H1-177, overexpressing nm23-H1 alone (Figure 24). The clone MDA-H1-177 value observed is reduced by a mean of almost 40% compared to the MDA-C100 cell line (Figure 24), as it was described previously (Leone et al., 1993a), thus confirming the role of NM23-H1 in inhibition of cellular motility.

In order to study the contribution of H-PRUNE PDE activity to cell motility we performed the motility assay on MDA-C100, MDA-H1-177, MDA-prune (clone #3 and #4), MDA-pruneΔ (clone #10 and #11) and MDA-prune4DΔ (clone #19 and #20). We choose these mutants because of their different ability to influence H-PRUNE PDE activity. We observed a 40% decrease of cell motility in MDA-pruneΔ clones and almost a complete decrease (90%) in MDA-prune4DΔ both compared to MDA-prune stable clones (Figure 25A). To verify if H-PRUNE PDE activity contribute alone to cell motility in breast cancer cell lines, we tested the clones overexpressing a well characterized PDE (PDE5A) in MDA-C100 (MDA-PDE5A clone #14 and #16). No increase in cell motility was observed in both PDE5A overexpressing clones (Figure 25A), thus indicating that the only H-PRUNE PDE activity is able to induce cell motility in this conventional cellular model.

In addition, it has been reported (Freije et al., 1997a; MacDonald et al., 1996) that the nm23H1-S120G (a mutant showing an impaired interaction with H-PRUNE) (Reymond et al., 1999) and nm23H1-P96S (a mutant that retains its ability to bind H-PRUNE) proteins are able to induce cellular motility. We investigated the role of H-PRUNE in cellular motility overexpressing mutants alone and together with H-PRUNE and correlated this to cellular motility.

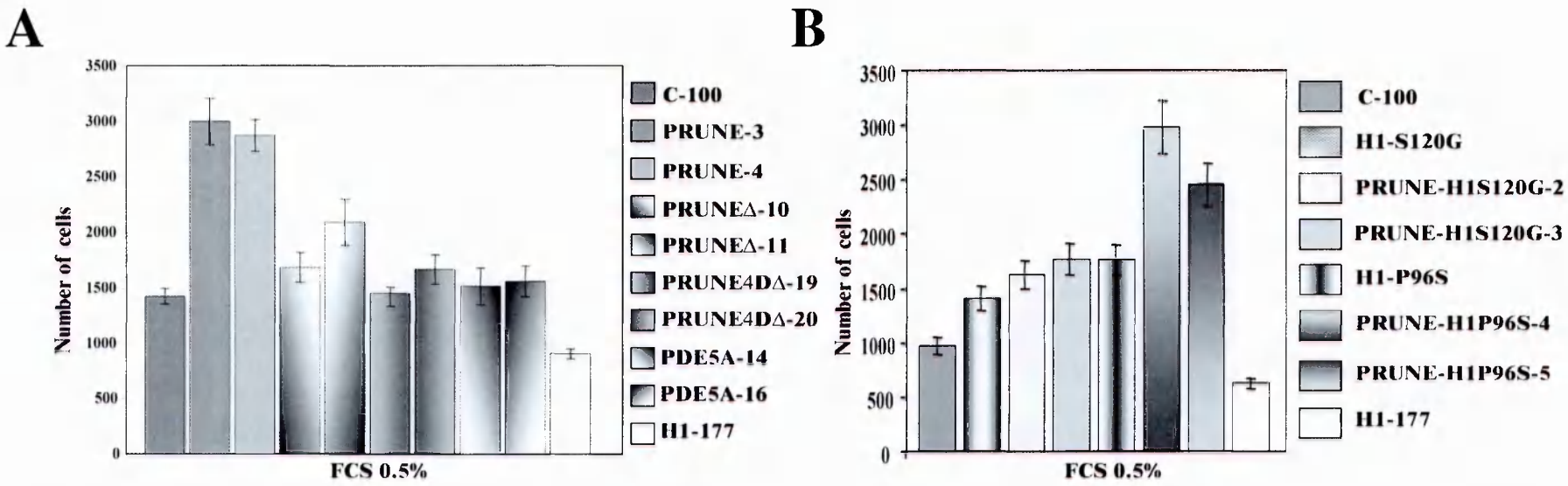

Figure 25. ***In vitro*** **motility assay.**

A) Cellular motility of MDA-C100 (control cell line), MDA-prune (clone #3 and #4), MDA-pruneΔ (clone #10 and #11), MDA-prune4DΔ (clone #19 and #20), MDA-PDE5A (clone #14 and #16) and MDA-H1-177 cell lines was measured after attraction by 0.5% FCS, as the number of cells subjected to motility and counted, as visualized and counted under the microscope (MDA-C100/MDA-prune $p<0.01$; MDA-pruneΔ/MDA-prune $p<0.025$; MDA-prune4DΔ/MDA-prune $p<0.001$; MDA-prune/MDA-PDE5A $p<0.004$).

B) Cellular motility of MDA-C100 (control cell line) and MDA-nm23H1-S120G, MDA-nm23H1-S120G-prune (clone #2 and #3), MDA-nm23H1-P96S, MDA-nm23H1-P96S-prune (clone #4 and #5) cell lines, overexpressing nm23-H1 mutants alone or with h-prune was measured after attraction by 0.5% FCS, as the number of cells subjected to motility and counted, as visualized and counted under the microscope (MDA-C100/MDA-nm23H1-S120G-prune $p<0.008$; MDA-C100/MDA-nm23H1-P96S-prune $p<0.005$; MDA-nm23H1-P96S-prune/MDA-nm23H1-S120G-prune $p<0.003$). All the motility assays histograms represent the number of cells and the arithmetical means±SD for three independent experiments performed in duplicate.

The MDA-nm23H1-S120G-prune clones show an almost 60% increase in motility as compared to the MDA-C100 control cell line, while the MDA-nm23H1-P96S-prune clones show a 200% increase in motility when compared to MDA-C100 cells (Figure 25B).

In conclusion, our findings indicate that overexpression of H-PRUNE in MDA-C100 cells increase their cellular motility. H-PRUNE is able to promote cell motility reducing NM23-H1 anti-metatstatic function. This effect is not observed when H-PRUNE is overexpressed in the presence of the impaired interacting nm23H1-S120G mutant, thus postulating a role of NM23-H1-H-PRUNE complex on increasing cellular motility.

In vivo H-PRUNE PDE activity

In vitro studies of H-PRUNE PDE activity in the presence of NM23-H1 have demonstrated a correlation between the direct physical interaction of H-PRUNE and NM23-H1 and the increase of H-PRUNE PDE activity (Figure 13A). To correlate H-PRUNE PDE activity and/or H-PRUNE NM23-H1 complex formation contribution to motility, each stable clone used in the motility assay was analysed for specific H-PRUNE cAMP-PDE activity on immuno-precipitated protein. Through these analyses, the MDA-prune clones have an increase of 8-folds cAMP-PDE activity as compared to the MDA-C100 clone (Figure 26). Instead, the MDA-pruneΔ clones have a decrease of 0.5-folds cAMP-PDE activity as compared to the MDA-prune clones and this correlates to their cell motility properties (Figure 26). In addition, we found that H-PRUNE PDE activity in MDA-H-PRUNE compared to double stable clones MDA-H1-177-prune is increased of 1.4-folds (Figure 26). These results show a direct correlation of H-PRUNE PDE activity to cell motility.

Clone name	h-prune PDE activity ($pmol \times min^{-1} \times \mu g^{-1}$)	Motility (number of cells)
MDA C-100	3.8±0.7	1548±84
MDA H1-177	2.2±0.4	928±73
MDA PRUNE #3	35±5.3	2812±294
MDA PRUNE #4	28.7±2.5	3272±271
MDA PRUNEΔ #10	16.8±1.2	1682±64
MDA PRUNEΔ #11	14.6±0.9	2087±97
MDA PRUNE-H1 #7	18.8±2.6	2048±93
MDA PRUNE-H1 #8	22±4.2	2006±87
MDA H1S120G	2.4±0.8	1328±54
MDA PRUNE-H1S120G #2	4.4±1.6	1624±89
MDA PRUNE-H1S120G #3	5.3±1.4	1767±108
MDA H1P96S	3.0±0.3	1742±38
MDA PRUNE-H1P96S #4	19.2±0.3	2982±184
MDA PRUNE-H1P96S #5	11.6±0.4	2448±143

Figure 26. ***In vivo*** **h-prune PDE activity.**
MDA-C100 (control cell line), MDA-prune (clone #3 and #4) and MDA-pruneΔ (clone #10 and #11) cell lines were treated with 8.0 μM dipyridamole for 24h. Cellular motility was measured after attraction by 0.5% FCS, as visualized and counted under the microscope (MDA-prune clone #3 and #4, $p<0.04$). Motility assay histograms represent the number of cells as arithmetical means±SD for three independent assays each conducted in duplicate.

Furthermore, the MDA-nm23H1-S120G-prune clones have a 3-folds decrease of H-PRUNE PDE activity as compared to the MDA-nm23H1-P96S-prune clones (Figure 26), thus implying a direct correlation between H-PRUNE cAMP-PDE activity, cellular motility and protein-protein interactions. In conclusion, we noted a direct correlation between H-PRUNE PDE function and protein-protein interactions, resulting in a significant influence on cellular motility.

H-PRUNE inhibitor influence on breast cancer stable clones

Since the ability of H-PRUNE to hydrolyze cAMP was inhibited selectively *in vitro* by dipyridamole (Figure 13B), we decided to elucidate H-PRUNE physiological role in MDA-MB-435 breast cancer cell line. We choose to use H-PRUNE overexpressing MDA clones and, as additional controls MDA-pruneΔ clones, because of a partial reduction (40%) of H-PRUNE PDE activity as discussed above (Figure 6B and 10B), to verify at which extent dipyridamole was able to inhibits their activities and correlate them to cellular motility. Both the MDA-prune and pruneΔ clones were incubated with dipyridamole (8 μM, a 10-fold higher concentration with respect to its IC_{50}) for 24 h to obtain the complete enzyme inactivation and then the motility assay was repeated as described above. After treatment with dipyridamole, the MDA-prune and MDA-pruneΔ clones showed a reduction in average of 40% and 20% in motility, respectively, showing that the inhibitor acts against H-PRUNE PDE activity thus inferring on a substantial decrease in cellular motility (Figure 27). These results are of pharmacological impact, because of partial success in the use of dipyridamole in combination with other drugs in clinical trials in breast (Budd et al., 1990, Budd et al., 1994) and gastric and intestinal carcinoma (Hejna et al., 1999).

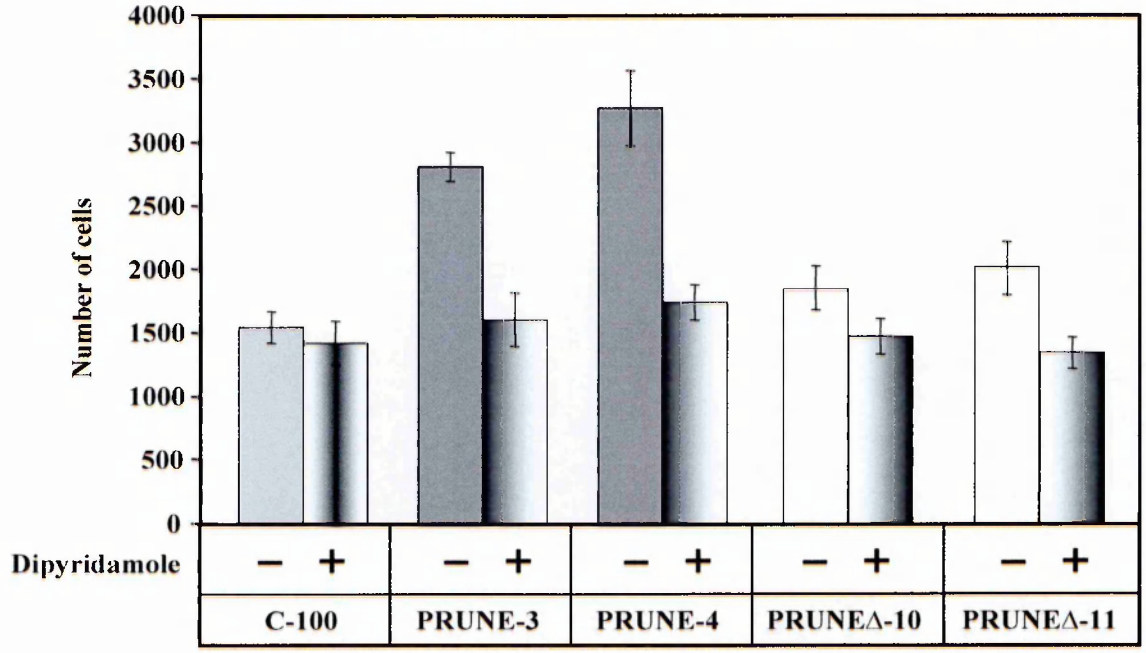

Figure 27. Inhibition of h-prune PDE activity and cell motility.

MDA-C100 (control cell line), MDA-prune (clone #3 and #4) and MDA-pruneΔ (clone #10 and #11) cell lines were treated with 8.0 μM dipyridamole for 24h. Cellular motility was measured after attraction by 0.5% FCS, as visualized and counted under the microscope (MDA-prune clone #3 and # 4, $p<0.04$). Motility assay histograms represent the number of cells as arithmetical means±SD for three independent assays each conducted in duplicate.

Breast carcinoma study on metastases affected patients

To verify *in vivo* the oncogenic role of H-PRUNE we have randomly selected fifty-nine cases for which metastasis have been reported (TxNxM1 according to TNM classification which describes the anatomical extent of disease). Analysis was performed on a multiple tissue array (MTA) containing primary tumour tissues cases that showed metastasis at the time of diagnosis or during follow-up (at least five years of follow-up; date of diagnosis: 1992-97). Immunohistochemical analyses of normal as well as no metastatic cancer tissues were performed (Figure 28A and B). Immunohistochemical analysis on MTA was performed using two antibodies that recognize specifically H-PRUNE and NM23-H1/-H2, respectively (Figure 28C and D).

According to immuno-histopathology grading, twenty-two cases (37%) with cytogenetic amplification of *H-PRUNE* chromosomal region, presented high H-PRUNE protein expression in contrast to the low or moderate expression level of NM23-H1, thus suggesting that about one third of breast metastasis formation may be due to both *h-prune* amplification and overexpression with concurrent diminished level of the NM23-H1 suppressor metastasis function. In addition, seven cases (12%) do not present *h-prune* amplification but possess high H-PRUNE protein level while NM23-H1 level is low. This suggests the presence of an alternative mechanism of H-PRUNE overexpression independent from gene amplification.

For the remaining 37 out of 59 (63%) cases with TxNxM1 tumors, we can hypothesize the involvement of an alternative pathogenetic pathway responsible for metastasis formation. These data indicate a metastasis-promoting role of H-PRUNE protein in breast carcinoma.

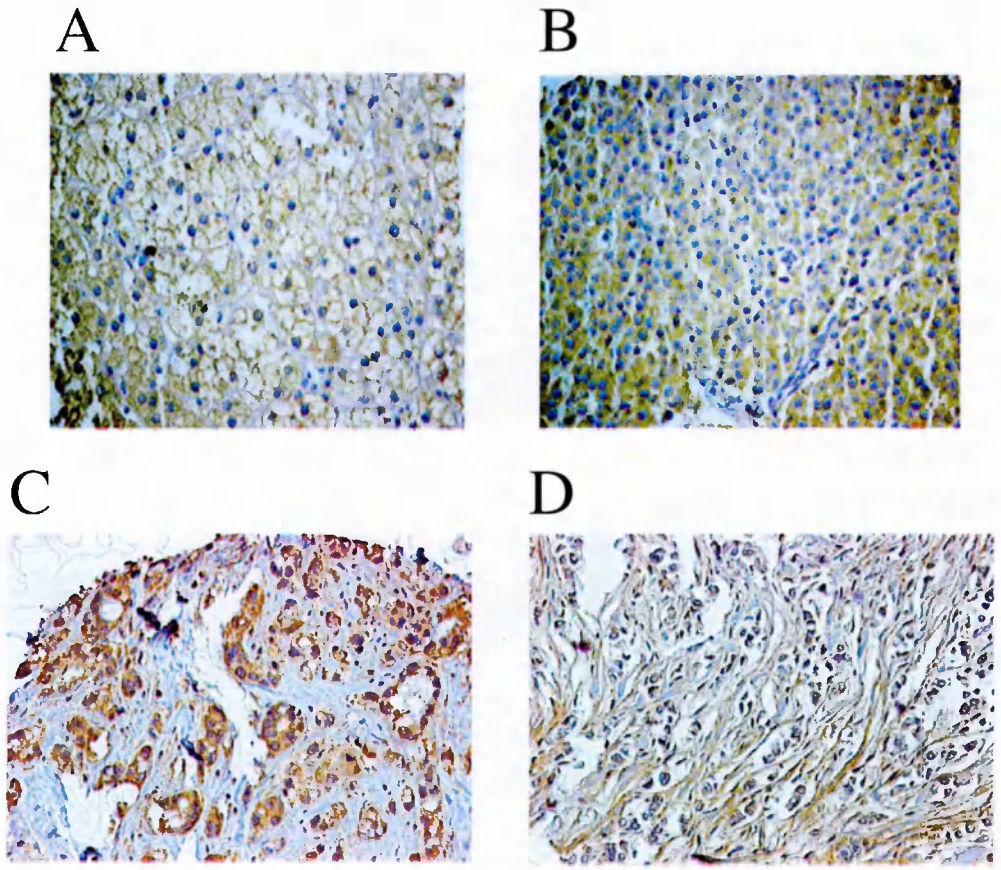

Figure 28. Immunohistochemical analysis on breast cancer cohorts.

A) 400X magnification of immunohistochemical analysis on normal tissue with low expression (+) of h-prune

B) 400X magnification of immunohistochemical analysis on a tumour cohort with low expression (+) of h-prune.

C) 200X magnification of immunohistochemical analysis on a tumour metastatic cohort with high expression (+++) of h-prune.

D) 200X magnification of immunohistochemical analysis on a tumour metastatic cohort with low (0/+) nm23-H1 expression.

cAMP content in MDA stable clones

In order to identify the molecular mechanism responsible of the increased motility effect, we have investigated to which extent the increase in cell motility was depending on the cAMP content of the MDA-MB-435 clones overexpressing H-PRUNE protein. For this reason we have analysed MDA-prune #3 and # 4 clones using a cAMP detecting immunoassay. The two MDA clones overexpressing h-prune show a reduction of ~25% in cAMP content (Figure 29), indicating that a correlation between H-PRUNE PDE activity and increase of cellular motility of the MDA-prune clones is observed together with a reduction of free cAMP nucleotides levels in these cells.

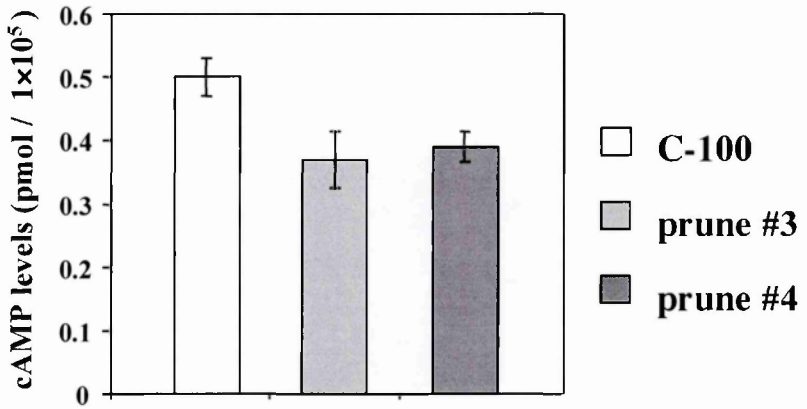

Figure 29. cAMP content of the MDA stable breast cancer clones overexpressing the h-prune protein. cAMP levels were determined by an immunoassay (R&D systems). For the quantitative determination of cAMP in MDA-C100 and MDA-prune #3 and #4 stable clones, 0.1 M HCl was added to a pellet of 1×10^5 cells to prepare the lysates. Each experiment was repeated three times in duplicate.

Bioinformatic analysis of differentially expressed genes in breast cancer stable clones

In order to verify the gene expression profile of the stable clones overexpressing nm23-H1 alone and/or in combination with h-prune, gene expression profiling was performed in Dr. Zollo's laboratory (D'Angelo et al., 2004). Expression levels of several genes involved in metastasis processes were found differentially regulated (P value ≤ 0.05) in the clone MDA-H1-177-prune (clone #8) compared to MDA-H1-177.

We found up-regulated, in the above described cellular model, genes known to be involved in cytoscheleton re-organization (*phosphatidylinositol 4-kinase type II*), protease activation (*proteasome 26S subunit, Nedd4 binding protein 2*), oncogenesis (*L-plastin, Rab1B, BRCA1-interacting protein -BRAP2)*, protein phosphorylation and nuclear transport (*Casein Kinase 2 interacting protein 1-CKIP1*). Furthermore, we found other two genes, correlated to motility, up-regulated in the clone overexpressing h-prune and nm23-H1 with respect to nm23-H1 overexpressing alone: the *dynein, light intermediate polypeptide 1 (DNALI1)* and of the *pleiotrophin.* Moreover, four genes, involved in extracellular matrix contacts and cellular adhesion (*plakophilin, LIM*), cytoscheleton re-organization (*plakin*) and in the oncosuppressor activity (*EXT1*), were found down regulated in the MDA-H1-177-prune #8 clone.

In summary, genes involved in processes linked to oncogenesis were discovered significantly altered in their level of expression, thus indicating a contribution of H-PRUNE to the higher oncogenic potential of the breast cancer cell line analysed (MDA-MB-435).

Discussion

H-PRUNE biochemical characterization

The human *PRUNE* gene was identified on the basis of homology with the *Drosophila prune* gene, first identified on the basis of a mutant phenotype (Reymond et al., 1999). The study of the new gene included different steps and approaches in order to perform a functional characterization of the protein product. The Drosophila model represented an important starting point to direct the studies of the human gene. In fact, in Drosophila mutations in the *prune* gene affected only eye colour (brownish purple in contrast to the wild-type red eye) but have no effect on viability and fertility. The association of prune mutation with a mutation in the abnormal wing disc gene (*awd/K-pn*; also named Killer-of-Prune) result in a lethal phenotype characterized by development of pseudo-melanotic tumours, thus, suggesting a synergism between the *prune* and *awd* genes. The human orthologue of *Awd* is *NM23-H1*, the first metastasis suppressor gene identified, which encodes for a nucleoside diphosphate kinase (NDPK) (Steeg, 1988).

A clustering analysis of the human and *Drosophila* PRUNE proteins shows that the proteins belong to the DHH family, which includes several phosphoesterases, such as the RecJ nuclease from bacteria and the pyrophosphatases from yeast and bacteria (Aravind and Koonin, 1998b). These enzymes hydrolyse phosphoester bonds in a broad spectrum of substrates at different affinities including single non-adenine-containing triphosphates (CTP, GTP, TTP), polynucleotides, DNA and RNA, producing single mono- and diphosphate nucleotides. The DHH proteins possess four conserved motifs, five invariant Aspartates and two conserved positively charged residues.

Structural analyses based on the two proteins belonging to the DHH superfamily, namely the RecJ nuclease and the inorganic pyrophosphatase (Ahn et al., 2001; Yamagata et al., 2002), suggested that H-PRUNE is likely to possess a metal-ion-dependent phosphoesterase activity. Moreover, the PRUNE proteins contain the DHR form (typical of some known PDEs) as substitution of the canonical DHH (Motif-3) that is observed in all other members of the DHH family. The cyclic nucleotide phosphodiesterases catalyses the hydrolysis of 3':5'-cyclic nucleotides to their corresponding nucleoside 5'-monophosphates.

Furthermore, a leucine zipper domain (positions from 157 to 185) was found in H-PRUNE primary sequence, thus suggesting a possible involvement of H-PRUNE in DNA binding capability and/or transcriptional activation.

The sequence alignments and structural analysis indicate that H-PRUNE could possess exonuclease, pyrophosphatase, polyphosphatase, phosphodiesterase and/or transcriptional activation activities. Among all the putative H-PRUNE activities, we decided to investigate first the phosphodiesterase activity, which act on cyclic nucleotides well known as second messengers and correlated to signal transduction. Additionally, the interaction between H-PRUNE and the NM23-H1 isoform that has NDPK activity, which is known to function on nucleotides, suggested us to focus our attention on the characterization of the cyclic nucleotides phosphodiesterase activity and its role in cellular signalling.

We demonstrated that mammalian H-PRUNE possesses a cyclic nucleotide phosphodiesterase activity (Figure 6B) and produced a mutant (H-PRUNEΔ) that contains substitutions in the conserved motif 3 of the DHH family. The H-PRUNEΔ shows a reduction of the PDE activity (Figure 6B), indicating that motif 3 is important for the PDE activity.

In order to define the putative catalytic site, a mutation analysis at single and multiple site in histidine (127), argine (128), and proline (129) of motif 3 and in the aspartic acids D28, D106, D126, D179 present respectively in motif 1, 2, 3 and 4 was performed. We determined PDE activity of all the mutants produced (Figure 10B). The analysis revealed that all the aminoacids mutated (except the aminoacid D106) are involved in PDE activity with different influence, indicating that motifs 1, 3 and 4 are most likely part of the catalytic site.

The characterization of the catalytic properties of recombinant H-PRUNE, expressed in Sf-9 cells, revealed that the affinity of H-PRUNE PDE for cAMP is 2.5-fold higher than that for cGMP. V_{max} with cGMP is 1.25-fold faster than that with cAMP (Figure 11A and B). The conserved motif 3 region is potentially responsible for the binding of Mg^{2+} ions as predicted by protein modelling (Figure 2A). In fact, H-PRUNE PDE activity is stimulated by $MgCl_2$ and is reduced by $MnCl_2$ but the H-PRUNEΔ, mutated in DHR (motif 3) shows a reduced PDE activity influenced at lower extent by the presence of the ions (Figure 12B). Nevertheless, we observed that H-PRUNE is also able to function in the absence or at low metal ion concentrations (Figure 12A).

Since H-PRUNE is able to interact with NM23-H1 and NM23H1-P96S but this interaction is impaired with NM23H1-S120G, a mutation occurring in advanced stages of neuroblastoma, we tested if H-PRUNE PDE activity could be influenced by physical interaction with NM23-H1 *in vitro*. We observed an increase in H-PRUNE PDE activity as a result of the protein-protein interaction, indicating a mechanism of regulation between the two proteins (Figure 13A).

In order to identify the physiological role of H-PRUNE we tested a panel of eight PDE inhibitors, which have an important pharmacological application as anti-

inflammatory agents, anti-depressants, anti-proliferative agents, antihypertensive and cardiovascular agents. We found that dipyridamole is able to inhibit H-PRUNE PDE activity with a significant IC_{50} value (IC_{50} 0.78μM) (Figure 13B). H-PRUNE is sensitive, like most other PDEs, to the non selective inhibitor IBMX with an IC_{50} of 40.2μM; also, vinpocetine, a specific inhibitor for PDE1C inhibits H-PRUNE PDE activity (IC_{50} 22.3μM). Dipyridamole, a selective inihibitor of H-PRUNE, is able to inhibit various PDEs as PDE5, 6, 9, 10 and 11. It will be of interest to examine other inhibitors to determine a more specific or selective inhibitor for H-PRUNE.

To date, we cannot exclude that H-PRUNE possess other activities as exonuclease, phosphoesterase or polyphosphatases, thus potentially defining for H-PRUNE, belonging to the DHH superfamily, a new family of phosphodiesterases.

H-PRUNE and sarcoma tumours

H-PRUNE maps to 1q21 chromosomal region, frequently amplified in a variety of human cancers. In some tumour types, this aberration is more frequent in metastatic than in primary lesions, associated with short overall survival (Tarkkanen et al., 1999), and/or chemotherapy resistance (Kudoh et al., 1999). These findings suggest that possible target genes could be involved in metastasis-related processes, for instance by inhibiting possible metastasis suppressor proteins, or in mechanisms of drug resistance. In sarcomas the amplification of 1q21 has been reported (Forus et al., 1995a,b; Szymanska et al., 1996), and the NM23-H1 expression is generally highly associated to high metastatic stages (Royds et al., 1997).

On the basis of the amplification of 1q21 chromosomal region and of the *NM23-H1* expression level (generally high) in sarcomas, we decided to study the expression levels of H-PRUNE in these mesenchymal tumours.

Amplification of *H-PRUNE* at various levels in 18 out of 19 sarcoma samples has been observed (Forus et al., 2001), suggesting that amplification and increased expression of H-PRUNE could be a mechanism for inhibition of NM23-H1 activity. In the more aggressive sarcoma types, LMS, MFH and MS, *H-PRUNE* amplification was generally accompanied by moderate to high protein levels (Figure 14). All these samples expressed NM23-H1 protein, mostly at low or moderate levels. Thirteen of the patients in this group showed amplification of *H-PRUNE*, and among those, nine developed metastases, and seven of those died of cancer. For the patients with an unknown copy number of *H-PRUNE* (16 LS and MFH cases) there was no clear correlation between H-PRUNE and/or NM23-H1 protein expression and prognosis. Nevertheless, the four patients that developed metastases and died all showed moderate to high expression levels of H-PRUNE, and low to moderate levels of NM23-H1.

The number of patients analysed is too low to draw any conclusion on the association of *H-PRUNE* amplification and overexpression with metastasis events in sarcoma or disease outcome, but it is remarkable that the expression levels of the gene is generally higher in aggressive tumours than in the relatively benign well-differentiated liposarcomas (WDLPS).

Indeed, the study of H-PRUNE and NM23-H1 in sarcoma suggested that amplification and overexpression of H-PRUNE could abrogate the possible regulatory function of NM23-H1. Such a mechanism could be comparable to the effect of amplification of MDM2 and CDK4/CCND1 on p53 and pRb1, respectively. Increased expression of these oncoproteins, caused by increased copy numbers of the respective genes, has been shown to inhibit the function of the two tumour suppressors (Khatib et al., 1993; Momand et al., 1992; Oliner et al., 1992).

The finding that *H-PRUNE* is amplified and overexpressed both in aggressive tumours and tumours of borderline malignancy is similar to what has been reported for MDM2 in sarcomas (Forus et al., 1993). The increased expression of H-PRUNE in tumours of borderline malignancy indicates that H-PRUNE could partecipate to the neoplastic transformation at different levels. In fact, tumorigenesis is a multistep process characterized by increase in cell proliferation, escape from apoptosis program, and increase in motility and invasiveness as the final steps.

In fact, we focused our attention on H-PRUNE contribution to proliferation and we performed an *in vitro* proliferation assay showing that overexpression of H-PRUNE increases proliferation in both transiently transfected and infected NIH3T3 cells (Figure 15 and 16).

Furthermore, the literature data correlating low expression of NM23-H1 to tumour aggressiveness are rather conflicting, and the exact role of NM23-H1 as a metastasis suppressor is not clear to date. There are several reports that link NM23-H1 to cell growth and proliferation. In some cases, decreasing levels of NM23-H1 is associated with increased proliferation (Caligo et al., 1997), whereas in other studies, the opposite has been shown (Cippolini et al., 1997).

Finally, the study of H-PRUNE in sarcoma supports the hypothesis of H-PRUNE, as the negative regulator of NM23-H1. H-PRUNE is generally amplified and overexpressed in our sarcoma collection and even if the number of case is too low to draw any conclusion, this first part of the thesis work was very important to direct the studies on other two tumours of interest, neuroblastoma and breast cancer, described as follow.

H-PRUNE and neuroblastoma tumours

In order to elucidate H-PRUNE role in oncogenesis, we decided to investigate H-PRUNE in neuroblastoma, a pediatric tumour and an intriguing model for NM23-H1 function and its protein partner. In fact, the interaction of H-PRUNE with NM23-H1 results impaired with the gain of function mutation, NM23H1-S120G, frequently encountered in neuroblastoma (Chang et al., 1994; Hailat et al., 1991; Lascu et al., 1997) and interestingly, high levels of NM23-H1, identified as a non metastatic gene, are generally associated to high metastatic potential in neuroblastoma cell-lines and in affected patients (Godfried et al., 2002).

H-PRUNE was found predominantly into the cytoplasm of transiently transfected COS-7 cells and of breast cancer cells (Reymond et al., 1999; D'Angelo et al. 2004). However, we found in several NB cell lines and *in vivo* cohorts a preferential nuclear localization of H-PRUNE using both immunofluorescence and immunohistochemical analyses of endogenous protein detection (Figures 17 and 21).

H-PRUNE interacts with NM23-H1 protein, a nucleoside diphosphate kinase (NDPK-A) (Reymond et al., 1999). The NM23-H2 isoform, with a predominant nuclear localization (Kraeft et al., 1996), has been implicated in transcription regulation of *CMYC* "via" its specific binding to a single strand DNA, a nuclease-hypersensitive polypurine/polypyrimidine element (NHE-PuF) (Berberich and Postel, 1995; Postel et al., 1993; Postel et al., 1996; Postel, 1996).

We investigated the capability of H-PRUNE to bind to the nuclear NM23-H2 protein (NDPK-B). By co-immunoprecipitation experiments we demonstrated that H-PRUNE binds to NM23-H2 wild-type protein (Figure 17B and C; Figure 18B) and to NM23-H2-N69H (Figure 19A), a mutant form impaired into the DNA binding. In addition H-PRUNE is not able to bind to the most occurring mutation, associated to

metastatic potential in melanoma cancer, NM23H2-S122P (Figure 19C and E). The interaction of H-PRUNE is also impaired with NM23H2-H118F, a catalytically inactive form of NM23-H2 (Figure 19B and D). Evidences indicate that H-PRUNE-NM23-H2 interaction is serine phosphorylation dependent (region containing S120, S122, S125) and based on Casein Kinase I phosphorylation (Garzia et al., submitted). How this function and nuclear binding regulation between these two proteins mechanistically is carried out is, to date, under investigation.

To elucidate H-PRUNE role in neuroblastoma, we used the SH-SY5Y cell line, an *in vitro* model, to observe if H-PRUNE overexpression could influence the expression of the other genes of interest. For this reason, we investigated NM23-H1 and NM23-H2 expression in SH-SY5Y neuroblastoma cell line overexpressing h-prune and we observed an increase at protein levels of both NM23-H1 and NM23-H2 (Figure20A), suggesting a potential role of H-PRUNE in neuroblastoma, directly or indirectly, correlated to the H-PRUNE protein partners (NM23-H1 and -H2 isoforms).

Moreover, an *in vivo* immunohistochemical analysis of H-PRUNE, nm23-H1 and nm23-H2 on several NB cohorts was performed and revealed over 47 NB cohorts (classified between stages 1, 2, 3 4), a significant increase of nm23-H1, nm23-H2 and H-PRUNE protein expression. In particular, comparing stage 1-2 (NB early onset tumour) and stage 4 (highly aggressive and pro-metastatic tumours) an increase of nm23-H1, nm23-H2 and H-PRUNE protein levels was encountered (Figure 21). The *in vitro* and the *in vivo* analyses tightly correlate H-PRUNE overexpression associated to nm23-H1 and nm23-H2 overexpression in both cases. To explain the correlation, we hypothesized a mechanism of regulation between these three genes (*H-PRUNE, NM23-H1 and NM23-H2*).

Sequence alignments indicated the presence of a leucine zipper domain in H-PRUNE suggesting that it could act as a DNA binding protein and/or a transcription factor in the nucleus of NB cells. Thus, we investigated the capability of H-PRUNE to increase directly *nm23-H1* and *nm23-H2* mRNA expression levels and by transactivation assays, we found that H-PRUNE does transactivate nm23-H2 mRNA expression but has no effect on nm23-H1 promoter. These results shed light on the new role of H-PRUNE protein in the nucleus compartment as a transcriptional activator of NM23-H2 protein.

Because of the over-expression observed of *NM23-H1* and *NM23-H2* genes in neuroblastoma SH-SY5Y cell line upon H-PRUNE over-expression and the trans-activation capability of nm23-H2 on *CMYC* promoter region, we further investigated the potential role of NM23-H2 directly on *nm23-H1* mRNA expression. We found that NM23-H2 is able to increase *NM23-H1* expression. The *in vitro* transactivation assays were supported by *in vivo* ChIP analyses. Indeed, we identified the binding region of H-PRUNE on *nm23-H2* promoter (Figure 22B) and the binding region of NM23-H2 on *nm23-H1* promoter (Figure 22C). Thus, we identified a new function of H-PRUNE correlated to its nuclear localization; in fact, H-PRUNE is able to bind to *nm23-H2* promoter and regulate the transcription of *NM23-H2*.

To explain H-PRUNE increased expression in stage 4 of NB, we analyzed *h-prune* promoter region and we found two putative E-boxes, by sequence analysis comparison. We hypothesized that H-PRUNE overexpression *in vivo* could be directly influenced by *MYCN,* a gene frequently amplified in NB tumours and encoding for a transcription factor binding the E-boxes. By luciferase reporter assays (performed in Dr. Zollo's laboratory) we demonstrated that *MYCN* increases slightly H-PRUNE expression, and by ChIP analysis we showed that MYCN is able to

weakly bind the region containing one of the two E-boxes found (E-box 2) (Figure 22A), suggesting that *MYCN* could be responsible of H-PRUNE increased levels in NB cohorts. Thus, we propose a new mechanism involving MYCN, H-PRUNE, NM23-H1 and NM23-H2 to explain NM23-H1 and -H2 increase in advanced stages of neuroblastomas.

The mRNA increase of both *NM23-H1* and *NM23-H2* genes, included in 17q21.3 chromosomal region, was previously reported (Godrfried et al., 2002) for advanced stages of neuroblastoma, either in affected patients or in neuroblastoma cell lines. In Neuroblastoma 17q gain and *MYCN* amplification are important negative prognostic factors (Bown et al., 1999; Seeger et al., 1985). Then, the NM23-H1 and H2 up-regulation in Neuroblastoma can be due to gene dosage (17q gain) and/or to direct or indirect transcriptional regulation (*MYCN* overexpression), as reported into the discussion section by Godfried et al. (2002).

In our analysis, the mRNA increase of *NM23-H1* and *-H2* could be explained by a mechanism of transcriptional regulation between H-PRUNE, NM23-H1 and NM23-H2, where the first key actor might be *MYCN* increased copy number.

In fact, to explain H-PRUNE overexpression associated to the progression of NB as observed in *in vivo* analyses, we demonstrated here the direct role of MYCN on *h-prune* promoter (Figure 22A).

Altogether, these results indicate a nuclear pathway of action in NB development involving *MYCN* amplification. MYCN transactivates *H-PRUNE* expression through its binding to the E-box, and H-PRUNE in turn induces NM23-H2 expression. Then, we found that NM23-H2 is able to transactivate *NM23-H1* mRNA expression levels. We postulate here H-PRUNE oncogenic action in NB malignancy by a transcriptional loop between different genes, including activation of

NM23-H1 and NM23-H2, as presented in a model (Figure 30). Although the molecular findings presented here need a more comprehensive analysis in a larger NB affected patient group, our results indicate a new nuclear function of H-PRUNE in combination with *MYCN* increase copy number (already known as marker of malignancy and poor prognosis in advanced neuroblastoma), and a new transcriptional activation mechanism involving H-PRUNE and, NM23-H1, NM23-H2 which can be new potential target for clinical intervention to prevent NB progression and cancer development.

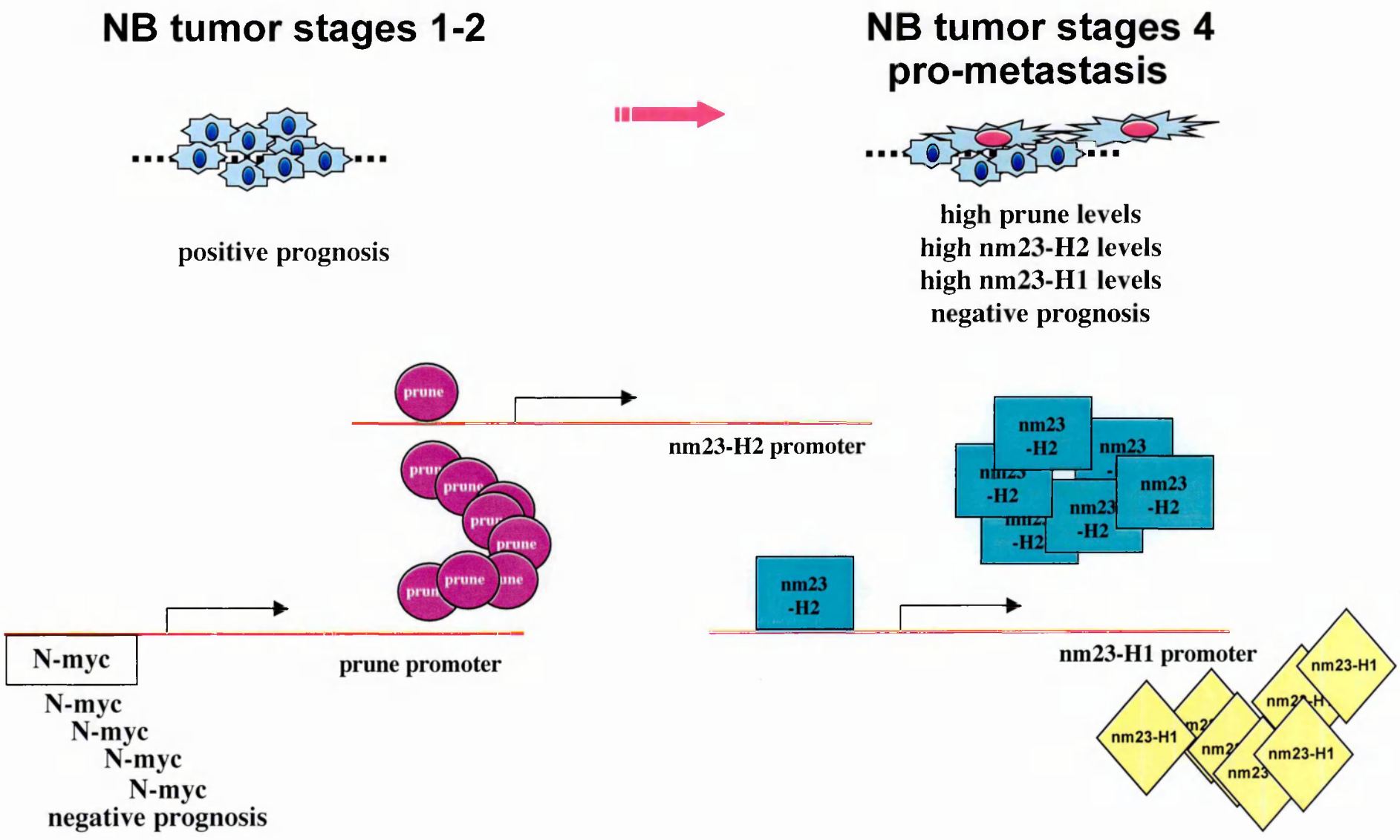

Figure 30. Model of Neuroblastoma development by h-prune, nm23-H2 and nm23-H1 pathway of action.

H-PRUNE and breast cancer

The anti-motility effect of NM23-H1 is widely demonstrated in breast cancer by several reports (Freije et al., 1997a; Freije et al., 1997b; Leone et al., 1993a).

A part of this thesis work demonstrated that H-PRUNE and the NM23s protein levels are unbalanced in sarcoma, suggesting that H-PRUNE may negatively regulate NM23-H1 anti-metastatic function. An increase in H-PRUNE expression is directly correlated with aggressiveness of those tumours and cancer progression (Forus et al., 2001). Since the literature has postulated that the anti-metastatic activity of NM23-H1 is independent of the NDPK activity (Wagner et al., 1997), we investigated at which extent the H-PRUNE influences cellular motility, which represents one of the first cellular acquired functions by the cancer cell to migrate away from the primary tumor site.

In order to study the influence of H-PRUNE PDE activity on cell motility, we overexpressed H-PRUNE, H-PRUNEΔ and H-PRUNE4DΔ in breast cancer model, and observed that overexpression of the wild type protein induces cell motility, while a decrease of its PDE function (H-PRUNEΔ, H-PRUNE4DΔ) corresponds to a decrease of cell motility (Figure 24 and 25A). Indeed, we observed for the mutant H-PRUNE4DΔ an 80% reduction of PDE activity and overexpression in MDA clone do not show significant increase in cell motility, thus excluding that other potential H-PRUNE activities are responsible of increasing motility. To correlate specifically H-PRUNE PDE activity to cell motility, we overexpressed PDE5A, in the same cellular model and tested for cell motility (Figure 25A). PDE5A, chosen for its sensitivity to dipyridamole (IC_{50} 0.9μM), did not affect MDA breast cell motility, thus indicating

that only H-PRUNE PDE function is responsible of increasing cell motility in breast cancer cells.

In addition, we observed that overexpression of H-PRUNE in a high NM23-H1 expression background displays a decreased motility phenotype and a lower H-PRUNE PDE activity compared to the cells overexpressing H-PRUNE alone (Figure 24). Although, H-PRUNE PDE activity is increased *in vitro* upon interaction with NM23-H1 (Figure 13A), this effect is not observed *in vivo*. These phenomena can be explained by different processes, influencing the H-PRUNE-NM23H1 complex formation: in fact, the protein-protein complex formation might depend on the presence of different oligomeric and/or post-translationally modified NM23-H1 forms (for example: serine phosphorylation) (Steeg, 2003).

In order to test the hypothesis that the negative regulation of H-PRUNE on the NM23 anti-metastatic function is due to an increase in PDE activity as a result of the protein-protein interaction, we investigated what effect two NM23-H1 mutants hold on H-PRUNE PDE activity. These protein mutants are NM23H1-P96S, able to physically interact with H-PRUNE, and NM23H1-S120G, that does not interact with H-PRUNE (Reymond et al., 1999); both mutants transfected in breast cancer cells (MDA-435) are able to suppress the endogenous anti-motility effect of the NM23-H1 wild-type protein (Freije et al., 1997a, MacDonald et al., 1996). Additionally, we show that breast cancer cells overexpressing H-PRUNE in a high NM23-H1-S120G expression background have lower cellular motility in comparison to cells overexpressing H-PRUNE in a high NM23-H1-P96S background (Figure 25B), thus further indicating that the physical interaction between these two proteins may be responsible for the motility promoting role. Furthermore, the H-PRUNE-NM23-H1-S120G clone has almost 66% lower PDE activity compared to the PDE value

observed in the clone overexpressing both H-PRUNE and NM23-H1-P96S (Figure 26), thus definitively indicating a correlation between protein-protein interaction, H-PRUNE cAMP-PDE activity and cellular motility effects.

In addition, the use of dipyridamole severely reduced the motility of the stable H-PRUNE breast clones and at less extent the H-PRUNEΔ overexpressing clones (Figure 27). Although dipyridamole might not be the most effective H-PRUNE cAMP PDE inhibitor and further experiments have to be performed to identify a new highly specific compound, these findings are of pharmacological interest. It is common opinion, that anti-coagulants such as dipyridamole and similar drugs exert their function on interfering the blood-clotting pathway activation through inhibition of adhesion of metastatic cells to capillary walls. These results are an added value to those presented *in vivo* (Haaz et al., 1996) describing the positive effect of dipyridamole and fluorouracil (FU) combination in chemotherapy and in several clinical trials; examples are in breast (Budd et al., 1994) and gastric and intestinal carcinoma (Hejna et al., 1999). Dipyridamole in combination with protease inhibitors, interferon, and 5-fluoroUracil inhibits metastasis formation. In view of the results reported here, we believe that the use of dipyridamole might hold promise for prevention and treatment of breast metastases spread and a large controlled investigation study might provide further evidences.

Moreover, we confirmed *in vivo* the data observed on cellular motility activation *in vitro,* using a significant number of breast cancer tissues from TxNxM1 patients. In fifty-nine tumours from cases presenting distal metastasis, *H-PRUNE* was found amplified in copy number and overexpressed in twenty-two cases (37%), whereas *NM23-H1* was found expressed at lower levels in all analysed cases (Figure 28). The data presented are indicating that H-PRUNE up-regulates genes involved in

metastasis and its activity *in vivo* increases the risk of more aggressive tumour behaviour, contributing negatively to the clinical outcome in breast cancer patients. The results reported here have important pharmacological consequences, as drugs able to selectively inhibit H-PRUNE PDE activity can be used in treatment of breast carcinoma, in order to block H-PRUNE pro-metastasis malignancy function.

Overall, these experiments shed light on the role of H-PRUNE on promotion of cellular motility and metastases influencing negatively the NM23-H1 anti-metastatic function. Our model of the role of H-PRUNE in cancer progression invokes in general its amplification in tumour cells. The amplification leads to an increased H-PRUNE PDE activity in the cytoplasmic compartment, thus influencing negatively the suppressor of metastasis function of the NM23s. The activation of the H-PRUNE PDE activity is due to a physical interaction with the NM23-H1 protein; the complex formation results in a substantial decrease of the level of free NM23-H1 forms, thus influencing cell proliferation, cellular motility and metastatic processes (Figure 31).

How H-PRUNE-NM23 protein complex influences NM23-H1 metastasis suppressor function by promoting motility, it is not yet known. These questions and their following experimental plans will be aims of future research efforts.

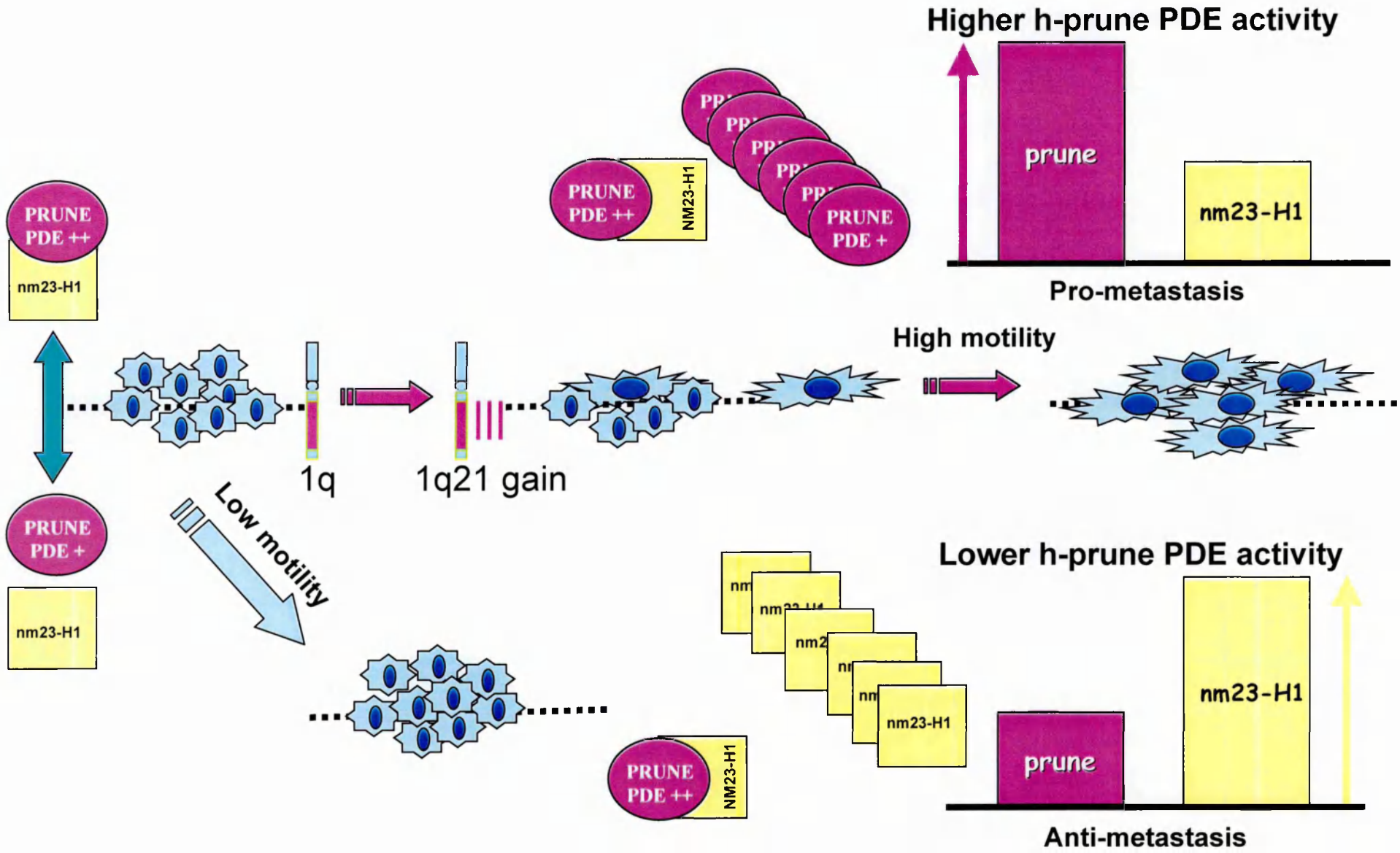

Figure 31. A model representing h-prune pro-metastatic function in breast cancer.

Further specific investigations to address the biological functions of H-PRUNE and NM23 in other model organisms should help in uncovering the potential significance of this pathway in metastasis as well as in cellular motility and development.

H-PRUNE PDE overexpression and molecular changes

The study of H-PRUNE in breast cancer, previously described, revealed that H-PRUNE overexpression in the MD-MB-435 breast carcinoma cell line causes the increase of cell motility associated either to H-PRUNE PDE activity or to the complex formation with NM23-H1 (D'Angelo et al., 2004).

In order to identify the molecular mechanism responsible of this phenomenon, we have investigated to which extent the increase in cell motility was depending on the cAMP content of the MDA-MB-435 clones overexpressing H-PRUNE protein. For this reason we have analysed MDA-prune #3 and # 4 clones using a cAMP detecting immunoassay. The two MDA clones overexpressing H-PRUNE show a reduction of ~25% in cAMP content (Figure 29), indicating that a correlation between H-PRUNE PDE activity and increase of cellular motility of the MDA-prune clones is observed together with a reduction of free cAMP nucleotides levels in these cells.

In *Dictyostelium*, Wessels et al. (2000) reported a direct link between cAMP cellular gradient (increase and decrease in a spatially and temporary manner) and cellular motility during chemotaxis processes. A model in which frontal waves of spatial gradient of cAMP, frequency of lateral pseudopodal formation and turning, direct the motility of the cell shows how cAMP regulates and drives pseudopodal

extention. How these findings and other working hypothesis are linked to H-PRUNE protein function in mammalian cellular motility are topics of further studies.

The features of metastatic cells are acquisition of invasive ability, changes in adhesion, initiation of motility and extra-cellular matrix proteolysis. We focused our attention on motility of metastatic cells and demonstrated that H-PRUNE is responsible of an increase of cell motility.

In order to verify the molecular changes occurring in tumour cells as a consequence of H-PRUNE and NM23-H1 protein overexpression, a gene expression profiling analysis of breast MDA clones, overexpressing nm23-H1 alone (MDA-H1-177) and together with H-PRUNE (MDA-H1-177-prune #8), was performed in Dr. Zollo's laboratory (D'Angelo et al., 2004).

The thesis work focused the attention on the study, by PubMed literature analyses, of the genes found differentially expressed in breast cellular models and discuss their potential function as being key actors on changing the biology of the cell and influencing the motility processes. A graphic cell representation is shown in Figure 32.

In the clone overexpressing both H-PRUNE and NM23-H1 (MDA-H1-177-prune #8), we found up-regulated the phosphatidylinositol 4-kinase type II (PI 4-K) (Heilmeyer et al., 2003), a key enzyme involved in the modelling of the actin cytoskeleton and into the activation of protein kinase C (Subrahmanyam et al., 2003) (Figure 32). One of the major pathways of signaling in mammalian cells involves the turnover of phosphatidylinositol (PI) and the generation of diacylglycerol (DAG) for protein Kinase C (PKC) activation and inositol-1,4,5-triphospate (IP3) for intracellular Ca2+ mobilization.

Figure 32. A cellular model representation describing genes differentially expressed as observed in the hprune-nm23-H1 overexpressing breast carcinoma clone (MDA-H1-177-prune #8). Double edge arrows indicate the putative interactions with known proteins involved in cell cycle and cell motility. Genes found up-regulated in the h-prune-nm23-H1 clone are shown in red; genes down-regulated are shown in blue.

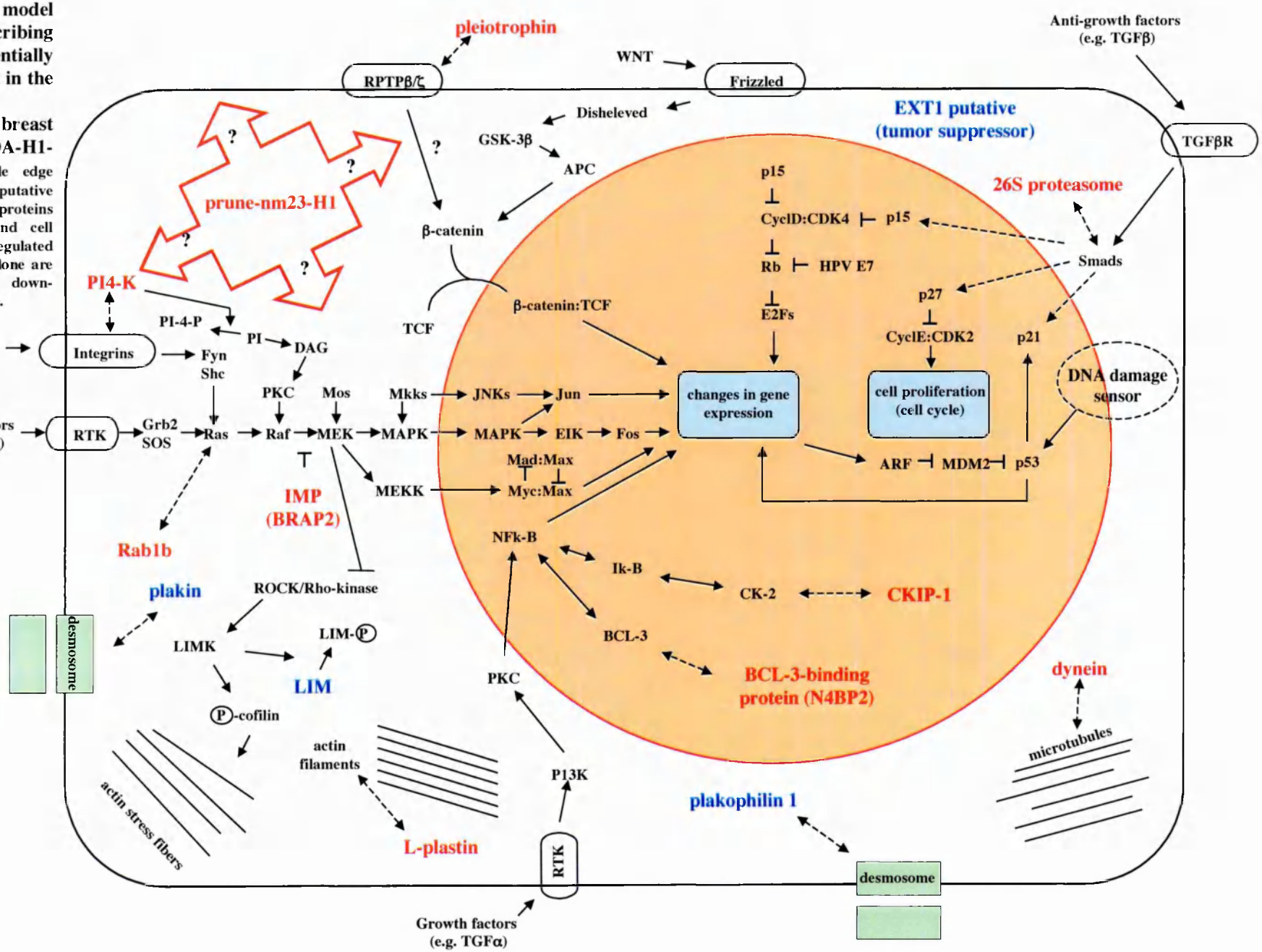

PI 4-kinases convert PI into PI-4-phosphate (PI-4-P), a highly relevant intermediate in multiple phosphatidylinositide signaling pathways. The enzyme activities have been classified into type II and type III, based on their sensitivity to adenosine and wortmannin. Type II PI 4- kinases are implicated in early signaling cascades during T cell activation. In addition to their putative role in mitogenic signal transduction, PI 4-kinases are also implicated in integrin-mediated signaling mechanisms, cytoskeletal reorganization and secretion. PI-4-P and PI-4,5-P2 themselves can interact with actin-binding proteins to regulate actin polymerization. The demonstration of physical association between $\alpha 3\beta 1$ integrin and PI 4-K suggests a link between integrin activation and metabolism of phosphoinositides (Berditchevski et al., 1997). Indeed, cell attachment is mediated by transmembrane receptors in the integrin family triggers signal transduction cascades that regulate cell proliferation, apoptosis, morphology, and cellular motility (Hynes et al., 2002; Blaess et al., 2004).

We additionally observed the up-regulation of 26S proteasome (Figure 32). Recent studies of the Smad family proteins, which are the signal transducers of the TGF-beta family ligands, have revealed the ability of Smads to interact with various components of the 26S proteasome system allowing to connect with those induced by many other extracellular regulators, thereby regulating a wide range of biological activities, including motility (Wang, 2003).

The overexpression of H-PRUNE in the MDA breast carcinoma clones up-regulates also the expression of Nedd4 binding protein 2 (N4BP2) (Figure 32). Yeast two-hybrid screening identified the N4BP2 protein and its full-length protein was referred to as BCL-3-binding protein (Watanabe et al., 2003). Several additional studies showed a correlation of bcl-3 induction in epithelial Na^+ transport processes.

Furthermore, plastins, members of a family of actin-binding protein, which exhibit a tissue-specific expression pattern were found up-regulated (Figure 32). L-plastin, which is specifically expressed in hematopoietic cell lineage, involved in the control of cell adhesion and motility was found up-regulated in the clones with high motility properties (MDA-H1-177-prune #8). This protein is also frequently expressed in cell lines derived from mammary solid tumors and therefore might be involved in cancer invasion and metastasis. One example is the experiment performed by Zheng et al. (1999), where they demonstrated the suppression of prostate carcinoma cell invasion by expression of antisense L-plastin gene.

In addition, the small GTPase Rab1b results up-regulated as the consequence of the overexpression of both H-PRUNE and NM23-H1 (Figure 32). Rab1b is essential for the transport from endoplasmic reticulum (ER) to Golgi. The secretory pathway in mammalian cells consists of a linear assembly of dynamic compartments. Transport and recycling between these compartments occur through generation of intermediates from the donor compartment and the delivery of such intermediates to the appropriate acceptor compartment. In the early secretory pathway, two isoforms of Rab1, Rab1a and Rab1b, have been shown to be required for protein transport from the endoplasmic reticulum (ER) to the cis-Golgi (Pind et al., 1994). Rabs have been proposed to act in a variety aspects of vesicular transport, including vesicle formation, motility, docking, and fusion. However, despite considerable advances in the discovery of some of its molecular mechanisms, the exact role of Rab function remains to be completely deciphered. Rabs proteins interact with Ras, a small guanosine triphosphate binding protein, which plays an important role in signal transduction pathways that influence cellular proliferation, apoptosis, cytoskeletal organization, and other important biological processes (Li and Sparano, 2003;

Kennedy and Davis, 2003; James et al., 2003). Ras mutations that result in constitutive activation of the Ras pathway are common in certain human cancers, and transfection of cell lines with mutant Ras induces tumorigenesis.

In the MDA clone, with an increased level of motility (MDA-H1-177-prune #8), up-regulation of Impedes Mitogenic signal Propagation (IMP), previously reported as a BRCA1-interacting protein 2 (Brap2), has also been observed (Figure 32). The IMP is a Ras effector that negatively regulates MAP kinase activation by limiting the formation of Raf-MEK complexes (Matheny et al., 2004). The protein was identified by its ability to bind to the nuclear localization signal of BRCA1. This latest protein, located into the cytoplasm, regulates negatively nuclear targeting transport by retaining proteins with a nuclear localization signal into the cytoplasm.

Among the genes up-regulated in the MDA-H1-177-prune #8 we additionally have found a novel Casein Kinase 2 Interacting Protein, designated CKIP-1 (Bosc et al., 2000) (Figure 32). CKIP-1 is a new component of PI3-K signaling in muscle differentiation. This protein additionally might regulate Casein Kinase (CK2) function, an essential, highly conserved, serine/threonine protein kinase present in all eukaryotic cells. Indirectly, CKIP-1 overexpression by binding to CK2 regulate a broad range of cellular proteins located in a variety of cellular compartments overall influencing transcription, translation, morphogenesis, and cell cycle progression.

Moreover, four genes, involved in extracellular matrix contacts and cellular adhesion (plakophilin, LIM), cytoscheleton re-organization (plakin) and in the oncosuppressor activity (EXT1), were found down regulated in the MDA-H1-177-prune #8 clone (Figure 32).

Desmosomes (DMs) are specialized cadherin-mediated adhesion complexes showing stability and rigidity to tissues under mechanical stress. These structures are

dynamic and continual renewal of stratifying epidermis layers involves both rapid synthesis and degradation of cellular junctions. Desmosomal adhesion may be compromised in invading and transitional metastases cell carcinomas, leading to a possible tumor suppressor function of desmosomal attachment (Tselepis et al., 1998; South et al., 2003) demonstrated that lack of plakophilin 1 increases keratinocyte migration and reduces desmosome stability, thus indicating a undoubted role of plakophilin in cell adhesion mechanisms.

One of the major signaling pathways involved in tumor metastasis is the Rho/ROCK/LIM kinase pathway, involved in the regulation of the actin cytoskeleton (Yoshioka et al., 2003). The skeletal muscle LIM protein 1 (SLIM1) localizes in an integrin-dependent manner to the nucleus and focal adhesions where it functions downstream of integrin activation to promote cell spreading and migration. LIM expression is down-regulated in the clones analyzed (MDA-H1-177-prune #8), indicating an alteration in a pathway correlated to cell migration.

Among the molecular mechanisms changes in gene expression in the MDA clones due to H-PRUNE and NM23-H1 overexpression, we observed down-regulation of plakin, appertaining to the family of adhesion junction plaque proteins, involved in the extracellular matrix contacts (Leung et al., 2001).

Supporting the hypothesis of the contribution of H-PRUNE to the higher oncogenic potential of the MDA breast carcinoma cell line analyzed (MDA-H1-177-prune #8) we observed the down-regulation of Exostose 1 gene, a putative tumour suppressor (Figure 32). Hereditary multiple exostoses, a dominantly inherited genetic disorder, characterized by multiple cartilaginous tumors, is caused by mutations in members of the EXT gene family, EXT1 or EXT2 (Senay et al., 2000). The proteins encoded by these genes, EXT1 and EXT2, are endoplasmic reticulum-localized type

II transmembrane glycoproteins that possess or are tightly associated with glycosyltransferase activities involved in the polymerization of heparan sulfate.

Interestingly, we found other two genes, correlated to motility, up-regulated in the clone overexpressing H-PRUNE and NM23-H1 with respect to NM23-H1 overexpressing alone.

The first gene encodes the dynein, light intermediate polypeptide 1 (DNALI1) (Figure 32). The motor protein cytoplasmic dynein is responsible for most of the minus-end-directed microtubule traffic within cells, obtaining from ATP hydrolysis to generate force and move in a step-like manner on microtubules. Dynein contains four evolutionarily conserved AAA (ATPase associated with various cellular activities) domains that are thought to bind nucleotide. Cytoplasmatic dynein is associated in vivo with vimentin intermediate filament and directly interacts with kinesin 1, coordinating motor activity (Ligon et al., 2004).

Furthermore, in the MDA clone overexpressing H-PRUNE we have found up-regulated the pleiotrophin (HB-GAM) (Figure 32), a protein involved in tumor growth, in the regulation of cell motility (Rauvala et al., 2000) and in the activation of tumor angiogenesis (Souttou et al., 2001). The pleiotrophin (PTN) and the namely heparin-binding growth factors belong to the midkine (MK) family. Pleiotrophin is expressed in embryonic and early post-natal fiber pathways of the nervous system, and it enhances axonal growth/guidance by binding to N-syndecan (syndecan-3) at the neuron surface. Widespread deregulation of pleiotrophin and midkine is found in many known human cancers and derived tumor cell lines, and it is known that pleiotrophin blocks tumor cell signaling, thus limited cell proliferation and tumor growth and metastasis in animal models (Zhang et al., 1999).

Understanding the molecular mechanism of the cellular motility and deciphering which other partners are acting together with H-PRUNE-NM23-H1 protein complex is now our major research direction. Certainly the above described breast carcinoma cellular model is our starting point to unravel new pathways correlated to cellular motility process and cancerogenesis. The cellular models presented here, will be a useful source to interpret the comprehensive protein networks responsible of cell migration, the first occurring event responsible of the enhancement of metastastic cellular processes.

Conclusions

This thesis has reviewed the biochemical activity of H-PRUNE and its functional role in correlation to NM23-H1, an anti-metastatic protein, in three different tumour types: sarcoma, neuroblastoma, and breast cancer. First, we have identified its phosphodiesterase activity and characterized its kinetic properties. H-PRUNE PDE activity is enhanced by the physical interaction with NM23-H1, and is suppressed by dipyridamole, a selective inhibitor of H-PRUNE.

We propose here two different models of action of H-PRUNE with respect to NM23-H1 anti-metastatic function, in correlation to H-PRUNE different cellular compartmentalization.

In sarcoma and in breast cancer, H-PRUNE localizes to the cytoplasm and high levels of H-PRUNE expression are associated with low levels of NM23-H1, suggesting a role of negative regulation of NM23-H1. In particular, we have demonstrated that both H-PRUNE PDE activity and H-PRUNE-NM23-H1 complex increase cell motility in MDA-MB-435 breast cancer cell line. In addition, H-PRUNE overexpression in the MDA-MB-435 cell line influences pathways and the expression of other genes, indicating its role in oncogenesis and metastatic processes. Moreover, we have found that dipyridamole, H-PRUNE selective inhibitor is able to reduce H-PRUNE pro-motility effect *in vitro*, suggesting that the selective H-PRUNE inhibitor could be a potential therapeutic drug for metastic diseases.

Furthermore, since H-PRUNE shows a nuclear localization in neuroblastoma cell lines and high levels of H-PRUNE, NM23-H1, and NM23-H2 have been found in advanced stages of the tumour, neuroblastoma resulted an intriguing model of study. In fact, we have demonstrated a new function of H-PRUNE associated to its nuclear localization, as being able to bind to the *NM23-H2* promoter and

transactivate its expression. In our model H-PRUNE contributes, both directly and indirectly, to NM23-H1 and NM23-H2 increased expression levels, suggesting that H-PRUNE positively regulates NM23s, which are associated to high metastatic potential in neuroblastoma.

Because of the H-PRUNE PDE function characterized and its role in cancer by increasing the metastatic potential in breast carcinoma and neuroblastoma, and because of its specific expression in brain development (Reymond et al., 1999), a conditional KO animal model will be an useful source to study its additional function by tissue specific functional ablation during mouse development. The recombinant vector containing both arms required for recombination has been additionally produced in my PhD laboratory bench work thesis. The construct will be injected into ES murine cells in order to generate chimerae and then, conditional KO mice, which will be an useful tool to elucidate H-PRUNE function in mouse development.

Finally, H-PRUNE is a novel phosphodiesterase and it is involved in tumour progression, regulating by different mechanisms the NM23-H1 anti-metastatic function. The overexpression of H-PRUNE has been associated to advanced stages of various types of tumours and the protein could be a potential target for clinical intervention.

The mouse model will be useful to clarify H-PRUNE role in development and further investigations will be addressed in order to elucidate the role of H-PRUNE-NM23-H1 complex in metastatic pathways.

References

Ahn S, Milner AJ, Futterer K, Konopka M, Ilias M, Young TW and White SA. (2001) The "open" and "closed" structures of the type-C inorganic pyrophosphatases from Bacillus subtilis and Streptococcus gordonii. *J Mol Biol* **313**, 797-811.

Aravind L. (1999) An evolutionary classification of the metallo-beta-lactamase fold proteins. *In Silico Biol* **1**, 69-91.

Aravind L and Koonin EV. (1998a) The HD domain defines a new superfamily of metal-dependent phosphohydrolases. *Trends Biochem Sci* **23**, 469-472.

Aravind L and Koonin EV. (1998b) A novel family of predicted phosphoesterases includes *Drosophila* prune protein and bacterial RecJ exonuclease. *Trends Biochem Sci* **23**, 17-19.

Backer JM, Mendola CE, Kovesdi I, Fairhurst JL, O'Hara B, Eddy RL Jr, Shows TB, Mathew S, Murty VV, Chaganti RS. (1993) Chromosomal localization and nucleoside diphosphate kinase activity of human metastasis-suppressor genes NM23-1 and NM23-2. *Oncogene* **8**, (2):497-502.

Barlund M, Monni O, Kononen J, Cornelison R, Torhorst J, Sauter G, Kallioniemi OLLI-P, Kallioniemi A. (2000) Multiple genes at 17q23 undergo amplification and overexpression in breast cancer. *Cancer Res* **1**, 60(19):5340-5344.

Beavo JA and Brunton LL. (2002) Cyclic nucleotide research -- still expanding after half a century. *Nat Rev Mol Cell Biol* **3**, 710-718.

Berberich SJ and Postel EH. (1995) PuF/NM23-H2/NDPK-B transactivates a human cmyc promoter-CAT gene via a functional nuclease hypersensitive element. *Oncogene* **10**, 2343-2347.

Berditchevski F, Tolias KF, Wong K, Carpenter CL, Hemler ME. (1997) A novel link between integrins, transmembrane-4 superfamily proteins (CD63 and CD81), and phosphatidylinositol 4-kinase. *J Biol Chem* **272**, 2595-2598.

Biggs J, Tripoulas N, Hersperger E, Dearolf C, Shearn A. (1988) Analysis of the lethal interaction between the prune and Killer of prune mutations of Drosophila. *Genes Dev* **2**, 1333-1343.

Blaess S, Graus-Porta D, Belvindrah R, Radakovits R, Pons S, Littlewood-Evans A, Senften M, Guo H, Li Y, Miner JH, Reichardt LF, Muller U. (2004) Beta1-integrins are critical for cerebellar granule cell precursor proliferation. *J Neurosci* **24**, 3402-3412.

Bosc DG, Graham KC, Saulnier RB, Zhang C, Prober D, Gietz RD, Litchfield DW. (2000) Identification and characterization of CKIP-1, a novel pleckstrin homology domain-containing protein that interacts with protein kinase CK2. *J Biol Chem* **275**, 14295-14306.

Bown N. (2001) Neuroblastoma tumour genetics: clinical and biological aspects. *J Clin Pathol* **54**, 897-910.

Bown N, Cotterill S, Lastowska M, O'Neill S, Pearson AD, Plantaz D, Meddeb M, Danglot G, Brinkschmidt C, Christiansen H *et al.* (1999) Gain of chromosome arm 17q and adverse outcome in patients with neuroblastoma. *N Engl J Med* **340**, 1954-1956.

Bradford MM. (1976) A rapid and sensitive method for the quantitation of microgram quantities of protein utilizing the principle of protein-dye binding. *Anal Biochem* **72**, 248-254.

Brodeur GM. (2003) Neuroblastoma: biological insights into a clinical enigma. *Nat Rev Cancer* **3**, (3):203-216. Review.

Brodeur GM, Maris JM, Yamashiro DJ, Hogarty MD, White PS. (1997) Biology and genetics of human neuroblastomas. Rev. *J Pediatr Hematol Oncol* **19**, (2):93-101.

Budd GT, Herzog P and Bukowski RM. (1994) Phase I/II trial of dipyridamole, 5-fluorouracil, leukovorin, and mitoxantrone in metastatic breast cancer. *Invest New Drugs* **12**, 283-287.

Budd GT, Jayaraj A, Grabowski D, Adelstein D, Bauer L, Boyett J, Bukowski R, Murthy, S. and Weick, J. (1990) Phase I trial of dipyridamole with 5-fluorouracil and folinic acid. *Cancer Res* **50**, 7206-7211.

Caligo MA, Cipollini G, Berti A, Viacava P, Collecchi P, Bevilacqua G. (1997) NM23 gene expression in human breast carcinomas: loss of correlation with cell proliferation in the advanced phase of tumor progression. *Int J Cancer* **20**, 74(1):102-111.

Chang CL, Zhu XX, Thoraval DH, Ungar D, Rawwas J, Hora N, Strahler JR, Hanash SM and Radany E. (1994) Nm23-H1 mutation in neuroblastoma [letter]. *Nature* **370**, 335-336.

Chou MM and Blenis J. (1995) The 70 kDa S6 kinase: regulation of a kinase with multiple roles in mitogenic signalling. *Curr Opin Cell Biol* **7**, (6):806-814.

Cimpean A, Stefan C, Gijsbers R, Stalmans W, Bollen M. (2004) Substrate-specifying determinants of the nucleotide pyrophosphatases/phosphodiesterases NPP1 and NPP2. *Biochem J.* 1, **381**(Pt 1):71-77.

Cipollini G, Berti A, Fiore L, Rainaldi G, Basolo F, Merlo G, Bevilacqua G, Caligo MA. (1997) Down-regulation of the nm23.h1 gene inhibits cell proliferation. *Int J Cancer* **9**, 73(2):297-302.

Corvi R, Amler LC, Savelyeva L, Gehring M, Schwab M. (1994) MYCN is retained in single copy at chromosome 2 band p23-24 during amplification in human neuroblastoma cells. *Proc Natl Acad Sci U S A.* **7**, 91(12):5523-5527.

Cuny M, Kramar A, Courjal F, Johannsdottir V, Iacopetta B, Fontaine H, Grenier J, Culine S, Theillet C. (2000) Relating genotype and phenotype in breast cancer: an analysis of the prognostic significance of amplification at eight different genes or loci and of p53 mutations. *Cancer Res* **15**, 60(4):1077-1083.

D'Angelo A, Garzia L, André A, Carotenuto P, Aglio V, Guardiola O, Arrigoni G, Cossu A, Palmieri G, Aravind L, Zollo M. (2004) Prune cAMP phosphodiesterase binds nm23-H1 and promotes cancer metastasis. *Cancer Cell* **5**, 137-149.

Du J and Hannon GJ. (2002) The centrosomal kinase Aurora-A/STK15 interacts with a putative tumor suppressor NM23-H1. *Nucleic Acids Res* **15**, 30(24):5465-5475.

Ejeskar K, Aburatani H, Abrahamsson J, Kogner P and Martinsson T. (1998) Loss of heterozygosity of 3p markers in neuroblastoma tumours implicate a tumour-suppressor locus distal to the FHIT gene. *Br J Cancer* **77**, 1787-1791.

Engel M, Veron M, Theisinger B, Lacombe ML, Seib T, Dooley S, Welter C. (1995) A novel serine/threonine-specific protein phosphotransferase activity of Nm23/nucleoside-diphosphate kinase. *Eur J Biochem* **15**, 234(1):200-207.

Enzinger FM and Weiss SW. (1995). Soft tissue tumors, 3rd edn. Mosby-Year Book Inc., St. Louis.

Fan Z, Beresford PJ, Oh DY, Zhang D and Lieberman J. (2003) Tumor suppressor NM23-H1 is a granzyme A-activated DNase during CTL-mediated apoptosis, and the nucleosome assembly protein SET is its inhibitor. *Cell* **112**, 659-672.

Fawcett L, Baxendale R, Stacey P, McGrouther C, Harrow I, Soderling S, Hetman J, Beavo JA, Phillips SC. (2000) Molecular cloning and characterization of a distinct human phosphodiesterase gene family: PDE11A. *Proc Natl Acad Sci U S A.* **28**, 97(7):3702-3707.

Fix A, Peter M, Pierron G, Aurias A, Delattre O, Janoueix-Lerosey I. (2004) High-resolution mapping of amplicons of the short arm of chromosome 1 in two neuroblastoma tumors by microarray-based comparative genomic hybridization. *Genes Chromosomes Cancer* **40,** (3):266-270.

Fletcher CD. (2002) Distinctive soft tissue tumors of the head and neck. *Mod Pathol.* **15,** (3):324-330. Review

Florenes VA, Aamdal S, Myklebost O, Maelandsmo GM, Bruland OS and Fodstad O. (1992) Levels of nm23 messenger RNA in metastatic malignant melanomas: inverse correlation to disease progression. *Cancer Res* **52**, 6088-6091.

Fong CT, White PS, Peterson K, Sapienza C, Cavenee WK, Kern SE, Vogelstein B, Cantor AB, Look AT and Brodeur GM. (1992) Loss of heterozygosity for chromosomes 1 or 14 defines subsets of advanced neuroblastomas. *Cancer Res* **52**, 1780-1785.

Forus A, D'Angelo A, Henriksen J, Merla G, Maelandsmo GM, Florenes VA, Olivieri S, Bjerkehagen B, Meza-Zepeda LA, del Vecchio Blanco F, Muller C, Sanvito F, Kononen J, Nesland JM, Fodstad O, Reymond A, Kallioniemi OP, Arrigoni G, Ballabio A, Myklebost O and Zollo M. (2001) Amplification

and overexpression of PRUNE in human sarcomas and breast carcinomas-a possible mechanism for altering the nm23-H1 activity. *Oncogene* **20**, 6881-6890.

Forus A, Florenes VA, Maelandsmo GM, Meltzer PS, Fodstad O, Myklebost O. (1993) Mapping of amplification units in the q13-14 region of chromosome 12 in human sarcomas: some amplica do not include MDM2. *Cell Growth Differ* **4**, (12):1065-1070.

Forus A., Weghuis DO, Smeets D, Fodstad O, Myklebost O, Guerts van Kessel A. (1995a) Comparative genomic hybridization analysis of human sarcomas: I. Occurrence of genomic imbalances and identification of a novel major amplicon at 1q21-q22 in soft tissue sarcomas. *Genes Chromosomes Cancer* **14**, (1): 8-14.

Forus A., Weghuis DO, Smeets D, Fodstad O, Myklebost O, Guerts van Kessel A. (1995b) Comparative genomic hybridization analysis of human sarcomas: II. Identification of novel amplicons at 6p and 17p in osteosarcomas. *Genes Chromosomes Cancer* **14**, (1): 15-21.

Freije JM, Blay P, MacDonald NJ, Manrow RE and Steeg PS. (1997a) Site-directed mutation of Nm23-H1. Mutations lacking motility suppressive capacity upon transfection are deficient in histidine- dependent protein phosphotransferase pathways in vitro. *J Biol Chem* **272**, 5525-5532.

Freije JM, Lawrence JA, Hollingshead MG, De la Rosa A, Narayanan V, Grever M, Sausville EA, Paull K and Steeg PS. (1997b) Identification of compounds with preferential inhibitory activity against low-Nm23-expressing human breast carcinoma and melanoma cell lines. *Nat Med* **3**, 395-401.

Galperin MY, Natale DA, Aravind L. and Koonin EV (1999) A specialized version of the HD hydrolase domain implicated in signal transduction. *J Mol Microbiol Biotechnol* **1**, 303-305.

Garzia L, Andre A, Amoresano A, D'Angelo A, Martusciello R, Cirulli C, Tsurumi T, Marino G and Zollo M. (2003) Method to express and purify nm23-H2 protein from Baculovirus infected cells. *Biotechniques* **35**, 384-391.

Garzia L, D'Angelo A, Volinia S, Andrè A, Cirulli C, Amoresano A, Marino G, Campanella C, Zollo M. (2004) Phosphorylation of nm23-H1 and nm23-H2 by CKIδinduces complex formation with h-prune and cellular motility. Submitted.

Gervasi F, D'Agnano I, Vossio S, Zupi G, Sacchi A, Lombardi D. (1996) Nm23 influences proliferation and differentiation of PC12 cells in response to nerve growth factor. *Cell Growth Differ* **7**, (12):1689-1695.

Godfried MB, Veenstra M, v Sluis P, Boon K, v Asperen R, Hermus MC, v Schaik BD, Voute TP, Schwab M, Versteeg R. (2002) The N-myc and c-myc downstream pathways include the chromosome 17q genes nm23-H1 and nm23-H2. *Oncogene* **21**, 2097-2101.

Grand CL, Powell TJ, Nagle RB, Bearss DJ, Tye D, Gleason-Guzman M, Hurley LH. (2004) Mutations in the G-quadruplex silencer element and their relationship to c-MYC overexpression, NM23 repression, and therapeutic rescue. *Proc Natl Acad Sci U S A.* **20**, 101(16):6140-6145. Epub 2004 Apr 12.

Guin GH, Gilbert EF and Jones B. (1969) Incidental neuroblastoma in infants. *Am J Clin Pathol* **51**, 126-136.

Guo C, White PS, Weiss MJ, Hogarty MD, Thompson PM, Stram DO, Gerbing R, Matthay KK, Seeger RC, Brodeur GM *et al.* (1999) Allelic deletion at 11q23 is common in MYCN single copy neuroblastomas. *Oncogene* **18**, 4948-4957.

Haaz MC, Fischel JL, Formento P, Renee N, Etienne MC and Milano G. (1996) Impact of different fluorouracil biochemical modulators on cellular dihydropyrimidine dehydrogenase. *Cancer Chemother Pharmacol* **38**, 52-58.

Hailat N, Keim DR, Melhem RF, Zhu XX, Eckerskorn C, Brodeur GM, Reynolds CP, Seeger RC, Lottspeich F, Strahler JR. (1991) High levels of p19/nm23 protein in neuroblastoma are associated with advanced stage disease and with N-myc gene amplification. *J Clin Invest* **88**, 341-345.

Hamby CV, Abbi R, Prasad N, Stauffer C, Thomson J, Mendola CE, Sidorov V and Backer JM. (2000) Expression of a catalytically inactive H118Y mutant of nm23-H2 suppresses the metastatic potential of line IV Cl 1 human melanoma cells. *Int J Cancer* **88**, 547-553.

Hamby CV, Mendola CE, Potla L, Stafford G and Backer JM. (1995) Differential expression and mutation of NME genes in autologous cultured human melanoma cells with different metastatic potentials. *Biochem Biophys Res Commun* **211**, 579-585.

Hanahan D, Weinberg RA. (2000) The hallmarks of cancer. *Cell* **7**, 100(1):57-70. Review.

Hartsough MT, Clare SE, Mair M, Elkahloun AG, Sgroi D, Osborne CK, Clark G and Steeg PS. (2001) Elevation of breast carcinoma Nm23-H1 metastasis suppressor gene expression and reduced motility by DNA methylation inhibition. *Cancer Res* **61**, 2320-2327.

Hartsough MT, Morrison DK, Salerno M, Palmieri D, Ouatas T, Mair M, Patrick J, Steeg PS. (2002) Nm23-H1 metastasis suppressor phosphorylation of kinase suppressor of Ras via a histidine protein kinase pathway. *J Biol Chem* **30**, 277(35):32389-32399. Epub 2002 Jun 24.

Hartsough MT and Steeg PS. (1998) Nm23-H1: genetic alterations and expression patterns in tumor metastasis. *Am J Hum Genet* **63**, 6-10.

Hartsough MT and Steeg PS. (2000) Nm23/nucleoside diphosphate kinase in human cancers. *J Bioenerg Biomembr* **32**, 301-308.

Heilmeyer LM Jr, Vereb Jr, Vereb G, Kakuk A, Szivak I. (2003) Mammalian phosphatidylinositol 4-kinases. *IUBMB Life* **55**, 59-65.

Hejna M, Raderer M and Zielinski CC. (1999) Inhibition of metastases by anticoagulants. *J Natl Cancer Inst* **91**, 22-36.

Hennessy C, Henry JA, May FE, Westley BR, Angus B, Lennard TW. (1991) Expression of the antimetastatic gene nm23 in human breast cancer: an association with good prognosis. *J Natl Cancer Inst* **20**, 83(4):281-285.

Howlett AR, Petersen OW, Steeg PS and Bissell MJ. (1994) A novel function for the nm23-H1 gene: overexpression in human breast carcinoma cells leads to the formation of basement membrane and growth arrest. *J Natl Cancer Inst* **86**, 1838-1844.

Hynes RO, Lively JC, McCarty JH, Taverna D, Francis SE, Hodivala-Dilke K, Xiao Q. (2002) The diverse roles of integrins and their ligands in angiogenesis. *Cold Spring Harb Symp Quant Biol* **67**, 143-153.

James RM, Arends MJ, Plowman SJ, Brooks DG, Miles CG, West JD, Patek CE. (2003) K-ras proto-oncogene exhibits tumor suppressor activity as its absence promotes tumorigenesis in murine teratomas. *Mol Cancer Res* **1**, 820-825.

Janoueix-Lerosey I, Penther D, Thioux M, de Cremoux P, Derre J, Ambros P, Vielh P, Benard J, Aurias A and Delattre O. (2000) Molecular analysis of chromosome arm 17q gain in neuroblastoma. *Genes Chromosomes Cancer* **28**, 276-284.

Kallioniemi A, Kallioniemi O-P, Sudar D, Rutovitz D, Gray JW, Waldman F and Pinkel D. (1992) Comparative genomic hybridization for molecular cytogenetic analysis of solid tumors. *Science* **258**, 818-821.

Kaneko Y and Knudson AG. (2000) Mechanism and relevance of ploidy in neuroblastoma. *Genes Chromosomes Cancer* **29**, 89-95.

Kantor JD, McCormick B, Steeg PS and Zetter BR. (1993) Inhibition of cell motility after nm23 transfection of human and murine tumor cells. *Cancer Res* **53**, 1971-1973.

Kennedy NJ, Davis RJ. (2003) Role of JNK in tumor development. *Cell Cycle* **2**, 199-201.

Khatib ZA, Matsushime H, Valentine M, Shapiro DN, Sherr CJ and Look AT. (1993) Coamplification of the CDK4 gene with MDM2 and GLI in human sarcomas. *Cancer Res* **15**, 53(22):5535-5541.

Kikkawa S, Takahashi K, Takahashi K, Shimada N, Ui M, Kimura N, Katada T. (1990) Conversion of GDP into GTP by nucleoside diphosphate kinase on the GTP-binding proteins. *J Biol Chem* **15**, 265(35):21536-21540. Erratum in: J Biol Chem 1991 Jul 5, 266(19):12795.

Kimura N, Shimada N, Ishijima Y, Fukuda M, Takagi Y, Ishikawa N. (2003) Nucleoside diphosphate kinases in mammalian signal transduction systems: recent development and perspective. *J Bioenerg Biomembr* **35**, (1):41-47. Review.

Kraeft SK, Traincart F, Mesnildrey S, Bourdais J, Veron M and Chen LB. (1996) Nuclear localization of nucleoside diphosphate kinase type B (nm23-H2) in cultured cells. *Exp Cell Res* **227**, 63-69.

Kudoh K, Takano M, Koshikawa T, Hirai M, Yoshida S, Mano Y, Yamamoto K, Ishii K, Kita T, Kikuchi Y, Nagata I, Miwa M, Uchida K. (1999) Gains of 1q21-q22 and 13q12-q14 are potential indicators for resistance to cisplatin-based chemotherapy in ovarian cancer patients. *Clin Cancer Res* **5**, (9):2526-2531.

Lacombe ML, Milon L, Munier A, Mehus JG, Lambeth DO. (2000) The human Nm23/nucleoside diphosphate kinases. *J Bioenerg Biomembr* **32**, (3):247-258. Review.

Lascu I, Chaffotte A, Limbourg-Bouchon B, Veron M. (1992) A Pro/Ser substitution in nucleoside diphosphate kinase of Drosophila melanogaster (mutation killer of prune) affects stability but not catalytic efficiency of the enzyme. *J Biol Chem* 25, **267**(18):12775-81.

Lascu I, Schaertl S, Wang C, Sarger C, Giartosio A, Briand G, Lacombe ML and Konrad M. (1997) A point mutation of human nucleoside diphosphate kinase A found in aggressive neuroblastoma affects protein folding. *J Biol Chem* **272**, 15599-15602.

Leone A, Flatow U, VanHoutte K and Steeg PS. (1993a) Transfection of human nm23-H1 into the human MDA-MB-435 breast carcinoma cell line: effects on tumor metastatic potential, colonization and enzymatic activity. *Oncogene* **8**, 2325-2333.

Leone A, Seeger RC, Hong CM, Hu YY, Arboleda MJ, Brodeur GM, Stram D, Slamon DJ and Steeg PS. (1993b) Evidence for nm23 RNA overexpression,

DNA amplification and mutation in aggressive childhood neuroblastomas. *Oncogene* **8**, 855-865.

Leung CL, Liem RK, Parry DA, Green KJ. (2001) The plakin family. *J Cell Sci* **114**, 3409-3410.

Li T and Sparano JA. (2003) Inhibiting Ras signaling in the therapy of breast cancer. *Clin Breast Cancer* **3**, 405-416; discussion 17-20.

Ligon LA, Tokito M, Finkelstein JM, Grossman FE, Holzbaur EL. (2004) A direct interaction between cytoplasmic dynein and kinesin I may coordinate motor activity. *J Biol Chem* **30**, 279(18):19201-19208. Epub 2004 Feb 24.

Liotta LA and Kohn EC. (2001) The microenvironment of the tumour-host interface. *Nature* **17**, 411(6835):375-379. Review.

Lombardi D, Lacombe ML and Paggi MG. (2000) Nm23: unraveling its biological function in cell differentiation. *J Cell Physiol* **182**, 144-149.

Lombardi D, Sacchi A, D'Agostino G, Tibursi G. (1995) The association of the Nm23-M1 protein and beta-tubulin correlates with cell differentiation. *Exp Cell Res* **217**, (2):267-271.

Ma D, McCorkle JR, Kaetzel DM. (2004) The metastasis suppressor NM23-H1 possesses 3'-5' exonuclease activity. *J Biol Chem* **23**, 279(17):18073-18084. Epub 2004 Feb 11.

MacDonald NJ, De la Rosa A, Benedict MA, Freije JM, Krutsch H, Steeg PS. (1993) A serine phosphorylation of Nm23, and not its nucleoside diphosphate kinase activity, correlates with suppression of tumor metastatic potential. *J Biol Chem* **5**, 268(34):25780-25789.

MacDonald NJ, Freije JM, Stracke ML, Manrow RE and Steeg PS. (1996) Site-directed mutagenesis of nm23-H1. Mutation of proline 96 or serine 120

abrogates its motility inhibitory activity upon transfection into human breast carcinoma cells. *J Biol Chem* **271**, 25107-25116.

Mao H, Liu H, Fu X, Fang Z, Abrams J and Worsham MJ. (2001) Loss of nm23 expression predicts distal metastases and poorer survival for breast cancer. *Int J Oncol* **18**, 587-591.

Maris JM and Matthay KK. (1999) Molecular biology of neuroblastoma. *J Clin Oncol* **17**, 2264-2279.

Maris JM, Weiss MJ, Mosse Y, Hii G, Guo C, White PS, Hogarty MD, Mirensky T, Brodeur GM, Rebbeck TR. *et al.* (2002) Evidence for a hereditary neuroblastoma predisposition locus at chromosome 16p12-13. *Cancer Res* **62**, 6651-6658.

Marshall B, Isidro G, Martins AG and Boavida MG. (1997) Loss of heterozygosity at chromosome 9p21 in primary neuroblastomas: evidence for two deleted regions. *Cancer Genet Cytogenet* **96**, 134-139.

Matheny SA, Chen C, Kortum RL, Razidlo GL, Lewis RE, White MA. (2004) Ras regulates assembly of mitogenic signalling complexes through the effector protein IMP. *Nature* **427**, 256-260.

Meltzer SJ, O'Doherty SP, Frantz CN, Smolinski K, Yin J, Cantor AB, Liu J, Valentine, M, Brodeur GM and Berg PE. (1996) Allelic imbalance on chromosome 5q predicts long-term survival in neuroblastoma. *Br J Cancer* **74**, 1855-1861.

Momand J, Zambetti GP, Olson DC, George D, Levine AJ. (1992) The mdm-2 oncogene product forms a complex with the p53 protein and inhibits p53-mediated transactivation. *Cell* **26**, 69(7):1237-1245.

Mora J, Cheung NK, Oplanich S, Chen L and Gerald WL. (2002) Novel regions of allelic imbalance identified by genome-wide analysis of neuroblastoma. *Cancer Res* **62**, 1761-1767.

Muleris M, Almeida A, Gerbault-Seureau M, Malfoy B, Dutrillaux B. (1994) Detection of DNA amplification in 17 primary breast carcinomas with homogeneously staining regions by a modified comparative genomic hybridization technique. *Genes Chromosomes Cancer* **10**, (3):160-70.

Muller W, Schneiders A, Hommel G, Gabbert HE. (1998) Expression of nm23 in gastric carcinoma: association with tumor progression and poor prognosis. *Cancer* **15**, 83(12):2481-2487.

Niitsu N, Okabe-Kado J, Okamoto M, Takagi T, Yoshida T, Aoki S, Hirano M and Honma Y. (2001) Serum nm23-H1 protein as a prognostic factor in aggressive non-Hodgkin lymphoma. *Blood* **97**, 1202-1210.

Nilsson M, Meza-Zepeda LA, Mertens F, Forus A, Myklebost O, Mandahl N. (2004) Amplification of chromosome 1 sequences in lipomatous tumors and other sarcomas. *Int J Cancer* **10**, 109(3):363-369.

Oliner JD, Kinzler KW, Meltzer PS, George DL and Vogelstein B. (1992) Amplification of a gene encoding a p53-associated protein in human sarcomas. *Nature* **2**, 358(6381):80-83.

Orevi N, Falk R (1975) Temperature-sensitive prune (pn) mutations of Drosophila melanogaster. *Mutat Res* **33**, 193-200.

Otsuki Y, Tanaka M, Yoshii S, Kawazoe N, Nakaya K, Sugimura H. (2001) Tumor metastasis suppressor nm23H1 regulates Rac1 GTPase by interaction with Tiam1. *Proc Natl Acad Sci U S A.* **10**, 98(8):4385-4390. Epub 2001 Mar 27.

Ouatas T, Salerno M, Palmieri D, Steeg PS. (2003) Basic and translational advances in cancer metastasis: Nm23. J Bioenerg Biomembr. **35**, (1):73-9. Review.

Pear WS, Nolan GP, Scott ML, and Baltimore D (1993) Production of High-Titer Helper-Free Retroviruses by Transient Transfection *Proc Natl Acad Sci U S A* **90**, 8392-8396.

Pind SN, Nuoffer C, McCaffery JM, Plutner H, Davidson HW, Farquhar MG, Balch WE. (1994) Rab1 and Ca2+ are required for the fusion of carrier vesicles mediating endoplasmic reticulum to Golgi transport. *J Cell Biol* **125**, 239-252.

Postel EH. (1996) NM23/Nucleoside diphosphate kinase as a transcriptional activator of c-myc. *Curr Top Microbiol Immunol* **213 (Pt 2),** 233-252.

Postel EH. (1999) Cleavage of DNA by human NM23-H2/nucleoside diphosphate kinase involves formation of a covalent protein-DNA complex. *J Biol Chem.* **6**, 274(32):22821-22829.

Postel EH, Berberich SJ, Flint SJ and Ferrone CA. (1993) Human c-myc transcription factor PuF identified as nm23-H2 nucleoside diphosphate kinase, a candidate suppressor of tumor metastasis. *Science* **261,** 478-480.

Postel EH, Weiss VH, Beneken J and Kirtane A. (1996) Mutational analysis of NM23-H2/NDP kinase identifies the structural domains critical to recognition of a c-myc regulatory element. *Proc Natl Acad Sci U S A* **93,** 6892-6897.

Randazzo PA, Northup JK, Kahn RA. (1991) Activation of a small GTP-binding protein by nucleoside diphosphate kinase. *Science* **8**, 254(5033):850-853.

Rauvala H, Huttunen HJ, Fages C, Kaksonen M, Kinnunen T, Imai S, Raulo E, Kilpelainen I. (2000) Heparin-binding proteins HB-GAM (pleiotrophin) and amphoterin in the regulation of cell motility. *Matrix Biol* **19**, (5):377-387

Reymond A, Volorio S, Merla G, Al-Maghtheh M, Zuffardi O, Bulfone A, Ballabio A and Zollo M. (1999) Evidence for interaction between human PRUNE and nm23-H1 NDPKinase. *Oncogene* **18**, 7244-7252.

Rosengard AM, Krutzsch HC, Shearn A, Biggs JR, Barker E, Margulies IM, King CR, Liotta LA, Steeg PS. (1989) Reduced Nm23/Awd protein in tumour metastasis and aberrant Drosophila development. *Nature* **9**, 342(6246):177-180.

Ross JS and Fletcher JA. (1999) HER-2/neu (c-erb-B2) gene and protein in breast cancer. *Am J Clin Pathol* **112**, 53-67. Review.

Royds JA, Robinson MH, Stephenson TJ, Rees RC, Fisher C (1997) The association between nm23 gene expression and survival in patients with sarcomas. *Br J Cancer* **75**, 1195-1200.

Salerno M, Ouatas T, Palmieri D, Steeg PS. (2003) Inhibition of signal transduction by the nm23 metastasis suppressor: possible mechanisms. *Clin Exp Metastasis*. **20**, (1):3-10. Review.

Sambrook J, Fritsch EF, and Maniatis T. (1989) Molecular cloning. A laboratory manual. 2a ed. USA, Cold Spring Harbor Laboratory Press.

Savelyeva L, Schwab M. (2001) Amplification of oncogenes revisited: from expression profiling to clinical application. *Cancer Lett* **26**, 167(2):115-123. Review.

Schaertl S, Geeves MA and Konrad M. (1999) Human nucleoside diphosphate kinase B (Nm23-H2) from melanoma cells shows altered phosphoryl transfer activity due to the S122P mutation. *J Biol Chem* **274**, 20159-20164.

Schneider J, Pollan M, Jimenez E, Marenbach K, Martinez N, Volm M, Marx D, Meden H. (2000) nm23-H1 expression defines a high-risk subpopulation of

patients with early-stage epithelial ovarian carcinoma. *Br J Cancer* **82**, (10):1662-1670.

Schwab M. (1991) Enhanced expression of the cellular oncogene MYCN and progression of human neuroblastoma. *Adv Enzyme Regul* **31**, 329-338.

Schwab M. (1997) MYCN Amplification in Neuroblastoma: a Paradigm for the Clinical Use of an Oncogene. *Pathol Oncol Res* **3**, (1):3-7.

Schwab M. (1998) Amplification of oncogenes in human cancer cells. *Bioessays* **20**, (6):473-479.

Schwab M, Westermann F, Hero B, Berthold F. (2003) Neuroblastoma: biology and molecular and chromosomal pathology. *Lancet Oncol* **4**, (8):472-480. Review.

Seeger RC, Brodeur GM, Sather H, Dalton A, Siegel SE, Wong KY and Hammond D. (1985) Association of multiple copies of the N-myc oncogene with rapid progression of neuroblastomas. *N Engl J Med* **313**, 1111-1116.

Senay C, Lind T, Muguruma K, Tone Y, Kitagawa H, Sugahara K, Lidholt K, Lindahl U, Kusche-Gullberg M. (2000) The EXT1/EXT2 tumor suppressors: catalytic activities and role in heparan sulfate biosynthesis. *EMBO Rep* **1**, 282-286.

Sleeman JP. (2000) The lymph node as a bridgehead in the metastatic dissemination of tumors. Recent Results *Cancer Res* **157**, 55-81.

Smith SH, Weiss SW, Jankowski SA, Coccia MA, Meltzer PS. (1992) SAS amplification in soft tissue sarcomas *Cancer Res* **1**, 52(13):3746-3749.

Sobin LH, Fleming ID. TNM Classification of Malignant Tumors, fifth edition (1997). Union Internationale Contre le Cancer and the American Joint Committee on Cancer. *Cancer* **1**, 80(9):1803-1804.

South AP, Wan H, Stone MG, Dopping-Hepenstal PJ, Purkis PE, Marshall JF, Leigh IM, Eady RA, Hart IR, McGrath JA. (2003) Lack of plakophilin 1 increases keratinocyte migration and reduces desmosome stability. *J Cell Sci* **116**, 3303-3314.

Souttou B, Raulais D, Vigny M. (2001) Pleiotrophin induces angiogenesis: involvement of the phosphoinositide-3 kinase but not the nitric oxide synthase pathways. *J Cell Physiol* **187**, 59-64.

Srivatsa PJ, Cliby WA, Keeney GL, Dodson MK, Suman VJ, Roche PC, Podratz KC. (1996) Elevated nm23 protein expression is correlated with diminished progression-free survival in patients with epithelial ovarian carcinoma. *Gynecol Oncol* **60**, (3):363-372.

Steeg PS. (2003) Metastasis suppressors alter the signal transduction of cancer cells. *Nat Rev Cancer* **3**, 55-63.

Steeg PS, Bevilacqua G, Kopper L, Thorgeirsson UP, Talmadge JE, Liotta LA, Sobel ME. (1988) Evidence for a novel gene associated with low tumor metastatic potential. *J Natl Cancer Inst* **6**, 80(3):200-204.

Subrahmanyam G, Rudd CE, Schneider H. (2003) Association of T cell antigen CD7 with type II phosphatidylinositol-4 kinase, a key component in pathways of inositol phosphate turnover. *Eur J Immunol* **33**, 46-52.

Subramanian C, Cotter MA 2nd, Robertson ES. (2001) Epstein-Barr virus nuclear protein EBNA-3C interacts with the human metastatic suppressor Nm23-H1: a molecular link to cancer metastasis. *Nat Med* **7**, (3): 350-355.

Szymanska J, Tarkkanen M, Wiklund T, Virolainen M, Blomquist C, Asko-Seljavaara S, Tukiainen E, Elomaa I and Knuutila S. (1996). Gains and losses

of DNA sequences in liposarcomas evaluated by comparative genomic hybridization. *Genes Chromosomes Cancer* **15**, (2):89-94.

Takita J, Hayashi Y, Takei K, Yamaguchi N, Hanada R, Yamamoto K and Yokota J. (2000) Allelic imbalance on chromosome 18 in neuroblastoma. *Eur J Cancer* **36**, 508-513.

Takita J, Ishii M, Tsutsumi S, Tanaka Y, Kato K, Toyoda Y, Hanada R, Yamamoto K, Hayashi Y, Aburatani H. (2004) Gene expression profiling and identification of novel prognostic marker genes in neuroblastoma. *Genes Chromosomes Cancer* **40**, (2): 120-132.

Tanaka T, Sugimoto T, Sawada T. (1998) Prognostic discrimination among neuroblastomas according to Ha-ras/trk A gene expression: a comparison of the profiles of neuroblastomas detected clinically and those detected through mass screening. *Cancer* **15**, 83(8):1626-1633.

Tanaka S, Tajiri T, Noguchi S, Shono K, Ihara K, Hara T, Suita S. (2004) Clinical significance of a highly sensitive analysis for gene dosage and the expression level of MYCN in neuroblastoma. *J Pediatr Surg* **39**, (1): 63-68.

Tarkkanen M, Elomaa I, Blomqvist C, Kivioja AH, Kellokumpu-Lehtinen P, Bohling T, Valle J, Knuutila S. (1999) DNA sequence copy number increase at 8q: a potential new prognostic marker in high-grade osteosarcoma. *Int J Cancer* **20**, 84(2):114-121

Timmons L and Shearn A. (1996) Germline transformation using a prune cDNA rescues prune/killer of prune lethality and the prune eye color phenotype in Drosophila. *Genetics* **144**, 1589-1600.

Tirkkonen M, Tanner M, Karhu R, Kallioniemi A, Isola J, Kallioniemi OP. (1998) Molecular cytogenetics of primary breast cancer by CGH. *Genes Chromosomes Cancer* **21**, (3): 177-184.

Tonini GP, Longo L, Coco S and Perri P. (2003) Familial neuroblastoma: a complex heritable disease. *Cancer Lett* **197**, 41-45.

Tselepis C, Chidgey M, North A, Garrod D. (1998) Desmosomal adhesion inhibits invasive behavior. *Proc Natl Acad Sci U S A* **95**, 8064-8069.

Tseng YH, Vicent D, Zhu J, Niu Y, Adeyinka A, Moyers JS, Watson PH and Kahn CR. (2001) Regulation of growth and tumorigenicity of breast cancer cells by the low molecular weight GTPase Rad and nm23. *Cancer Res* **61**, 2071-2079.

Venkitaraman AR. (2002) Cancer susceptibility and the functions of BRCA1 and BRCA2. *Cell* **25**, 108(2):171-182. Review.

Wagner PD, Vu ND. (2000) Histidine to aspartate phosphotransferase activity of nm23 proteins: phosphorylation of aldolase C on Asp-319. *Biochem J* **15**, 346 Pt 3:623-630.

Wagner PD, Steeg PS, Vu ND. (1997) Two-component kinase-like activity of nm23 correlates with its motility- suppressing activity. *Proc Natl Acad Sci U S A* **94**, 9000-9005.

Wang T. (2003) The 26S proteasome system in the signaling pathways of TGF-beta superfamily. *Front Biosci* **8**, d1109-1127.

Watanabe N, Wachi S, Fujita T. (2003) Identification and characterization of BCL-3-binding protein: implications for transcription and DNA repair or recombination. *J Biol Chem* **278**, 26102-26110.

Wessels DJ, Zhang H, Reynolds J, Daniels K, Heid P, Lu S, Kuspa A, Shaulsky G, Loomis WF, Soll DR. (2000) The internal phosphodiesterase RegA is

essential for the suppression of lateral pseudopods during Dictyostelium chemotaxis. *Mol Biol Cell* **11**, 2803-2820.

Yamagata A, Kakuta Y, Masui R and Fukuyama K. (2002) The crystal structure of exonuclease RecJ bound to Mn2+ ion suggests how its characteristic motifs are involved in exonuclease activity. *Proc Natl Acad Sci U S A* **99**, 5908-12.

Yoshioka K, Foletta V, Bernard O, Itoh K. (2003) A role for LIM kinase in cancer invasion. *Proc Natl Acad Sci U S A* **100**, 7247-7252.

Zhang N, Yeh HJ, Zhong R, Li YS, Deuel TF. (1999) A dominant-negative pleiotrophin mutant introduced by homologous recombination leads to germ-cell apoptosis in male mice. *Proc Natl Acad Sci U S A* **96**, 6734-6738.

Zheng P, Eastman J, Van de Pol S, Pimplikar SW. (1998) *PAT1*, a microtubule-interacting protein, recognizes the basolateral sorting signal of amyloid precursor protein. *Proc. Natl. Acad. Sci. USA* **95**, 14745-14750.

Zheng J, Rudra-Ganguly N, Powell WC, Roy-Burman P. (1999) Suppression of prostate carcinoma cell invasion by expression of antisense L-plastin gene. *Am J Pathol* **155**, 115-122.

Acknowledgements

I would like to thank my director of studies Dr. Massimo Zollo for giving me the opportunity to work in his laboratory. I'm very thankful to him for his assistance, support, encouragement and ideas in project development. These thanks extend to Prof. Ashok Venkitaraman, my supervisor, for his interest in my work and for his help throughout my PhD course and in the preparation of this thesis.

I'm grateful to the Telethon Institute of Genetics and Medicine (TIGEM), and I appreciatively acknowledge the Director Prof. Andrea Ballabio for giving me the opportunity to work into the institute. A distinctive acknowledgement goes to Dr. Elena Rugarli, who has coordinated the first Open University program at TIGEM with patience and determination.

I thankfully acknowledge all the "Zollo's group" members, Veruska, Alessandra A., Livia, Pietro, Ombretta, Natascia, and Annamaria for their support and for sharing the additional data inserted in this PhD thesis to make a more comprehensive thesis work.

An exclusive thanks is for my special friend Adriano who always listened to me and gave me strength, encouragment, and esteem. I'm thankful for sharing the "Lab 94" laboratory with Alessandro, Mariella, Giovanna, Manuela, Valeria N., Giusy, Dario, Claudia, Barbara R. and Sabrina, who made my "laboratory lifetime" enjoyable. I'm very grateful to Alessia and Stefano C. for sharing helpful discussions.

My PhD laboratory bench work thesis has also been pleasurable for discussing and working with Antonio T., Carmine Sp., Carmine S., Ciro, Enzo,

Federico, Silvana, Barbara Z., Bianca, Ester, MT, Stefano P., Manlio, Francesco, Valeria C., Alessandra N., Salvatore B., Fabio, MariaTeresa D., Filomena and AnnaMonica.

My thanks extend to Mario T. and Peo for their informatic support, and to all the TIGEM researchers who gave me trust and esteem.

I'm very thankful to my friends Patrizia and Gabriella and to all my "Castel Morrone's" friends who have always supported me.

Finally, my gratefulness goes to my mother Franca and my grandparents Alessandro and Maria, who let my dream become true.

Publications from this thesis

Forus A, **D'Angelo A**, Henriksen J, Merla G, Maelandsmo GM, Florenes VA, Olivieri S, Bjerkehagen B, Meza-Zepeda LA, del Vecchio Blanco F, Muller C, Sanvito F, Kononen J, Nesland JM, Fodstad O, Reymond A, Kallioniemi OP, Arrigoni G, Ballabio A, Myklebost O, Zollo M. Amplification and overexpression of PRUNE in human sarcomas and breast carcinomas-a possible mechanism for altering the nm23-H1 activity. *Oncogene.* 2001 Oct 18;20(47):6881-90.

Garzia L, Andre A, Amoresano A, **D'Angelo A**, Martusciello R, Cirulli C, Tsurumi T, Marino G, Zollo M. Method to express and purify nm23-H2 protein from baculovirus-infected cells. *Biotechniques.* 2003 Aug;35(2):384-8, 390-1.

D'Angelo A, Garzia L, Andre A, Carotenuto P, Aglio V, Guardiola O, Arrigoni G, Cossu A, Palmieri G, Aravind L, Zollo M Prune cAMP phosphodiesterase binds nm23-H1 and promotes cancer metastasis. *Cancer Cell.* 2004 Feb;5(2):137-49.

D'Angelo A. and Zollo M. Unraveling genes and pathways influenced by h-prune PDE overexpression: a model to study cellular motility. *Cell cycle.* June 2004, Volume 3, Issue 6.

Zollo M., André A., Cossu A., Sini MC., **D'Angelo A.**, Marino N., Budroni M., Tanda F., Arrigoni G., and Palmieri G. Overexpression of h-prune in breast cancer is correlated with advanced disease status. (2004) Submitted.

Garzia L., **D'Angelo A.**, Volinia S., Andrè A., Cirulli C., Amoresano A., Marino G., Campanella C., Zollo M. (2004) Phosphorylation of nm23-H1 and nm23-H2 by CKIδinduces complex formation with h-prune and cellular motility. Submitted.